

# **Potassium Channels in Prostate and Colonic Cancer**

DISSERTATION ZUR ERLANGUNG DES DOKTORGRADES DER  
NATURWISSENSCHAFTEN (DR.RER.NAT.) DER NATURWISSENSCHAFTLICHEN  
FAKULTÄT III – BIOLOGIE UND VORKLINISCHE MEDIZIN  
DER UNIVERSITÄT REGENSBURG



vorgelegt von  
Jiraporn Ousingsawat  
aus Bangkok, Thailand

Juni 2007



Promotionsgesuch eingereicht am: 13 August 2007

Die Arbeit wurde angeleitet von: Prof. Dr. Karl Kunzelmann

Prüfungsausschuss:

Vorsitzender:	Prof. Dr. Richard Warth
1. Gutachter	PD Dr. rer. nat. Rainer Schreiber
2. Gutachter	Prof. Dr. Edward Geissler
3. Prüfer:	Prof. Dr. Stephan Schneuwly
Ersatzperson:	Prof. Dr. Ernst Tamm



## Zusammenfassung

Kaliumionenkanäle nehmen Einfluss auf den Zellzyklus und die Zellproliferation. *In vitro* Untersuchungen an Krebszellen und bösartigen Tumoren zeigen eine erhöhte Expression verschiedener Typen von  $K^+$ - Kanälen, wie zum Beispiel spannungsabhängige  $K_v$ - Kanäle, Eag-1,  $Ca^{2+}$ - abhängige BK- Kanäle und den 2P- Domänenkanal TASK-3. In der vorliegenden Arbeit untersuchten wir den Beitrag von  $K^+$ - Kanälen zur Entwicklung von Karzinomen der Prostata und des Dickdarms. Funktionelle Untersuchungen wurden mittels Patch clamp und Ussingkammer an Zelllinien und tierischen Geweben durchgeführt und rektale Potentialmessungen wurden an Mäusen *in vivo* vorgenommen. Mittels Aktivatoren und Inhibitoren von Kaliumkanälen, sowie der RNA- Interferenz Technik konnte der Beitrag der unterschiedlichen Kaliumkanaltypen ermittelt werden. Weiterhin wurde die Expression der Kanalproteine mit semiquantitativer und real-time PCR, Westernblot und Immunhistochemie untersucht.

### **$Ca^{2+}$ - abhängige Kaliumkanäle (BK) unterstützen das Wachstum von Zellen des Prostatakarzinoms**

*KCNMA1* kodiert für die  $\alpha$ - Untereinheit des großen  $Ca^{2+}$ - abhängigen (BK)  $K^+$ - Kanals und liegt in Spätstadien hormoninsensitive Prostatakarzinome in amplifizierter Form vor. Im Gegensatz hierzu zeigten gutartige Prostatagewebe eine nur schwache Expression von BK. Die Rolle von BK Kanälen für die Proliferation von Zellen des Prostatakarzinoms wurde mit Hilfe von PC-3 Zellen untersucht. PC-3 Zellen repräsentieren das hormoninsensitive Prostatakarzinom und wurden mit hormonsensitiven LNCaP- Zellen und der gutartigen Zelllinie BPH-1 verglichen. In PC-3 Zellen war die Expression von BK-Kanälen deutlich erhöht und selektive Blockade mit dem BK- Inhibitor Iberiotoxin oder siRNA hemmte BK- Kanalströme und die Proliferation von PC-3 Zellen. BK- Kanäle wurden in isolierten Membranen nachgewiesen und konnten durch den Inhibitor Paxillin und durch siRNA unterdrückt werden. Eine hormonelle Aktivierung der BK- Kanäle durch Östrogene wurde nur in LNCaP und BPH-1 Zellen beobachtet. Die Ergebnisse liefern eindeutige Hinweise für die Rolle von BK- Kanälen beim Prostatakarzinom. Die BK- Kanalexpression kann als prognostischer Marker beim Prostatakarzinom gewertet werden und könnte ein wichtiges Zielprotein für die Behandlung fortgeschrittener Prostatakarzinome darstellen.

### **Der Elektrolyttransport und die Expression spannungsabhängiger Kaliumkanäle sind beim Kolonkarzinoms verändert**

Die Rolle von  $K^+$ - Kanälen für die Proliferation des Kolonkarzinoms wurde an drei verschiedenen Modellen untersucht: 1) An der humanen Kolonkarzinomzelllinie T<sub>84</sub>. 2) Am Kolon von Karzinogen- behandelten Mäusen. 3) Am Kolon von Mäusen mit einem

genetischen Defekt des Tumorsuppressorgens *APC*. Neben der abnormalen Kaliumkanalexpression wurden Veränderungen in der Expression von Ionenkanälen festgestellt, die für den Elektrolyttransport im Kolonepithel *in vivo* von entscheidender Bedeutung sind.

#### *Histologische Veränderungen während der Karzinogenese im Mäusekolon*

Unter der Behandlung mit den chemischen Karzinogenen DMH und MNU, konnte in der frühen Phase histologisch eine Entzündung im Mäusekolon beobachtet werden, die bei weiterer Behandlung zu einer Veränderung der Mukosaarchitektur und schließlich zu einer Epitheldysplasie führte. Dies stellen typische Vorstufen während der Entwicklung von der normalen Mukosa hin zum Kolonkarzinom dar. Mutationen im Tumorsuppressorgens *APC* werden in nahezu allen Fällen des humanen Kolonkarzinoms sowie den erblichen Formen der Adenomatosis Polyposis Coli gefunden. Heterozygote Tiere mit einem Defekt im *APC*-Gen entwickeln multiple Darmneoplasien, die im fortgeschrittenen Stadium in intestinale Karzinome übergehen. Die Expression der karzinomrelevanten Proteine  $\beta$ -Catenin und Phospho-Akt war in den Polypen von Dünn- und Dickdarm der heterozygoten *APC<sup>Min/+</sup>* Tiere erhöht.

#### *Veränderungen des Kochsalztransports während der Karzinogenese im Kolonepithel*

Die Behandlung mit den Karzinogenen DMH oder MNU führte in der frühen Phase zu entzündlichen Veränderungen im Kolon der Versuchstiere, die denen der DSS- induzierten Kolitis ähnlich waren. Weiterhin wurde eine Abnahme der amiloridhemmbaren  $\text{Na}^+$  Resorption und der cAMP- aktivierten  $\text{Cl}^-$  Sekretion beobachtet. Da die Expression der zugrunde liegenden Transportproteine ENaC und CFTR unverändert war, sind die Transportstörungen wahrscheinlich ein Resultat der reduzierten Aktivität der  $\text{Na}^+/\text{K}^+$ -ATPase. Im Gegensatz zu den Karzinogen- behandelten Tieren, fand sich im gesamten Kolon von *APC<sup>Min/+</sup>* Mäusen eine deutliche Zunahme der elektrogenen  $\text{Na}^+$ - Resorption, welche durch eine erhöhte Expression der drei ENaC- Untereinheiten bedingt war. Die Zunahme von ENaC im Kolon von *APC<sup>Min/+</sup>* Mäusen ist wahrscheinlich durch Aktivierung des intrazellulären mTOR-Akt Signalweges und die reduzierte Apoptose bedingt. Die Ergebnisse könnten erklären, weshalb es bei der Kolitis häufig zu Diarrhöen kommt, wohingegen bei intestinalen Tumoren häufig ein Wechsel zwischen Obstipation und Diarrhöe auftritt.

#### *Pathologische Expression von $\text{K}^+$ - Kanälen beim Kolonkarzinom*

In der vorliegenden Arbeit konnten wir die Bedeutung von  $\text{K}_v$  und BK  $\text{K}^+$ - Kanälen für die Proliferation von Kolonkarzinomzellen zeigen. In  $\text{T}_{84}$  Kolonkarzinomzellen fanden wir eine Vielzahl von  $\text{K}^+$ - Kanälen, wie z.B.  $\text{K}_v1.3$ ,  $\text{K}_v1.5$ ,  $\text{K}_v3.3/3.4$ ,  $\text{K}_v\text{LQT}$ , Eag-1, Erg-1 und die kalziumabhängigen  $\text{K}^+$ - Kanäle BK und SK4. Inhibitoren von  $\text{K}_v$ - Kanälen und siRNA für Eag-1 unterdrückten die Zellproliferation, wohingegen Blocker und siRNA für  $\text{Ca}^{2+}$ - abhängige  $\text{K}^+$ -

Kanäle keinen Einfluss auf die Proliferation von  $T_{84}$ - Zellen hatten.  $K_v$ - und Eag- Kanäle unterstützen die Regulation des intrazellulären pH und die  $Ca^{2+}$ - abhängige Signaltransduktion. Eine erhöhte Aktivität von  $K_v$  Kanälen wurde auch im Dickdarm von DMH- und MNU- behandelten Tieren festgestellt. Die Effekte der  $K_v$  Kanalinhhibitoren 4-AP und Astemizol auf den intestinalen Transport waren deutlich verstärkt bei den karzinogenbehandelten Mäusen. In der prämaligen Kolonschleimhaut von karzinogenbehandelten Mäusen finden sich daher  $K_v1.3$ ,  $K_v1.5$  und  $K_v3.1$  sowie Mitglieder der Eag- Kaliumkanalfamilie, die als onkogene Ionenkanäle wahrscheinlich zur Entwicklung des Kolonkarzinoms beitragen. Im proximalen Kolon von  $APC^{Min/+}$  Mäusen wurde ebenfalls ein erhöhter Astemizol- sensibler Transport beobachtet, was durch Aktivierung der mitogenen oder mTOR- abhängigen Signaltransduktion erklärt sein könnte. Akt aktiviert Erg, ein weiteres Mitglied der EAG Familie, wie auch BK Kanäle. Neben der Zunahme von Eag- Strömen wurde auch eine Zunahme der BK- Kanalaktivität im Kolon von  $APC^{Min/+}$  Mäusen festgestellt. Als Ursache für die Zunahme der BK- abhängigen Ströme wurde eine vermehrte Transkription der regulatorischen  $\beta 1$ - und  $\beta 2$ - Untereinheiten des BK- Kanals gefunden. Bemerkenswerterweise wurde auch in  $T_{84}$ - Zellen eine Zunahme der Expression von  $\beta$ - Untereinheiten beobachtet.

#### *Expression von Eag-1 in humanen Prostata- und Kolonkarzinomen*

Im Gegensatz zum gesunden humanen Kolon fanden wir in Gewebeproben humaner kolorektaler Karzinome ebenfalls eine Expression von Eag-1. Unsere Untersuchungen zeigen, dass eine Amplifikation des Eag-1- Gens in humanen Kolonkarzinomproben mit einer reduzierten Lebenserwartung verbunden ist. Eag-1 könnte daher als diagnostischer und prognostischer Marker der Kolonkarzinomerkrankung dienen. Zusammengenommen konnten wir zeigen, dass Kaliumkanälen für die Entwicklung und das Wachstums von Prostata- und Kolonkarzinomen eine Bedeutung zukommt. Eine Beziehung zwischen Tumor und molekularer sowie funktioneller Expression von  $K_v$ - Kanälen, vor allem Eag-1, sowie  $Ca^{2+}$ -abhängiger  $K^+$ - Kanäle konnte in verschiedenen Modellen festgestellt werden. Wir konnten zeigen, dass diese Kanäle die Zellproliferation unterstützen und deshalb wahrscheinlich auch das Wachstum des Karzinoms fördern. BK- und Eag- Kanäle wurden als Marker für eine negative Prognose des Karzinompatienten identifiziert. Die vorliegenden Ergebnisse könnten somit hilfreich sein, um die Diagnose und Behandlung dieser Karzinome zu verbessern und könnten einen Beitrag zur Prognose der Patienten leisten.





# CONTENTS

	<i>page</i>
Zusammenfassung	I
Contents	V
Chapter 1	Introduction
	Expression and function of K <sup>+</sup> channels in intestinal epithelial cells
	3
	K <sup>+</sup> channels and cell proliferation
	- Cell cycle, growth factors and K <sup>+</sup> channel activity
	6
	- Control of K <sup>+</sup> channel activity by growth factors
	6
	- Ca <sup>2+</sup> signaling and membrane voltage
	7
	- Regulation of intracellular pH
	8
	- Cell volume regulation
	9
	K <sup>+</sup> channels and apoptosis
	10
	Paradoxical role of K <sup>+</sup> channels in cell proliferation and apoptosis
	10
	Aims of the present study
	12
Chapter 2	<i>KCNMA1</i> gene amplification promotes tumor cell proliferation in human prostate cancer
	13
Chapter 3	Voltage-gated K <sup>+</sup> channels support proliferation of colonic carcinoma cells
	31
Chapter 4	Expression of voltage-gated potassium channels in human and mouse colonic carcinoma
	51
Chapter 5	Upregulation of colonic ion channels in <i>APC<sup>Min/+</sup></i> mice
	67
Summary	83
References	87
Appendix	105
Acknowledgements	111
Curriculum Vitae	113



## CHAPTER 1

### INTRODUCTION

Cancer is the second most common cause of death in developed countries. Although large progress was made in understanding the molecular process of cancer development, many details of carcinogenesis remain obscure and novel treatments are demanded. Meanwhile a wide spectrum of diagnostic and therapeutic procedures exist such as surgery, chemotherapy, radiation, hormone, and immune therapy. However, the overall mortality and morbidity of cancer remains very high. The present work tries to make a contribution to a better understanding of the carcinogenic process and may provide new avenues for diagnosis and treatment of colonic cancer.

Oncogenesis is a complicated process, involving a series of genetic alterations and signal transduction pathways. Expression and activity of ion channels may be affected during tumor development and growth of cancer, among many other changes. The role of these ion channels for proliferation and development of cancer, however, remains obscure. About 10 years ago, Wonderlin and Strobel summarized the effects of ion channel inhibitors on proliferation of various malign cell types (Wonderlin and Strobl, 1996). It was shown that activation of  $K^+$  channels is crucial for progression through the G1 phase of the cell cycle. The review disclosed some essential details regarding the role of  $K^+$  channels in cell proliferation and cancer. Over the past 10 years, there were many more reports identifying expression of particular types of  $K^+$  channels in cancer (Table 1). It was, however, entirely unclear to what degree  $K^+$  channels contribute to the development of colonic and prostate cancer.

**Table 1.**  $K^+$  channels or currents identified in cancer. Genes are named according to the Human Gene Nomenclature Committee (HGNC name).

<i><b><math>K^+</math> channel</b></i>	<i><b>HGNC name</b></i>	<i><b>Type of tumor</b></i>	<i><b>Reference</b></i>
<b>Voltage-gated <math>K^+</math> channels (<math>K_v</math>)</b>			
$K_v$		human ovarian cancer small lung cancer myeloblastic leukemia hepatocarcinoma colonic cancer schwannoma	Abdul and Hoosein, 2002b, Fieber, 2003, Pancrazio et al., 1993, Renaudo et al., 2004, Xu et al., 1996, Yao and Kwan, 1999, Zhanping et al., 2007, Zhou et al., 2003

**Table 1.** K<sup>+</sup> channels or currents identified in cancer (continued).

<i>K<sup>+</sup> channel</i>	<i>HGNC name</i>	<i>Type of tumor</i>	<i>Reference</i>
K <sub>v</sub> 1.3	<i>KCNA3</i>	oligodendrocyte progenitor cells glioma prostate cancer colonic cancer breast cancer melanoma	Abdul et al., 2003, Abdul and Hoosein, 2002a, Abdul and Hoosein, 2002b, Pardo, 2004
K <sub>v</sub> 1.5	<i>KCNA5</i>	gastric cancer human glioma	Lan et al., 2005, Preussat et al., 2003
K <sub>v</sub> 2.1	<i>KCNB1</i>	cervical carcinoma endometrial adenocarcinoma	Suzuki and Takimoto, 2004a
K <sub>v</sub> 3.4	<i>KCNC4</i>	oral squamous cell carcinoma	Chang et al., 2003
<b>Family of voltage-gated K<sup>+</sup> channels (<i>ether à go-go</i>)</b>			
K <sub>v</sub> 10.1 (Eag-1)	<i>KCNH1</i>	breast cancer cervical cancer human melanoma, neuroblastoma	Farias et al., 2004a, Meyer et al., 1999, Pardo et al., 1999
K <sub>v</sub> 11.1 (Erg-1)	<i>KCNH2</i>	intestinal metaplasia primary leukemia endometrial tumors colonic cancer glioblastoma cervical carcinoma endometrial adenocarcinoma human mammary gland adenoma neuroblastoma atrial tumor cells	Bianchi et al., 1998, Cherubini et al., 2000, Crociani et al., 2003, Lastraioli et al., 2004, Lastraioli et al., 2006, Masi et al., 2005, Pillozzi et al., 2002, Smith et al., 2002, Suzuki and Takimoto, 2004a, Wang et al., 2002
<b>Ca<sup>2+</sup>-activated K<sup>+</sup> channels</b>			
Large conductance Ca <sup>2+</sup> -activated K <sup>+</sup> channels (BK)	<i>KCNMA1</i>	breast cancer human glioma prostate cancer human astrocytoma	Basrai et al., 2002, Chang et al., 2003, Coiret et al., 2007, Gessner et al., 2005, Ouadid-Ahidouch et al., 2004a, Weaver et al., 2004
Intermediate conductance Ca <sup>2+</sup> -activated K <sup>+</sup> channels (IK or SK4)	<i>KCNN4</i>	breast cancer human glioma human melanoma human bronchial carcinoma pancreatic cancer	Cruse et al., 2006, Jager et al., 2004, Meyer et al., 1999, Ouadid-Ahidouch et al., 2004b, Weaver et al., 2004
Small conductance Ca <sup>2+</sup> -activated K <sup>+</sup> channels (SK1, SK2,SK3)	<i>KCNN1</i> , <i>KCNN2</i> , <i>KCNN3</i>	mammary cancer human glioma human melanoma	Meyer et al., 1999, Potier et al., 2006, Weaver et al., 2004

**Table 1.** K<sup>+</sup> channels or currents identified in cancer (continued).

<i>K<sup>+</sup> channel</i>	<i>HGNC name</i>	<i>Type of tumor</i>	<i>Reference</i>
<b>Two-pore domain K<sup>+</sup> channels</b>			
TASK-3	<i>KCNK9</i>	breast cancer lung cancer primary mouse embryo fibroblasts colonic cancer	(Kim et al., 2004, Mu et al., 2003a, Patel and Lazdunski, 2004)
<b>Inward rectifier K<sup>+</sup> channels</b>			
K <sub>ir</sub> 2.1	<i>KCNJ2</i>	human lung cancer	(Sakai et al., 2002)
K <sub>ir</sub> 3.1	<i>KCNJ3</i>	breast cancer lung cancer	(Plummer, III et al., 2004, Plummer, III et al., 2005, Stringer et al., 2001)
K <sub>ir</sub> 4.1	<i>KCNJ10</i>	glioma	(Nathke, 2006)
ATP-sensitive K <sup>+</sup> channels (K <sub>ir</sub> 6.1/K <sub>ir</sub> 6.2)	<i>KCNJ8/KCNJ11</i>	human breast cancer	(Klimatcheva and Wonderlin, 1999, Woodfork et al., 1995)

### Expression and function of K<sup>+</sup> channels in intestinal epithelial cells

Potassium channels are the largest and most diverse family of plasma membrane channels. They have essential functions in any cell type. In epithelial cells of the gastrointestinal tract, K<sup>+</sup> channels play an important role in i) absorption of nutrients and electrolytes, ii) secretion of K<sup>+</sup>, iii) regulation of cell volume and pH, and iv) cell proliferation, differentiation, and apoptosis (O'Grady and Lee, 2005, Warth and Barhanin, 2003). Potassium channels, typically located in the basolateral membrane of epithelial cells, provide the driving force for nutrient absorption and electrogenic transport. In both Na<sup>+</sup> absorbing and Cl<sup>-</sup> secreting epithelia, K<sup>+</sup> efflux via basolateral K<sup>+</sup> channels helps to sustain the negative membrane voltage necessary for Na<sup>+</sup> entry or Cl<sup>-</sup> exit across the luminal membrane. Large-, intermediate-, and small-conductance Ca<sup>2+</sup>-activated K<sup>+</sup> channels, as well as K<sub>ATP</sub> and 239B-sensitive K<sub>v</sub>LQT1 K<sup>+</sup> channels have been identified in small and large intestine (Warth and Barhanin, 2003).

Apart from the kidneys, the colonic epithelium contributes to K<sup>+</sup> homeostasis by fine tuning luminal K<sup>+</sup> secretion and absorption. Potassium absorption is mediated by the H<sup>+</sup>/K<sup>+</sup>-ATPase on the luminal side of the colonic epithelium and is regulated by aldosterone and nutritional K<sup>+</sup> intake (Lomax et al., 1994, Sandle and Butterfield, 1999). Luminal nucleotides induce K<sup>+</sup> secretion via activation of large conductance Ca<sup>2+</sup>-activated K<sup>+</sup> channels (BK) (Hay-Schmidt et al., 2003, Puntheeranurak et al., 2006, Sausbier et al., 2006) (Figure 1). Besides BK, there is evidence for a pH sensitive ROMK-type K<sup>+</sup> channel located on the luminal side (Warth and

Bleich, 2000). Similar to the small intestine, basolateral  $K^+$  channels in the colonic epithelium are essential to maintain a hyperpolarized membrane voltage and the electrical driving force for  $Cl^-$  secretion and  $Na^+$  absorption (Bleich and Warth, 2000, Devor et al., 1997). Basolateral  $K^+$  channels are activated either by an increase in intracellular  $Ca^{2+}$  or cAMP (Bleich et al., 1996, Kunzelmann and Mall, 2002, Mall et al., 1998, Sandle et al., 1994). So far, three types of  $K^+$  channels have been identified on the basolateral side;  $K_{v}LQT1$ , BK, and SK4. These channels have been studied in detail. Thus,  $K_{v}LQT1$  (*KCNQ1*) has a very low single channel conductance and is blocked by 293B. It can be activated by either cAMP or  $Ca^{2+}$ . In the colon, *KCNQ1* coassembles with the regulatory subunit *KCNE3* to produce an instantaneous  $K^+$  current. It is essential for basolateral  $K^+$  exit (Bleich and Warth, 2000) (Figure 1). BK channels have also been detected in mammalian colon. Expression of BK channels is high in the surface epithelium cells but reduced in lower crypt cells. (Burckhardt and Gögelein, 1992, Hay-Schmidt et al., 2003, Klaerke et al., 1996) However, this pattern of expression may change during inflammatory processes (Sandle et al., 2007). BK channels are inhibited by paxillin and iberiotoxin. Moreover, SK4 is another type of basolateral  $K^+$  channel expressed in the colonic epithelium. It is an intermediated conductance  $Ca^{2+}$ -activated  $K^+$  channel identified in murine and rabbit colon. SK4 is activated by increase in intracellular  $Ca^{2+}$  and 1-EBIO, and is inhibited by clotrimazole and TRAM-34 (Warth et al., 1999).

$K^+$  channel activity is also critical for cell volume regulation (Sarkadi and Parker, 1991). When swollen due to hypotonic stress, cells are able to re-adjust their volume by a mechanism known as regulatory volume decrease (RVD). RVD is accomplished by activation of both  $Cl^-$  and  $K^+$  channels, thereby releasing KCl and water from the cell. SK4 channels have been identified in small intestine (Okada et al., 2001) and colon (Umesaki et al., 1979) to contribute to cell volume regulation. The osmotic swelling results in an increase in the cytosolic  $Ca^{2+}$  concentration, which subsequently activates SK4 (Okada et al., 2001).

Apart from cell volume regulation,  $K^+$  channels control cell signaling via intracellular  $Ca^{2+}$ . The cell-negative  $K^+$  diffusion potential provides the driving force for both  $Ca^{2+}$  release from intracellular endoplasmic reticulum and  $Ca^{2+}$  influx through membrane localized  $Ca^{2+}$  channels (Schreiber, 2005).

Beyond these well recognized functions, epithelial  $K^+$  channels have been implicated in cell migration, proliferation, differentiation, and apoptosis in various cell types, including those of intestinal epithelia. After injury, early mucosal repair occurs by epithelial cell migration to reseal superficial wounds. Epithelial migration is activated by a rise in cytosolic  $Ca^{2+}$  concentration due

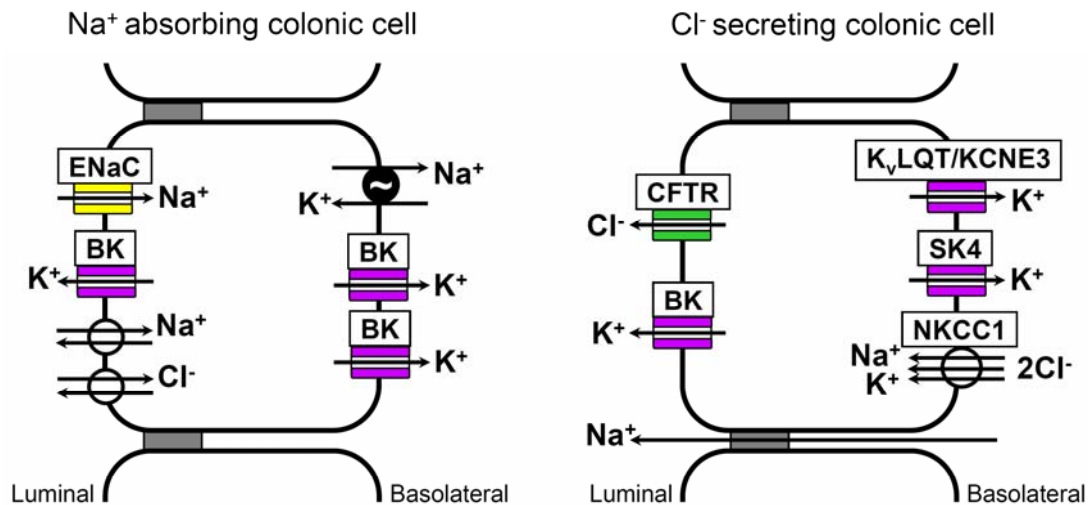


**Figure 1.** Simplified transport model of the mammalian colonic epithelium. Electrogenic Na<sup>+</sup> absorption via the epithelial Na<sup>+</sup> channel (ENaC) takes place in the surface epithelium and upper crypts of the distal colon. Electroneutral NaCl absorption (parallel Na<sup>+</sup>/H<sup>+</sup> and Cl<sup>-</sup>/HCO<sub>3</sub><sup>-</sup> exchange) dominates in the proximal colon. Large conductance Ca<sup>2+</sup>-activated K<sup>+</sup> channels (BK) are located in the luminal and basolateral membrane of surface epithelial cells. Expression of BK channels is more pronounced in the distal colon when compared to the proximal colon. BK channels are responsible for K<sup>+</sup> secretion and maintain the driving force for Na<sup>+</sup> absorption. Cl<sup>-</sup> secreting cells are located predominately in the crypt base. Cl<sup>-</sup> is taken up into the cell by the basolateral Na<sup>+</sup>-K<sup>+</sup>-2Cl<sup>-</sup> cotransporter NKCC1, and is secreted via luminal cystic fibrosis transmembrane conductance regulator (CFTR) Cl<sup>-</sup> channels. Cl<sup>-</sup> secretion is maintained by basolateral K<sub>v</sub>LQT1/KCNE3 and SK4 channels and is paralleled by secretion of K<sup>+</sup> via luminal K<sup>+</sup> channels and Na<sup>+</sup> transport through the paracellular shut (modified from Kunzelmann and Mall, 2002).

to activation of K<sub>v</sub> channels (Rao et al., 2002). Although K<sup>+</sup> channels have a clear role in proliferation and differentiation, as outlined in the next chapter, they paradoxically also have a central function during apoptosis of intestinal cells (Grishin et al., 2005). Thus, K<sup>+</sup> efflux increases twofold in apoptosis-induced IEC-6 rat epithelial cells. K<sup>+</sup> channel inhibitors prevent DNA fragmentation, caspase activation and loss of the mitochondrial membrane potential, resulting in attenuation of apoptotic cell death. Obviously, activation of large K<sup>+</sup> currents that lead to cell shrinkage in conjunction with apoptotic stimuli causes programmed cell death (review Kunzelmann, 2005).

### K<sup>+</sup> channels and cell proliferation

It has been shown that K<sup>+</sup> channels support cell proliferation. While K<sup>+</sup> transport affects many cellular parameters like membrane potential, cytosolic Ca<sup>2+</sup>, pH, and cell volume, a cell cycle specific function has also been attributed to K<sup>+</sup> channels. According to this, K<sup>+</sup> channels are expressed in a cell cycle-dependent manner.

***Cell cycle, growth factors and K<sup>+</sup> channel activity***

Cyclic oscillations in K<sup>+</sup> channel activity, which parallel the cell cycle, have been described for a number of somatic cell types including embryonic cells (Bregestovski et al., 1992, Day et al., 1993, Day et al., 1998, Meyer and Heinemann, 1998, Takahashi et al., 1993, Wonderlin and Strobl, 1996). During early mouse development, BK channel activity is oscillating with the cell cycle, being low in S and G<sub>2</sub>, and high in M and G<sub>1</sub> phases (Day et al., 1993). Apart from BK, *ether à go-go-related* (Erg) K<sup>+</sup> channels are also regulated in early mouse embryogenic development (Winston et al., 2004). High levels of Erg mRNA are detected in fertilized oocytes, but levels decline during embryonic development. Subcellular and membrane localization of Erg channels varies at different stages, and is changed by treatment with specific Erg inhibitors. Interestingly, these blockers reduce the transition to the blastocyst stage and the number of cells per blastocyst. Thus, both BK and Erg channels play a significant role in early embryonic development.

The functional importance of K<sup>+</sup> channels for cell cycling is further supported by inhibition of cell cycle initiation and/or procession due to application of K<sup>+</sup> channel inhibitors. For instance, tetraethylammonium (TEA), a non-specific K<sup>+</sup> channel blocker, inhibits proliferation in B lymphocytes by suppressing both K<sup>+</sup> currents and DNA synthesis. Interestingly, TEA inhibits proliferation by stopping the cell cycle in the G<sub>1</sub> phase, but has otherwise no influence on the transition from G<sub>0</sub> to G<sub>1</sub> phase (Amigorena et al., 1990). The same antagonist also induces G<sub>1</sub> arrest in oligodendrocyte progenitor cells. G<sub>1</sub> phase blockers such as rapamycin and deferoxamine mimic the anti-proliferative effects of K<sup>+</sup> channel blocker (Ghiani et al., 1999). In addition, TEA causes accumulation of p27 and p21, cyclins and cyclin-dependent kinase (Cdk) inhibitors. p27 and p21 bind and inactivate the G<sub>1</sub>/S-phase cyclin-Cdk complex (cyclin E-Cdk2) and the S-phase cyclin-Cdk complex (cyclin A-Cdk2), thereby arresting the cell in the G<sub>1</sub> phase. Accumulation of p27 and arrest of the cell in the G<sub>1</sub> phase by the K<sub>v</sub> blocker 4-aminopuridine (4-AP) has been reported for small cell lung cancer, leukemic Jurket cells, and myeloblastic cells (Renaudo et al., 2004, Xu et al., 1996). Taken all this together, activation of K<sub>v</sub> channels is required for cells to progress through the G<sub>1</sub> phase of the cell cycle. Other studies show a role of human Erg K<sup>+</sup> channels for transition from G<sub>1</sub> to S phase (Shao et al., 2005).

***Control of K<sup>+</sup> channel activity by growth factors***

Growth factors such as insulin, insulin-like growth factor-1 (IGF-1), transforming growth factor- $\beta$ 1 (TGF $\beta$ 1) and epidermal growth factor (EGF) activate receptor tyrosine kinases and stimulate cell proliferation. The same mitogens also control K<sup>+</sup> channel expression and activity. Insulin



increases BK channel activity in the native hippocampus and in recombinant BK-expressing HEK293 cells (O'Malley and Harvey, 2004). Channel activation is attenuated by specific inhibitors of mitogen-activated protein kinase (MAPK) but not by inhibitors of phosphatidylinositol 3-kinase (PI3K), indicating insulin-induced activation of BK channels via stimulation of the MAPK pathway. In human myeloblastic ML-1 cells,  $K_v$  channel activity is modulated by the insulin - PI3K - Akt pathway, controlling cell proliferation (Guo et al., 2005). IGF-1 activates  $K_v$  channels in HEK293 cells via the PI3K pathway, resulting in enhanced proliferation (Gamper et al., 2002). The effects of IGF-1 on  $K^+$  currents are blocked by inhibitors of PI3K and are mimicked by overexpression of phosphoinositide-dependent protein kinase-1 (PDK1) or serum- and glucocorticoid-dependent kinase-1 (SGK1). Both PDK1 and SGK1 are downstream targets of PI3K (Figure 2). Importantly, IGF-1-induced proliferation of HEK293 cells is inhibited by both  $K^+$  channel blockers and inhibitors of PI3K. TGF $\beta$ 1 stimulates BK channels through MAPK and PI3K signaling cascades (Lhuillier and Dryer, 2002). TGF $\beta$ 1 evokes phosphorylation of the proto-oncogen Akt (protein kinase B) and activates MAPK/Erk kinase (MEK). Inhibition of PI3K by wortmannin and LY294002 suppresses the stimulatory effects of TGF $\beta$ 1 on BK channel and Akt phosphorylation. PI3K and Erk represent parallel signaling cascades activated through TGF $\beta$ 1, which both stimulate BK channels (Figure 2). The epidermal growth factor EGF has also been shown to activate  $K^+$  channel activity in parallel to cell proliferation. EGF stimulation hyperpolarizes the membrane voltage of mouse fibroblasts (Magni et al., 1991) and mouse mammary epithelial cells (Enomoto et al., 1986). A similar hyperpolarization is obtained by application of  $Ca^{2+}$  ionophores, while the effects of EGF are blocked by charybdotoxin, TEA, or quinine. Thus,  $Ca^{2+}$ -activated  $K^+$  channels may support EGF-induced cell proliferation. In summary, an increase in  $K^+$  channel expression and activity appears to be a downstream event of growth factor signaling.

### ***Ca<sup>2+</sup> signaling and membrane voltage***

$Ca^{2+}$  is a major intracellular messenger that is also crucial for cell proliferation. The intracellular  $Ca^{2+}$  concentration ( $[Ca^{2+}]_i$ ) is tightly controlled and maintained at around 100 nM in resting cells. Increase in  $[Ca^{2+}]_i$  occurs by  $Ca^{2+}$  release from intracellular stores and  $Ca^{2+}$  entry from the extracellular space through different types of  $Ca^{2+}$  channels. In excitable tissues,  $Ca^{2+}$  influx occurs through voltage-gated  $Ca^{2+}$  channels. In non-excitable cells,  $Ca^{2+}$  entry occurs through store-operated  $Ca^{2+}$  channels (SOCs) and receptor-operated  $Ca^{2+}$  channels (ROCs) (Schreiber, 2005). These channels are activated by depletion of intracellular  $Ca^{2+}$  stores (endoplasmic reticulum) and by ligand binding, respectively. A hyperpolarized membrane voltage is essential to provide the driving force for  $Ca^{2+}$  entry and  $Ca^{2+}$  release (Figure 3A). Oscillations of  $[Ca^{2+}]_i$

have been observed during the cell cycle. These transient changes of  $[Ca^{2+}]_i$  occur at the exit from G0, during S phase, and at the end of M phase (Schreiber, 2005). Cytosolic  $Ca^{2+}$  activates gene transcription and triggers resting cells to re-enter the cell cycle and to initiate of DNA synthesis at the G1/S transition (Berridge, 1995).

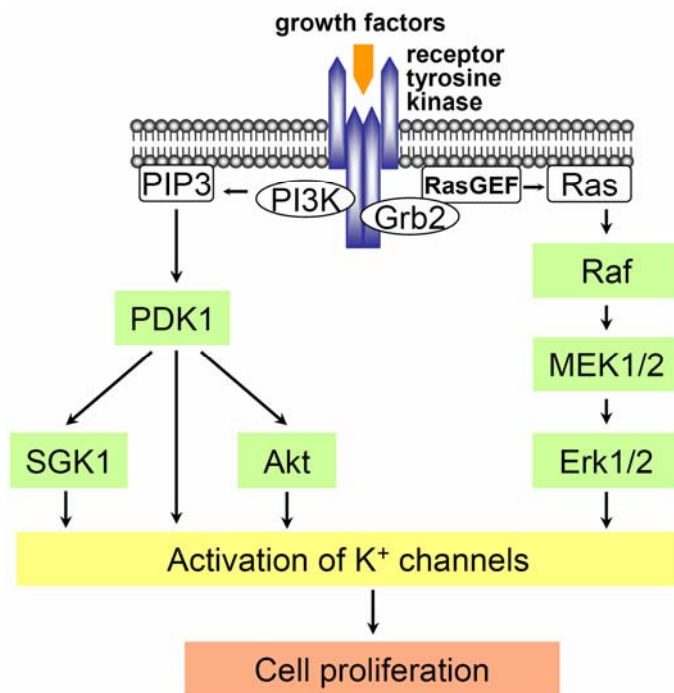


**Figure 2.** Growth factors stimulate cell proliferation by increasing expression and activity of  $K^+$  channels. Activation of receptor tyrosine kinase by growth factors triggers phosphatidylinositol 3-kinase (PI3K) and mitogen-activated protein kinase (MAPK). The PI3K generates phosphatidylinositol 3,4,5-triphosphate (PIP3) which serves as a docking site for phosphatidylinositol-dependent protein kinase-1 (PDK1). Subsequently, serum- and glucocorticoid-dependent kinase-1 (SGK1) and the protein kinase Akt are phosphorylated and activated by PDK1.  $K^+$  channels are regulated by phosphorylation via PDK1, SGK1, and Akt, which in turn stimulates cell proliferation. Activation of Ras is also triggered by receptor tyrosine kinase. Grb-2 adaptor protein binds to the receptor and to the Ras guanine nucleotide exchange factor (RasGEF). Ras, Raf (MAPKKK), MEK (MAPKK), and Erk (MAPK) are activated subsequently, which results in stimulation of  $K^+$  channels.

A negative membrane voltage induced by  $K^+$  channels provides the driving force for  $Ca^{2+}$  influx. Thus,  $K^+$  channel blockers inhibit cell cycle progression due to membrane depolarization (Lepple-Wienhues et al., 1996, Nilius and Wohlrab, 1992). Growth hormones such as epidermal growth factor (Pandiella et al., 1989) and bradykinin (Lang et al., 1991) induce sustained oscillations of the negative membrane voltage by alternating between depolarization and hyperpolarization. These oscillations in response to growth factor stimulation are  $Ca^{2+}$  dependent and are blocked by  $K^+$  channel inhibitors. Thus  $K^+$  channels provide the physiological basis for intracellular  $Ca^{2+}$  oscillations.

### **Regulation of intracellular pH**

Highly proliferative cancer cells produce a hypoxic and acidic microenvironment due to large amounts of metabolic acid, generated during glycolysis and synthesis of lactic acid. In tumor tissues extracellular pH ( $pH_e$ ) varies from 6.5 - 6.9, when compared to 7.0 - 7.5 in normal

tissues. In contrast, intracellular alkalinization has been demonstrated in tumors (Stubbs et al., 1995). Even in an acidic extracellular environment, cancer cells maintain an intracellular pH, which is about 0.2 – 0.4 pH units more alkaline than that of normal cells (Webb et al., 1999). Intracellular alkalinization is induced by an outward transport of protons by the  $\text{Na}^+/\text{H}^+$ -exchanger, vacuolar  $\text{H}^+$ -ATPase,  $\text{H}^+/\text{Cl}^-$  symporter, and monocarboxylate transporter (lactate-proton transporter) (Harguindeguy et al., 2005, Izumi et al., 2003). However, the  $\text{Na}^+/\text{H}^+$ -exchanger NHE1 is the main transporter, activated by growth factors and oncogens (Reshkin et al., 2000). Hyperactivity of NHE1 is observed during oncogenic transformation and development of malignant tumors. NHE1 exchanges intracellular  $\text{H}^+$  for extracellular  $\text{Na}^+$ , and therefore largely relies on the driving force provided by a low intracellular  $\text{Na}^+$  concentration. Cells maintain the chemical gradient for  $\text{Na}^+$  by pumping  $\text{Na}^+$  out of the cell through the  $\text{Na}^+/\text{K}^+$ -ATPase. Subsequently intracellular  $\text{K}^+$  needs to be recycled through basolateral membrane  $\text{K}^+$  channels (Figure 3A).  $[\text{Ca}^{2+}]_i$  and  $\text{pH}_i$  fluctuation during cell cycling are paralleled by fluctuations in  $[\text{Na}^+]_i$  and  $[\text{K}^+]_i$  (Morrill and Robbins, 1984). Therefore  $\text{K}^+$  channels substantially contribute to maintenance of intracellular pH.

### ***Cell volume regulation***

During cell cycle progression, large changes in cell volume occur. Cells must double their size before they divide, to maintain a constant average size over generations. Mitogens and growth factors activate NHE1,  $\text{Na}^+/\text{K}^+/\text{2Cl}^-$  cotransporter (NKCC1), non-selective cation channels, and nutrient transporters thereby increasing cell volume (Lang et al., 2000). Cell swelling activates  $\text{K}^+$  and  $\text{Cl}^-$  efflux by regulatory volume decrease (RVD). Thus, cells are capable of coping with changes in cell volume. The relationship between cell size and proliferation was investigated extensively in neuroblastoma and glioma cells. An intimate relationship was found between proliferation and cell volume, and either cell swelling or shrinkage was found to reduce proliferation (Dubois and Rouzaire-Dubois, 2004). Thus, cell proliferation is optimal within a certain range of cell volume. One possibility to explain how changes in cell volume affect cell proliferation, is the macromolecular crowding theory (Dubois and Rouzaire-Dubois, 2004, Ellis, 2001). Cell swelling and shrinkage lead to dilution and concentration, respectively, of cellular constituents, including macromolecules. Conformation and thus activity of macromolecules such as enzymes is largely dependent on their crowding and on the ratio of hydration versus osmotically active water. Relatively small changes in concentration lead to large changes in activity. Notably,  $\text{K}^+$  channel blockers like TEA, 4-AP, and  $\text{Cs}^+$  increase the cell volume and decrease the rate of cell proliferation. Proliferation is fully inhibited when cell volume increases

by 25% (Rouzair-Dubois and Dubois, 1998). These effects on volume regulation demonstrate another mechanism by which  $K^+$  channels control cell proliferation.

### **$K^+$ channels and apoptosis**

Programmed cell death or apoptosis is induced by extrinsic and intrinsic pathways. The extrinsic or death receptor pathway, requires binding of ligands such as CD95, tumor necrosis factor  $\alpha$  (TNF- $\alpha$ ) or Fas-ligand. The intrinsic pathway or the mitochondrial pathway is triggered by mitochondrial membrane depolarization or DNA damage, disruption of the mitochondrial membrane and release of cytochrome c. As an early hallmark of programmed cell death, apoptotic cells show cell shrinkage, termed apoptotic volume decrease (AVD), due to efflux of  $K^+$ ,  $Cl^-$ , and water (Figure 3B). Subsequent activation of caspase during the late phase of AVD leads to cleavage of nuclear lamin and DNA fragmentation via deoxyribonuclease activation. Consequently, apoptotic bodies are formed and digested by macrophages. AVD is inhibited by pharmacological blockers of  $K^+$  or  $Cl^-$  channels, but not by broad spectrum caspase inhibitors (Maeno et al., 2000). Activation of apoptosis decreases  $[K^+]_i$  considerably. Reduction in  $K^+$  efflux, by elevating  $[K^+]_e$  or  $K^+$  channel blockers prevents cell shrinkage and inhibits cell death (Bortner et al., 1997). Conversely, increase in  $K^+$  efflux stimulates apoptosis. Interestingly, maintaining  $[K^+]_i$  at physiological concentrations (140 mM) or  $K^+$  channel blockers directly inhibit apoptotic enzymes and cytochrome c release, thereby preventing apoptosis (Grishin et al., 2005, Hughes, et al., 1997, Hughes and Cidlowski, 1999). In contrast,  $K^+$ -ionophores (valinomycin) induce apoptosis in various cell types due to an increase in  $K^+$  efflux. Taken together, pronounced  $K^+$  efflux and reduced  $[K^+]_i$  is an initial step during programmed cell death. Various  $K^+$  channels have been implicated in apoptosis such as  $K_v$ , BK, two-pore  $K^+$  channels, hErg, ATP-sensitive  $K^+$  channels and inward rectifier  $K^+$  channels (reviewed in Burg et al., 2006). As mentioned before,  $Cl^-$  channels are also activated during apoptosis. In apoptotic cortical neurons  $Cl^-$  channel blockers inhibit outward rectifying  $Cl^-$  currents, prevent AVD, and attenuate apoptotic cell death (Wei et al., 2004). Several types of  $Cl^-$  channels are shown to contribute to cellular apoptosis such as CFTR (Barriere et al., 2001, Gottlieb and Dosanjh, 1996),  $Ca^{2+}$ -activated  $Cl^-$  channel (Elble and Pauli, 2001, Kim et al., 2003), cell volume regulatory  $Cl^-$  channels (Lang et al., 2004), and outwardly rectifying  $Cl^-$  channels (ORCC) (Szabo et al., 1998).

### **Paradoxical role of $K^+$ channels in cell proliferation and apoptosis**

Paradoxically,  $K^+$  currents have a role for proliferation and apoptosis. Even identical  $K^+$  channels were found to contribute to either proliferation or apoptosis. For instance, human Erg channels

facilitate tumor cell proliferation by  $\text{TNF-}\alpha$ , and also promote  $\text{H}_2\text{O}_2$ -induced apoptosis in various tumors (Wang et al., 2002, Wang, 2004). The intermediate conductance  $\text{Ca}^{2+}$ -activated  $\text{K}^+$  channel is important in AVD of human intestinal cells, but is also activated by growth factors (Okada et al., 2001, Tilly et al., 1993). The two-pore domain  $\text{K}^+$  channel TASK-3 has both an oncogenic potential in breast tumors, and a role during neuronal apoptosis (Patel and Lazdunski, 2004).

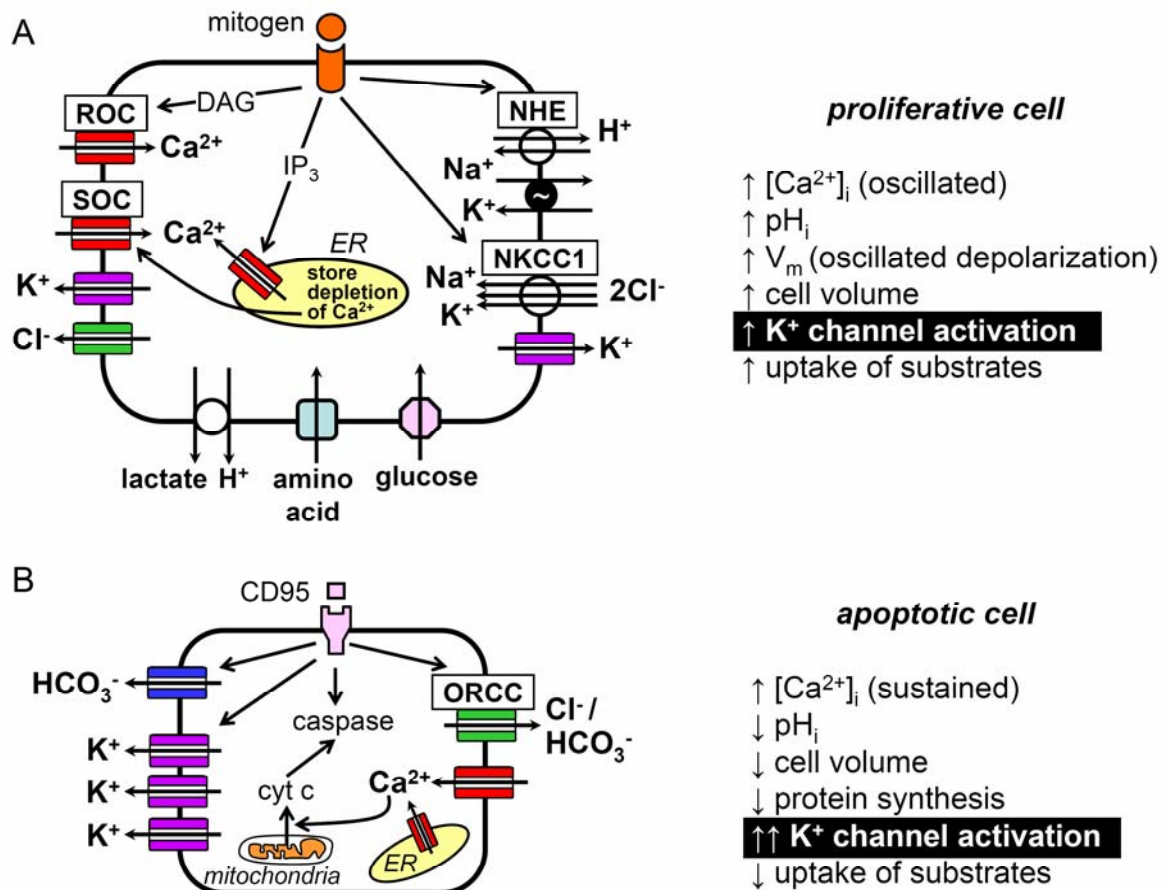


**Figure 3.** Role of  $\text{K}^+$  channels in cell proliferation and apoptosis. In proliferative cells (A), mitogens activate  $\text{Na}^+/\text{H}^+$  exchange (NHE), the  $\text{Na}^+/\text{K}^+-2\text{Cl}^-$  cotransporter (NKCC1), and uptake of substrates. This leads to an increase in cell volume.  $\text{H}^+$  efflux via NHE and lactate- $\text{H}^+$  transport causes cytosolic alkalinization, which triggers proliferation. Proliferating cells have a large  $\text{Cl}^-$  conductance that is essential for regulatory volume decrease (RVD).  $\text{K}^+$  channels are also activated by mitogens and control RVD and oscillations of the membrane potential, which provides the driving force for  $\text{Ca}^{2+}$  entry through store-operated  $\text{Ca}^{2+}$  channels (SOC) or receptor-operated  $\text{Ca}^{2+}$  channels (ROC). Intracellular  $\text{K}^+$  recycles through plasma membrane  $\text{K}^+$  channels to maintain the activity of the  $\text{Na}^+/\text{K}^+-\text{ATPase}$  and NKCC1. Therefore  $\text{K}^+$  channel activity indirectly supports cell proliferation via regulation of  $\text{Ca}^{2+}$  signaling, pH, and cell volume. B) Programmed cell death or apoptosis is induced by CD95 or Fas ligand. CD95 induces  $\text{HCO}_3^-$  efflux via  $\text{HCO}_3^-$  permeable anion channels and outwardly rectifying  $\text{Cl}^-$  channels (ORCC), thus causing acidosis. Cellular acidosis occurs during early phases of apoptosis. Activation of death receptors also activates  $\text{K}^+$  and  $\text{Cl}^-$  channels.  $\text{K}^+$  and  $\text{Cl}^-$  efflux causes cell shrinkage.

How can these opposite functions be reconciled? Principally, many of the homeostatic parameters are fundamentally different in proliferative and apoptotic cells. Cell proliferation leads to an increase in cell volume, whereas apoptotic cell death is characterized by a decrease in cell volume or cell shrinkage. In proliferative cells, activation of  $K^+$  channels is necessary to maintain cell volume via RVD, whereas in apoptotic cells activation of  $K^+$  channels leads to AVD cell shrinkage. The  $[K^+]_i$  in apoptotic cells drops to values below 50 mM, suggesting that  $K^+$  efflux exceed that of water efflux, while a drop in  $[K^+]_i$  is not observed in proliferative cells (Yu et al., 2001). Notably, proteolytic activation of caspases-3 and nuclease is facilitated by reduction of  $[K^+]_i$  (Hughes. et al., 1997). In general, the amplitude of  $K^+$  currents observed during apoptosis is much higher than that in proliferative cells (Patel and Lazdunski, 2004, Wang, 2004). Other noticeable differences concern intracellular  $Ca^{2+}$  signaling: Oscillatory  $Ca^{2+}$  rises are associated with proliferation and have not been observed during apoptosis (Berridge et al., 1998).  $Ca^{2+}$  release from endoplasmic reticulum (ER) is rapidly taken up by mitochondria and the ER. When mitochondria become overloaded with  $Ca^{2+}$ , mitochondrial metabolism will be disturbed, which activates programmed cell death. Therefore, a steady and high  $[Ca^{2+}]_i$  increase appears to be necessary for apoptosis.

### **Aims of the present study**

It was outlined above that  $K^+$  channels contribute to cell proliferation by controlling cell cycle transitions and affecting fundamental homeostatic parameters such as intracellular  $Ca^{2+}$ , pH, and cell volume. However, the current knowledge is fragmentary and lacks of a deeper understanding of the underlying mechanisms. As another major concern, most studies have only been performed in cell cultures and little is known about the role of  $K^+$  channels for tumor development *in vivo*. The series of experimental work presented here, aimed in a better understanding of the role of  $K^+$  channels in prostate and particularly colonic cancer. The objectives were as follow:

- To demonstrate the contribution of BK channels to proliferation of prostate cancer.
- To clarify the expression of  $K^+$  channels and their functions in the premalignant colon and colonic cancer.
- To elucidate more specifically the mechanisms by which  $K_v$  and EAG channels support cell proliferation in colonic cancer.
- To study changes in ion transport during the development of colonic cancer
- To investigate particularly the role of Eag-1 channels in human and mouse intestinal tumors.

## CHAPTER 2

### **KCNMA1 gene amplification promotes tumor cell proliferation in human prostate cancer**

#### **ABSTRACT**

Molecular mechanisms of prostate cancer progression are poorly understood. Here, we studied gene amplification of the large conductance calcium-activated potassium channel alpha subunit (*KCNMA1*), which is located at the chromosomal region 10q22. Fluorescence *in situ* hybridization (FISH) revealed *KCNMA1* amplification in 16% of 119 late-stage human prostate cancers and in the hormone-insensitive prostate cancer cell line PC-3. In contrast, *KCNMA1* amplification was absent in 33 benign controls, 32 precursor lesions and in 105 clinically organ-confined prostate cancers. Amplification was associated with mRNA and protein overexpression as well as increased density of BK channel protein and  $\beta$ -estradiol-insensitive BK currents in PC-3 cells as compared to non-amplified control cell lines. Specific blockade of BK channels by iberiotoxin or RNAi significantly inhibited  $K^+$  currents and growth of PC-3 cells. The data demonstrate that 10q22 amplification drives *KCNMA1* expression and cell proliferation. Thus, *KCNMA1* qualifies as a promising diagnostic and therapeutic target in patients with prostate cancer.

**Keywords:** prostate cancer; progression; amplification; BK channel; *KCNMA1*

## INTRODUCTION

Prostate cancer is the most frequent malignant tumor among males in developed countries and the second leading cause for cancer-related death (Hsing et al., 2000). Androgen withdrawal is an effective therapy for patients with advanced prostate cancer, but progression to hormone independence occurs ultimately in almost all patients after a few months or years (Petrylak et al., 2004). Although numerous non-hormonal agents have been evaluated in patients with hormone-refractory prostate cancer, these agents have limited anti-tumor activity with modest or no effect on survival (Petrylak et al., 2004). Therefore, identification and selected inhibition of molecular targets that mediate progression of prostate cancer are highly warranted.

The molecular mechanisms underlying progression to metastatic and hormone-refractory prostate cancer are poorly understood. High-level amplifications can pinpoint to genomic sites containing activated oncogenes with major biologic and therapeutic importance. We have recently identified an amplification at 10q22 prevailing in approximately 15% of hormone-refractory prostate cancers and in the hormone-insensitive prostate cancer cell line PC-3 (Bernardino et al., 1997, El Gedaily et al., 2001). Amplification of 10q22 appears to be absent or exceedingly rare in other tumor types, suggesting that this chromosomal region harbors genes that specifically drive progression of prostate cancer (Knuutila et al., 2000)

The *KCNMA1* gene is located at 10q22 and encodes the pore-forming  $\alpha$ -subunit of the large conductance  $\text{Ca}^{2+}$ -activated  $\text{K}^+$  channel (also known as BK-channel, Maxi  $\text{K}^+$  channel, slowpoke) that can tetramerize to a fully active BK channel (El Gedaily et al., 2001, Quirk and Reinhart, 2001). In mammalian tissues, *KCNMA1* is almost ubiquitously expressed along with four regulatory  $\beta$ -subunits *KCNMB1-4* (Orio et al., 2002, Rebhan et al., 1997).

Numerous functions have been attributed to BK channels, including modulation of smooth muscle tone of blood vessels and uterus (Amberg et al., 2003, Zhou et al., 2000), synaptic neurotransmitter release (Robitaille and Charlton, 1992) and epithelial transport (Kunzelmann and Mall, 2002). Most recently, attention has been drawn to the BK channel as a critical player in blood pressure regulation (Amberg and Santana, 2003) and in the neurotropic effect of ethanol (Davies et al., 2003). Hence, potassium channel-modulating agents have been suggested as therapeutic agents in neurological and cardiovascular disorders (Calderone, 2002).

Apart from this, growing evidence exist that  $\text{K}^+$  channels may also be involved in oncogenesis. For example, BK channel activation has been shown to drive tumor cell proliferation in astrocytoma (Basrai et al., 2002). Moreover, a previous report has suggested a role of potassium channels for the proliferation of prostate cancer (Van Coppenolle et al., 2004). Here,



we demonstrate that *KCNMA1* is amplified in a subset of late-stage prostate cancers *in vivo*, and that BK channel activity alters growth of human prostate cancer *in vitro*.

## MATERIALS AND METHODS

### *FISH probes*

The bacterial artificial chromosome (BAC) RP11-428p16, which contains major parts of the *KCNMA1* gene sequence, and the BAC RP11-417o11, which contains the whole genomic sequence of *PLAU*, were obtained from the Wellcome Trust Sanger Institute (Cambridge, UK). Growth conditions and DNA extraction were as recommended by the supplier. One microgram of purified plasmid DNA was labeled using a modified Bio Nick kit (Invitrogen, Carlsbad, CA, USA). The nucleotide solution of the nick kit was replaced by 0.2 mM each dCTP, dGTP, dTTP, 0.1 mM dATP, 500 mM Tris-HCl (pH 7.8), 50 mM MgCl<sub>2</sub>, 100 mM mercaptoethanol, 100 mg/ml nuclease-free bovine serum albumin (BSA), 1 ml Digoxigenin (Roche Diagnostics, Basel, CH), and 1 ml DNA Polymerase 1 (Invitrogen) was added. Nick translation was performed at 16°C for 90 min. The labeled FISH probes were purified by precipitation and re-dissolved in 50 µl H<sub>2</sub>O.

### *Clinical specimens*

The 298 formalin-fixed and paraffin-embedded clinical specimens on the prostate tissue microarray were from the archive of the Institute for Pathology, University Hospital Basel, Switzerland. The tissue microarray was constructed as described previously (Kononen et al., 1998). The size of each tissue spot was 0.6 mm. In addition, sections from eight frozen prostate tissue specimens were used for immunofluorescence. They were from four patients with hormone-refractory local recurrences treated by transurethral resection, two patients with clinically organ-confined disease treated by radical prostatectomy and from two patients with benign prostatic hyperplasia treated by transurethral resections. Specimens were kept anonymous, and the experiments were according to the guidelines of the ethical committee of the University of Basel.

### *Fluorescence in situ hybridization*

Paraffin removal (3 × 5 min in Xylene followed by 2 × 2 min ethanol 95% and air-drying) and enzymatic tissue pretreatment (Vysis pretreatment solution, 80°C, 15 min) of tissue sections mounted on glass slides were performed in a VP2000 Processor device (Vysis, Downers Grove, IL, USA). Slides were rinsed in water for 2 min, incubated in protease K solution (Vysis) at 37°C for 150 min and rinsed in water again. Subsequently, slides were dehydrated in an ascending ethanol series (70, 80, 95%) and air-dried. Then, a premixed hybridization cocktail containing

0.5 µl centromere 10 probe (CEP 10 Spectrum orange labeled; Vysis), 1.5 µl *KCNMA1* probe (digoxigenin labeled), 1 µl Cot DNA (Invitrogen) and 7 µl hybridization buffer (Vysis) was added to each slide. For probe and target DNA denaturation, slides were heated to 72°C for 10 min. Probes were allowed to hybridize overnight at 37°C in a humidified chamber. The next day, slides were washed in 2 × standard sodium citrate, 0.3%NP40, pH 7 - 7.5 at 72°C for 2 min. The *KCNMA1* probe was detected using the Dig detection kit (Roche Diagnostics). Amplification was defined as a signal ratio of gene probe/centromere 10  $\geq$  2 and at least five gene signals.

#### *Cell lines and cell culture*

We used the cell lines PC-3, LNCaP and BPH-1. PC-3 was originally established from a lumbar vertebral metastasis of a 62-year-old Caucasian man after treatment with diethylstilbestrol and bilateral orchiectomy (Kaighn et al., 1979). LNCaP cells were isolated from a needle aspiration biopsy of the left supraclavicular lymph node metastasis of a 50-year-old Caucasian man (Horoszewicz et al., 1980). BPH-1 originates from a 68-year-old patient with transurethral resection of the prostate for benign prostatic hyperplasia. The donor had not undergone hormonal therapy and did not have malignant disease. The cells were immortalized with a virus carrying the SV40T antigen and selected for resistance to geneticin. This cell line does not express androgen receptor and prostate specific antigen (Hayward et al., 1995).

For the growth assays, 6×25,000 cells were plated on a six-well plate (Falcon, Becton-Dickinson, Franklin Lakes, NJ, USA). PC-3 and BPH-1 were grown in 3 ml Opti-MEM (Invitrogen) + 10% fetal calf serum (FCS, BioConcept, Allschwil, CH). After 1 day, the medium was changed to Opti-MEM + 1% FCS. At day 2, the medium was changed to Opti-MEM + 0.4% Albumax (Invitrogen) containing iberiotoxin (Sigma, Fluka Production GmbH, St Louis, MO, USA) or 17β-estradiol (Sigma, Fluka Production GmbH). Iberiotoxin (IBMX) was diluted in phosphate-buffered saline (PBS) to a final concentration of 20 nM. 17β-estradiol was diluted in 70% ethanol to a final concentration of 1 nM. In contrast to PC-3 and BPH-1, LNCaP did not grow in Opti-MEM + 0.4% Albumax. Thus, the effects of estradiol and IBTX on growth of LNCaP were assayed in Opti-MEM + 5% FCS + 0.2% Albumax. This medium contains reduced serum and still allows growth of LNCaP. After two days of growth, cell numbers were counted using a Neubauer Chamber. The growth rate  $k$  was calculated as  $N(t) = N_0 \cdot e^{kt}$ ,  $t$  = time in days.

#### *Western blot and immunofluorescence*

Cells were lysed in sample buffer containing 1% sodium dodecyl sulfate (SDS) and 100 mmol/l dichlorodiphenyltrichloroethane. Protein concentrations were determined according to a modified Laury method. Lysates of PC-3 cells were resolved by 7% SDS-PAGE, transferred to Hybond-P

(Amersham Pharmacia Biotech, Freiburg, BRD) and incubated with anti-KCNMA1 polyclonal antibody (generous gift by Professor Dr P Ruth, Institute of Pharmacy, University of Tübingen, Germany). Proteins were visualized using a sheep anti rabbit immunoglobulin G, conjugated to horse radish peroxidase and ECL Advance Detection Kit (Amersham Pharmacia Biotech). For immunocytochemistry, PC-3, BPH-1 and LNCaP cells were grown on glass cover slips, washed three times in PBS and fixed in methanol at -20°C. After washing in PBS, cells were incubated for 10 min in blocking buffer containing 10% BSA and 10% fish skin gelatine (both from Sigma). Cells were incubated overnight at 4°C in blocking solution, containing the primary antibody (1:1000 dilutions). Subsequently, cells were washed in PBS and incubated with the fluorescein isothiocyanate (FITC)-linked secondary antibody for 1 h at 37°C. Tissues were counter stained with 4',6-diamidino-2-phenylindole dihydrochloride (DAPI) solution (Sigma) and embedded in Mowiol (Sigma). Immunofluorescence was detected using an Axiovert 200 microscope and MetaFluor imaging software. Immunofluorescence on frozen tissue sections was performed as described previously (Sausbier et al., 2006).

#### *RNA interference (RNA<sub>i</sub>)*

Transfection was performed following the siRNA transfection protocol for Lipofectamine 2000 (Qiagen, KJ Venlo, NL, USA). Briefly, 50,000 cells were plated in six-well plates (Falcon, Becton-Dickinson) one day before transfection. The transfection was performed in Opti-MEM (Invitrogen) for 4 h. The transfection mixture contained 5 µl of siRNA and Lipofectamine, each, in totally 3 ml Opti-MEM. After 4 h, the transfection mixture was replaced by Opti-MEM + 10% FCS. The siRNA sequences were: K1 gactggcagagtcctggtgt, K2 gtgggtctgtccttcctact, K3 gaccgtcctgagtgccatgt, K4 acgcc ctagaggtggctaca.

#### *Semiquantitative RT-PCR*

Cells washed with PBS were lysed in 350 microl RLT buffer (RNAeasy minikit, Qiagen). RNA extraction was done according to the protocol of Qiagen. cDNA synthesis was performed with 0.25 mg of total RNA using the superscript2 cDNA synthesis kit (Invitrogen). RT-PCR was performed using the LightCycler-system and the LightCycler FastStart DNA Master Hybridization Probes kit (Roche Diagnostics). Primers for G6PD and KCNMA1 hybridization products were obtained from TIB MolBiol (Berlin, BRD). PCR primers were: KCNMA1: KCNMA1\_s: cctggcctcctccatggt, KCNMA1\_a: ttctgggcctccttcgtct, G6PD: G6ex7,8 R ttct gcatcacgtcccga, G6ex6 S accactacctgggcaaggag. Hybridization probes were: KCNMA1: KCNMA1\_fl: agcgtccgccagagcaagat, KCNMA1\_lc: atgaagaggccccgaagaaagt, G6PD: G6ex\_FL: cagatggggccgaagatcctgtt, G6ex\_LC: caaatctcagcaccatgaggttctgcac. PCR conditions were:

activation: 10 min 95°C PCR cycle: 5 s at 95°C, annealing 5 s at 57°C, elongation 15 s at 72°C, 40 cycles. Raw data for *KCNMA1* expression were corrected by comparing to the related G6PD controls. Then these corrected values were compared to each other to obtain relative expression.

#### *Patch clamp experiments*

Cell culture dishes were mounted on the stage of an inverted microscope (IM35, Carl Zeiss AG, Oberkochen, BRD) and kept at 37°C. Patch clamp experiments were performed in the fast whole cell and cell excised inside/out configuration. The patch pipettes had an input resistance of 2-4 MΩ when filled with a solution containing (mmol/l) KCl 30, K-gluconate 95, NaH<sub>2</sub>PO<sub>4</sub> 1.2, Na<sub>2</sub>HPO<sub>4</sub> 4.8, ethyleneglycol tetraacetate 1, CaCl<sub>2</sub> 0.726, MgCl<sub>2</sub> 1.034, D-glucose 5, adenosine triphosphate 1 (32 Cl). The pH was adjusted to 7.2, the Ca<sup>2+</sup> activity was either 0.1 or 1 μmol/l. The access conductance was between 30 and 120 nS. In regular intervals, membrane voltages (V<sub>m</sub>) were clamped in steps of 10 mV from -50 to +50 mV and whole cell conductances were calculated according to Ohm's law. Currents (voltage clamp) and voltages (current clamp) were recorded using a patch clamp amplifier (EPC 7, List Medical Electronic, Darmstadt, Germany), the LIH1600 interface and PULSE software (HEKA) as well as Chart software (AD-Instruments). Data were analyzed using PULSE and Origin software. In membrane patches containing several BK channels, channel activity was determined by multiplying single channel Po with the number of active channels in the membrane patch. NS1619, IBTX, paxillin and 17β-estradiol were from Sigma.

#### *Statistical analysis*

Statistical significance was verified in the Figures 2, 5, and 6 with an analysis of variance test using JMP-IN software (release 5.1, SAS Institute GmbH, Heidelberg, BRD). Statistical significance was assumed when  $P < 0.05$ ;  $n = 3$  for these figures. For all patch clamp experiments, Students t-test  $P$ -values  $< 0.05$  were accepted to indicate statistical significance (\*).

## **RESULTS**

#### *KCNMA1 amplification and overexpression of BK channels*

Human prostate cell lines were analyzed for *KCNMA1* amplification by fluorescence *in situ* hybridization (FISH). Amplification, defined as a signal ratio of the *KCNMA1* gene/centromere of chromosome 10  $\geq 2$  and at least five gene signals, was present in the hormone-insensitive

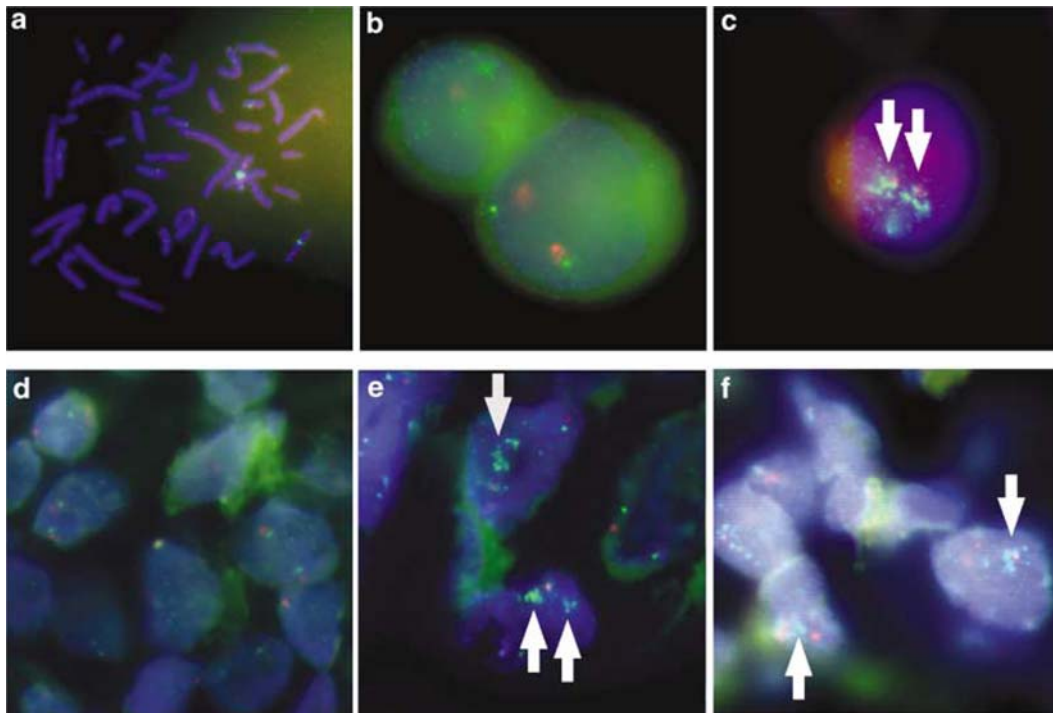


**Figure 1.** FISH with *KCNMA1*-specific BAC RP11-428P16. a) Metaphase control: Green *KCNMA1* signals and red centromere signals on chromosome 10. b) BPH-1, transformed benign prostate hyperplasia cell line, showing two signals for BAC probe and centromeric probe, each. c) PC-3, tumourigenic prostate cancer cell line with *KCNMA1* amplification at 10q22: two clusters of green probe signals and two red signals of centromere 10 (arrows). d) Tumor cells from clinical prostate cancer with normal probe copy number. e) and f) Prostate cancers with amplification. Dense clusters of green probe signals but only rare red centromeric signals (arrows). Blue channel: DAPI. Green channel: FITC (BAC RP11-428P16). Red channel: Spectrum Orange (centromere 10). Magnification  $\times 1000$ .

prostate cancer cell line PC-3 but not in the hormone-sensitive prostate cell lines BPH-1 or LNCaP (Figure 1). To explore whether this amplification also prevails *in vivo*, a series of 298 formalin-fixed and paraffin-embedded human prostate specimens was analyzed on a tissue microarray. We found amplification in 16.0% of 119 advanced prostate cancers including untreated locally aggressive tumors (20%), distant metastases (13%) and local recurrences (22%) from hormone-refractory tumors but not in benign prostatic hyperplasia, precursor lesions (high-grade prostatic intraepithelial neoplasia) and clinically localized prostate cancers (Table 1). These results suggest that amplification of *KCNMA1* is associated with progression to late-stage, metastatic and hormone-refractory human prostate cancer. The FISH results of *KCNMA1* were compared with *PLAU*, a previously suggested candidate target gene at 10q22 (Helenius et al., 2001). Comparable to *KCNMA1*, *PLAU* amplification was present in PC-3 but not in BPH-1 and LNCaP. Analysis of 133 specimens revealed a similar prevalence and distribution of *PLAU* amplification among the different tumor stages as *KCNMA1* amplification (Table 1). *PLAU*

amplification was absent in specimens of benign prostatic hyperplasia and in clinically localized prostate cancers but present in untreated locally aggressive tumors (14%), lymph node metastases (13%), distant metastases (13%) and in hormone-refractory local recurrences (12%). The difference in the prevalence of amplification of these two genes in the different subgroups of tumors stages was statistically not significant.

**Table 1.** Prevalence of *KCNMA1* and *PLAU* amplification in prostate cancer

Category	<i>KCNMA1</i>			<i>PLAU</i>		
	Number of cases	<i>KCNMA1</i> amplification (N)	<i>KCNMA1</i> amplification (%)	Number of cases	<i>PLAU</i> amplification (N)	<i>PLAU</i> amplification (%)
BPH	33	0	0	24	0	0
High-grade PIN	32	0	0	-	-	-
T1a/b	43	0	0	17	0	0
T2	62	0	0	7	0	0
T3/4	10	2	20	7	1	14.3
LN metastases	17	0	0	8	1	12.5
Distant metastases	47	7	13	30	4	13.3
Hormone-refractory local recurrences	45	10	22.2	43	5	11.6

Abbreviations: BPH, benign prostatic hyperplasia; LN metastases, pelvic or paraortal lymph node metastases; PIN, prostatic intraepithelial hyperplasia; T1a/b, incidentally detected prostate cancer in transurethral resection for presumed BPH; T2, clinically organ confined prostate cancer treated by radical prostatectomy; T3/4, clinically non-organ confined, locally advanced prostate cancer treated with palliative transurethral resection. FISH analysis on a prostate-specific tissue microarray (TMA). The BAC RP11-428P16 was used as *KCNMA1*-specific probe, the BAC RP11-417O11 was used as *PLAU*-specific probe and the centromeric probe for chromosome 10 as a reference. The total number of specimens evaluable for *KCNMA1* and *PLAU* was 298 and 133, respectively. Amplification was defined as a ratio between gene and reference of X2 and at least five gene signals.

To study whether amplification of *KCNMA1* results in overexpression, we compared the mRNA levels of *KCNMA1* in the amplified PC-3 cell line with the non-amplified cell lines BPH-1 and LNCaP using semiquantitative reverse transcriptase-polymerase chain reaction (RT-PCR). Expression of *KCNMA1* was significantly higher in PC-3 as compared to LNCaP and BPH-1, suggesting that *KCNMA1* amplification drives over-expression of the channel protein (Figure 2a). In fact, increased levels of *KCNMA1* protein in PC-3 as opposed to the control cell lines were documented by immunofluorescence (Figure 2b). The fluorescence intensity (mean of optical density  $\pm$  error of the mean) was significantly higher in PC-3 ( $27,759 \pm 2061$ ; 10 cells) than in

LNCaP ( $10,806 \pm 259$ ; 12 cells) and BPH-1 ( $317 \pm 19.2$ ; 13 cells;  $P < 0.0001$ ; stains were repeated twice). Immunofluorescence on human prostatic tissue revealed strong BK expression in smooth muscle cells of the fibromuscular stroma. This is in line with previous reports showing strong expression in smooth muscle of other sites such as blood vessels and colonic wall (McCobb et al., 1995, Sausbier et al., 2006). BK expression also prevailed in all six prostatic adenocarcinomas and the intensity varied from weak to moderate (Figure 3). None of the tumors met the criteria for *KCNMA1* gene amplification by FISH. One tumor had increased gene copy number of *KCNMA1* (5-7 gene signals and 4-5 reference signals) and showed moderate BK expression (Figure 3a). However, expression at a similar level was also found in tumors with a normal gene copy number (Figure 3f). Benign prostatic glands showed weak expression of BK.

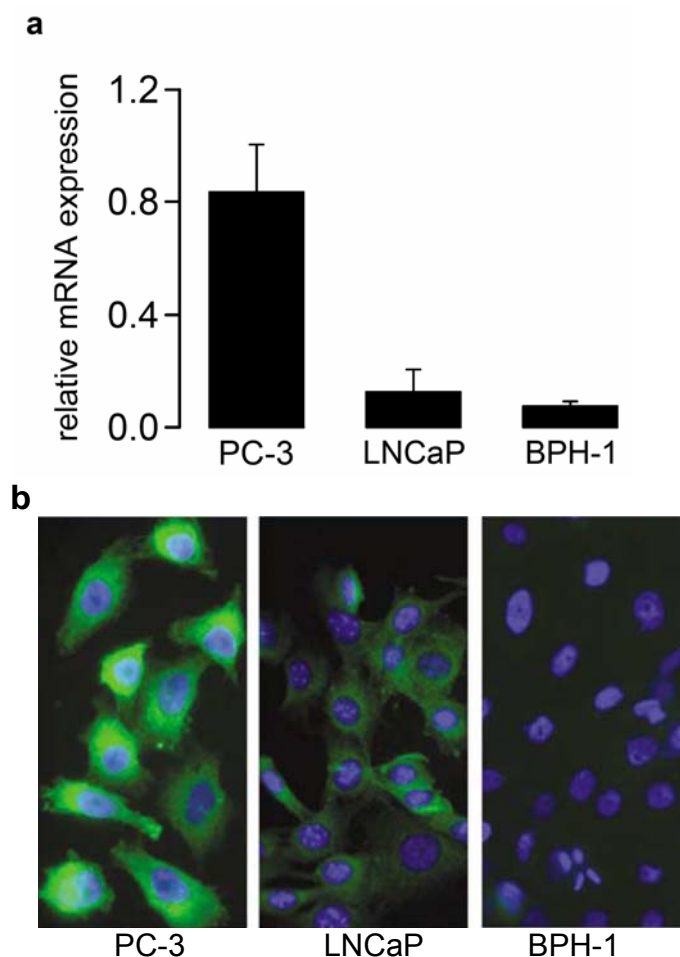


**Figure 2.** Expression of *KCNMA1*. a) mRNA expression of *KCNMA1* was significantly enhanced in the amplified prostate cancer cell line PC-3 as compared to the non-amplified cell lines LNCaP ( $P = 0.0002$ ) and BPH-1 ( $P = 0.0001$ ). Figure is drawn to be relative to the expression in PC-3. ( $n = 3$  for each group). b) Immunofluorescence of the prostate cancer cell lines PC-3, LNCaP and BPH-1. Protein expression of *KCNMA1* was strong in PC-3 cells, weak in LNCaP and indiscernible in BPH-1 ( $P < 0.0001$ ). Magnification  $\times 1000$ . Stains were repeated twice.

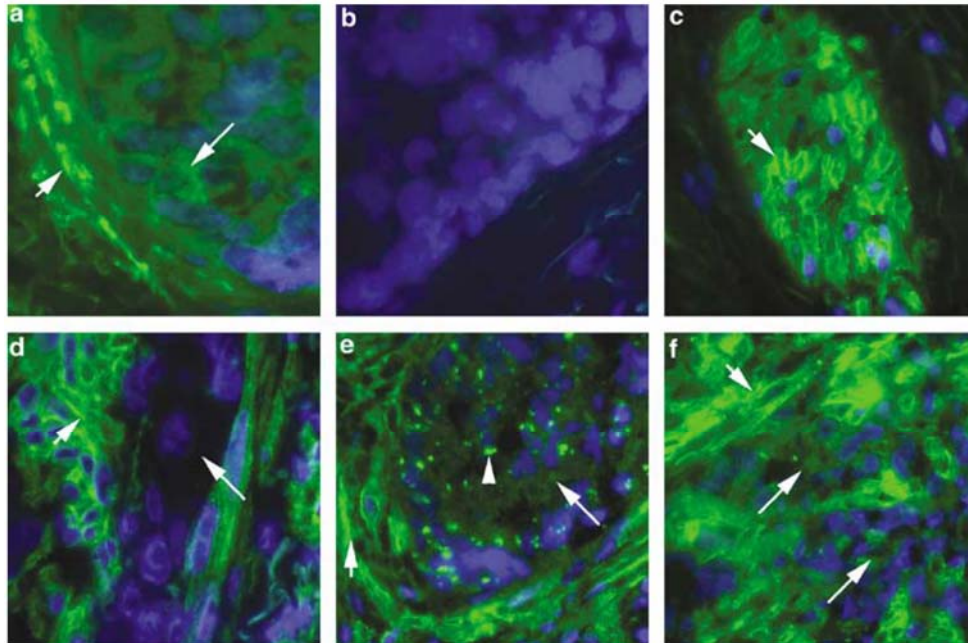


**Figure 3.** Immunofluorescence of anti-BK channel antibody on human prostate cancer tissue. Antibody labeled in green (FITC), nuclei counterstained in blue (DAPI). a) Well-detectable BK channel staining in the cytoplasm of hormone-refractory prostate cancer (long arrow), and strong staining in surrounding smooth muscle cells (short arrow). This tumor showed increased *KCNMA1* gene copy number by FISH. b) Negative control on the same specimen as (a). Absence of staining indicates specificity of the antibody. c) Bundle of smooth muscle cells in the same specimen as a). Note the very intense expression of the BK channel at the cellular membrane (short arrow). d) Hormone-refractory prostate cancer infiltrating between smooth muscle cells. Note the intense staining of the smooth muscle cells (short arrow) and the very weak staining of the tumor cells (long arrow). This tumor had normal *KCNMA1* gene copy number by FISH. e) Benign prostatic gland. Weak cytoplasmic immunofluorescence (long arrow). The bright spots in the cytoplasm represent autofluorescent lipofuscin granules that are typically present in benign prostatic glands (arrowhead). f) Hormone-insensitive prostate cancer infiltrating between smooth muscle cells. Well-detectable cytoplasmic and membranous immunofluorescence in tumor cells (long arrows) and strong positivity in adjacent smooth muscle cells (short arrow). This tumor had normal *KCNMA1* gene copy number by FISH. Magnifications: (a)-(d)  $\times 1000$ , (e)-(f)  $\times 630$ .

#### *BK channel currents in prostate cancer cells*

The prostate cell lines PC-3 and BPH-1 were used as *in vitro* models to study the influence of *KCNMA1* currents for cell proliferation. Functional expression of BK channels in PC-3 and BPH-1 cells was examined in patch clamp experiments. Iberitoxin (IBTX), a well-known and highly specific inhibitor of the BK channel (Galvez et al., 1990), reversibly inhibited whole cell current ( $I_m$ ) and conductance ( $G_m$ ) in PC-3 (Figure 4a and b). Inhibition of whole cell currents was paralleled by a depolarization of the membrane voltage ( $V_m$ ). Other than in PC-3 cells, IBTX had only minor effects on the whole cell current of LNCaP the benign BPH-1 cells and did not depolarize the membrane voltage (Figure 4c). Whole cell patch clamp experiments were performed in the same media as proliferation assays. Under these



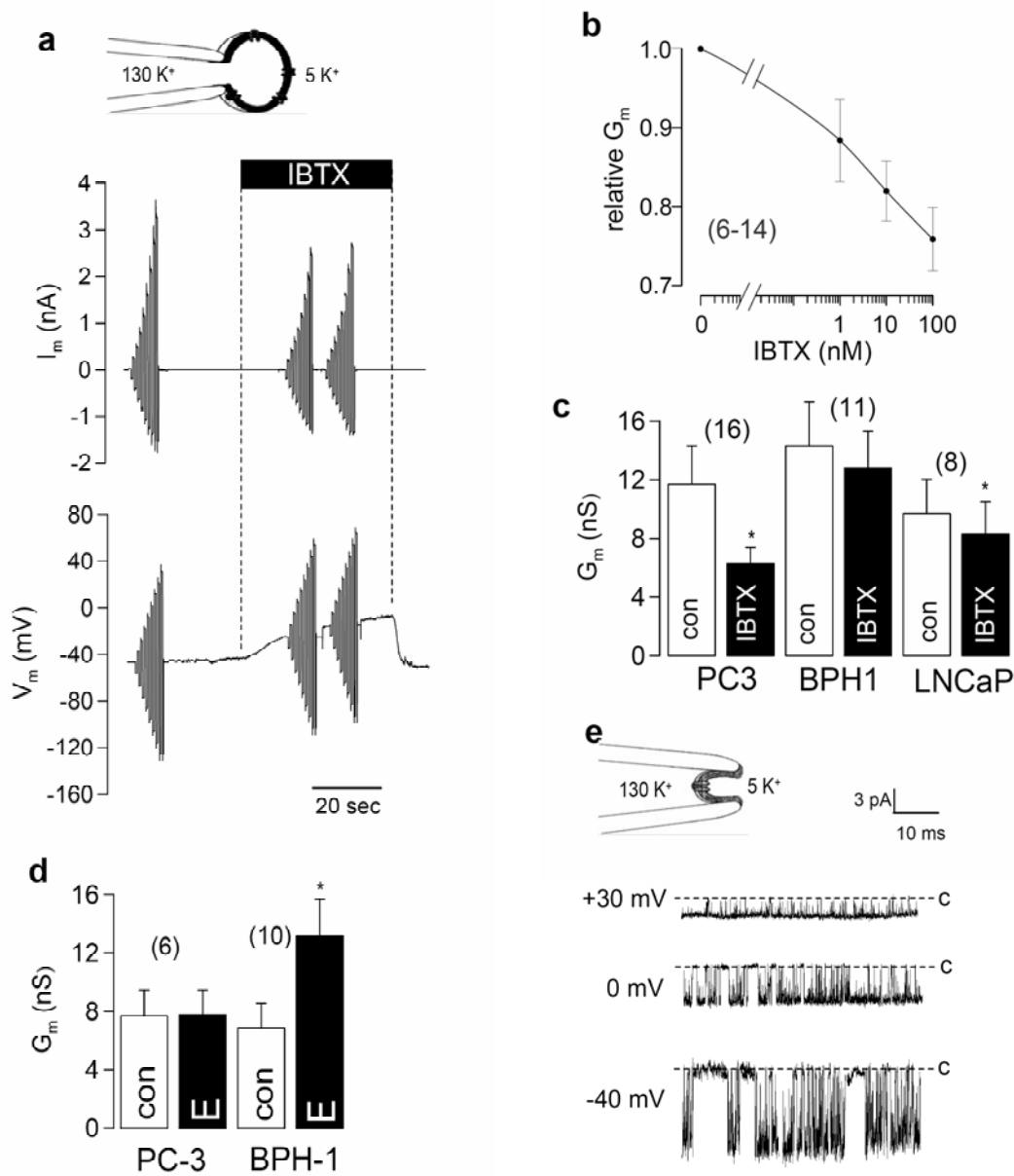


**Figure 4.** BK currents in prostate cancer cells. a) Continuous recording of the whole cell current ( $I_m$ , upper trace) and membrane voltage ( $V_m$ , lower trace) in a fast whole cell recording of a PC-3 cell. Symbol on top indicates configuration and concentrations of K<sup>+</sup>. IBTX (20 nmol/l) reduced the outward current and depolarized  $V_m$ . b) Concentration dependence of the inhibitory effect of IBTX on the whole cell conductance ( $G_m$ ) of PC-3 cells. c) Summary of the whole cell conductances ( $G_m$ ) of PC-3, BPH-1 and LNCaP cells and effects of IBTX (20 nmol/l) on  $G_m$  as compared to negative control (con). IBTX significantly reduced  $G_m$  in PC-3 and LNCaP ( $P < 0.001$  and  $P < 0.02$ , respectively). d) Summary of the whole cell conductances ( $G_m$ ) of PC-3 and BPH-1 cells and effects of 17 $\beta$ -estradiol (E, 10 mmol/l). 17 $\beta$ -estradiol led to a significantly increased  $G_m$  in BPH-1 ( $P < 0.01$ ). e) Single BK channel currents in inside out membrane patches at different clamp voltages. Channel openings are indicated by brief downward current deflections, while ---c indicates the closed state of the channel. Symbols indicate configuration and concentrations of K<sup>+</sup>. \*Significance (paired t-test); (n) = number of experiments.

“proliferative” conditions, the membrane voltage ( $V_m$ ) of both BPH-1 ( $-18 \pm 1.8$  mV,  $n = 13$ ) and PC-3 ( $-23 \pm 2.0$  mV,  $n = 17$ ) cells was depolarized. Although depolarization of  $V_m$  allows for activation of BK channels, IBTX inhibited membrane conductance was only found in PC-3 cells but not in BPH-1 cells. In Ringer solution both PC-3 and BPH-1 cells were hyperpolarized to  $-58 \pm 2.1$  mV ( $n = 14$ ) and  $-59 \pm 3.8$  mV ( $n = 17$ ) and IBTX sensitive membrane conductance was reduced (data not shown). Other  $\text{Ca}^{2+}$ -activated  $\text{K}^+$  channels such as small and intermediate conductance channels showed negligible contribution to the whole cell conductance of PC-3 and BPH-1 cells (data not shown).

The whole cell  $\text{K}^+$  conductance could not be augmented by the BK channel activator  $17\beta$ -estradiol in PC-3 (Valverde et al., 1999a), but was further enhanced along with a hyperpolarization of the membrane voltage in BPH-1 (Figure 4d). The results suggest a high activity of BK channels in PC-3 that cannot be further increased by  $17\beta$ -estradiol. These findings were supported by inside/out excision of membrane patches from PC-3 cells into a bath solution containing high  $\text{Ca}^{2+}$  concentration. Under these conditions, large conductance BK channels were regularly detected in PC-3 (Figure 4e), but only occasionally found in membrane patches of BPH-1. The open probability ( $P_o$ ) of the single channel was enhanced at depolarized membrane voltages, and the single channel conductance was about 220 pS at symmetrical  $\text{K}^+$  concentrations of 150 mM, which is characteristic for BK channels.

#### *Impact of BK channel activity on proliferation of prostate cancer cells*

We examined the response of PC-3, BPH-1 and LNCaP to modulation of BK channel activity (Figure 5). The basal growth rate was higher in PC-3 than in BPH-1 and was significantly inhibited by the BK channel inhibitor IBTX ( $P = 0.015$ ). This indicates a central role of BK channels for proliferation of PC-3 under normal growth conditions (Figure 5a). In contrast, there was no significant effect of IBTX on the growth of BPH-1 and LNCaP ( $P > 0.05$ , Figure 5b and c).  $17\beta$ -estradiol stimulated growth of BPH-1 ( $P = 0.0021$ ) and LNCaP ( $P = 0.0039$ ) but not PC-3 cells (Figure 5a-c). The growth effect of  $17\beta$ -estradiol was abolished by IBTX both in BPH-1 and LNCaP. This finding suggests that the steroid exerts its stimulatory effects on cell proliferation in BPH-1 and LNCaP through activation of BK channels. In contrast, rapidly growing PC-3 cells proliferate independently of  $17\beta$ -estradiol, as the abundantly expressed BK channels operate already at the high activity.

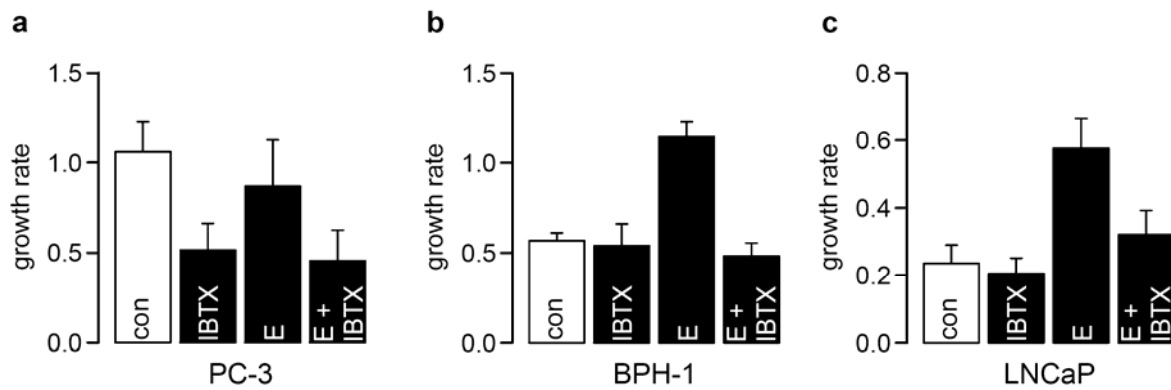


**Figure 5.** Growth rates of PC-3, BPH-1 and LNCaP cells in response to IBTX and 17 $\beta$ -estradiol (E). a) Growth of PC-3 cells was reduced in response to IBTX ( $P = 0.015$ ) and was not significantly influenced by 17 $\beta$ -estradiol. b) BPH-1 cells showed increased growth in response to 17 $\beta$ -estradiol ( $P = 0.0021$ ), which was prevented by IBTX ( $P = 0.0175$ ). (c) LNCaP cells showed increased growth in response to 17 $\beta$ -estradiol ( $P = 0.0039$ ), which was prevented by IBTX ( $P = 0.026$ ). Con = untreated control, IBTX = iberiotoxin, E = 17 $\beta$ -estradiol, E + IBTX = 17 $\beta$ -estradiol + iberiotoxin. y-axis: growth rate  $k$  as  $N(t) = N_0 \times e^{kt}$ .  $N(t)$ : number of cells at time  $t$ ,  $N_0$  = number of cells at time 0,  $t$  in days.

The role of BK channels for proliferation of prostate cancer cells was further substantiated by gene-specific mRNA silencing using RNA interference (RNA<sub>i</sub>). Four different types of anti-*KCNMA1* small interference RNA molecules (siRNA K1-K4) were transfected into PC-3 cells, which all significantly reduced *KCNMA1* mRNA expression and cell proliferation. The most potent *KCNMA1*-siRNA (K2) inhibited mRNA expression (Figure 6a) and cell proliferation (Figure 6b) by 80-90%, when compared to non-transfected cells (c-si) or cells transfected with scrambled sequence siRNA (scr). Expression of *KCNMA1* protein was largely reduced in siRNA K2-treated cells, when compared to non-transfected cells or cells transfected with scrambled sequence siRNA (Figure 6c). In whole cell patch clamp experiments, inhibition of the membrane conductance and depolarization of the membrane voltage by IBTX was significantly reduced in RNA<sub>i</sub>-treated cells (Figure 7a). The BK-inhibitor paxillin rather than IBTX was used for analysis of excised inside out membrane patches as paxillin is applicable to the cytosolic side of the membrane. Analysis of excised inside out membrane patches of RNA<sub>i</sub>-treated cells revealed largely attenuated BK channel activity ( $nP_o$ ) and a reduced effect of the BK channel blocker paxillin (Figure 7b). Inhibition of BK channel activity by paxillin was much reduced in RNA<sub>i</sub>-treated PC-3 cells and was not detectable in BPH-1 cells (Figure 7c). Taken together, the present data indicate a crucial role of *KCNMA1* for proliferation of advanced and hormone-refractory prostate cancer cells.

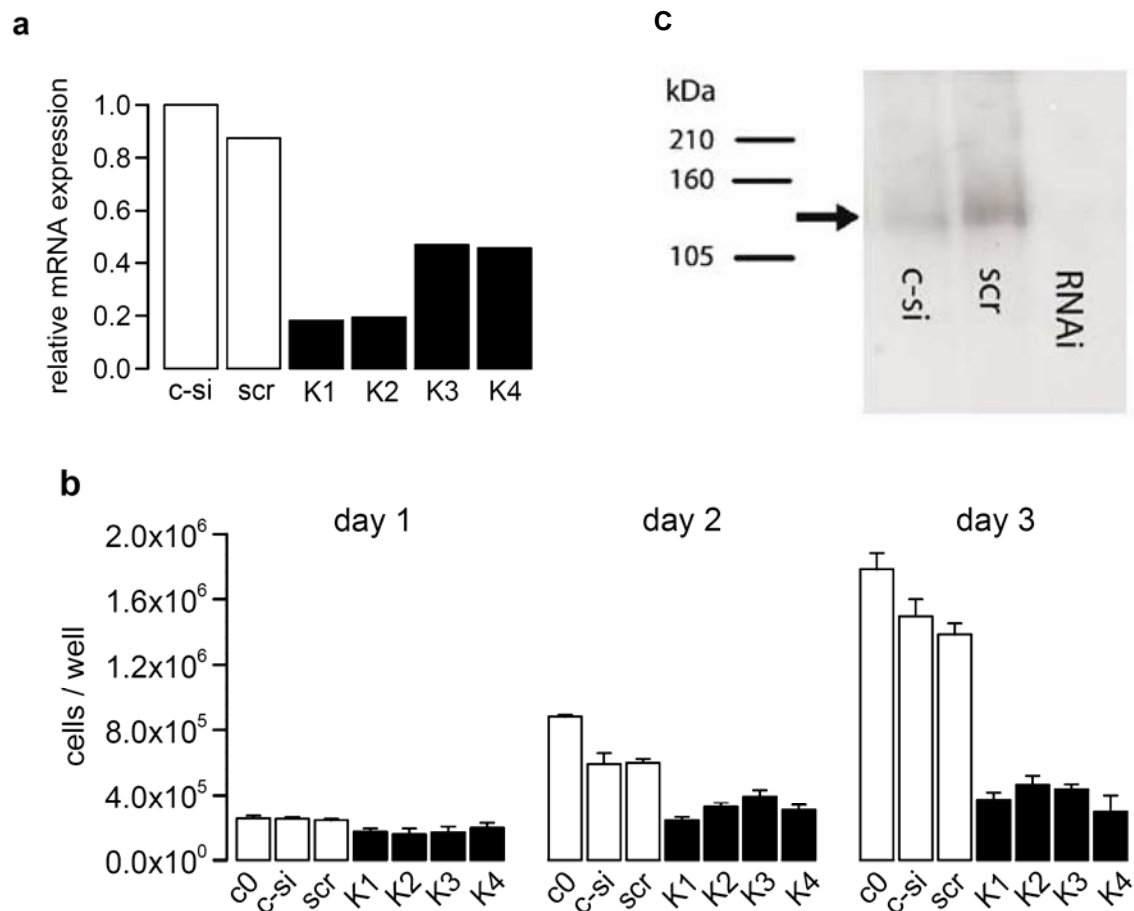


**Figure 6.** Inhibition of *KCNMA1* expression by RNA<sub>i</sub> in PC-3. a) RNA<sub>i</sub> reduced *KCNMA1* mRNA expression to 15–50% compared to non-transfected cells (c-si) or cells transfected with scrambled sequence RNA<sub>i</sub> (scr) ( $P = 0.005$  or  $P = 0.0021$ , respectively). Figure is drawn to be relative to the expression in the control (c-si). b) *KCNMA1*-RNA<sub>i</sub> using all four active siRNA K1-4 had a pronounced inhibitory effect on PC-3 cell growth. y-axis shows total number of cells per well. c) Western blot analysis of non-transfected (c-si) PC-3 cells and PC-3 cells which have been transfected with scrambled sequence (scr) and *KCNMA1*-RNA<sub>i</sub> (K2).

## DISCUSSION

There is mounting evidence that  $K^+$  channels play a crucial role in oncogenesis, and their potential as therapeutic targets in cancer has been recognized (Conti, 2004, Pardo et al., 1999, Pei et al., 2003, Wang, 2004). Here, we demonstrate that the large conductance  $Ca^{2+}$ -activated potassium channel (*KCNMA1*) is amplified at 10q22 in 16% of late-stage, metastatic and hormone-refractory human prostate cancers. In the cell line PC-3, amplification of *KCNMA1* is associated with overexpression of mRNA and protein, and a high density of BK channels in the cellular membrane as opposed to non-amplified cell lines. Importantly, growth inhibition by specific blockade of *KCNMA1* activity using IBTX and RNA<sub>i</sub> in the amplified prostate cancer cell

line PC-3 strongly argues for an oncogenic effect of *KCNMA1* amplification and functional overexpression. Expression of BK channel protein is not restricted to cell lines *in vitro* but also present in human prostate cancers *in vivo*. As well-detectable BK expression was found in tumors without *KCNMA1* amplification, factors other than increased gene dosage must also be involved in the regulation of BK expression in prostate cancer.

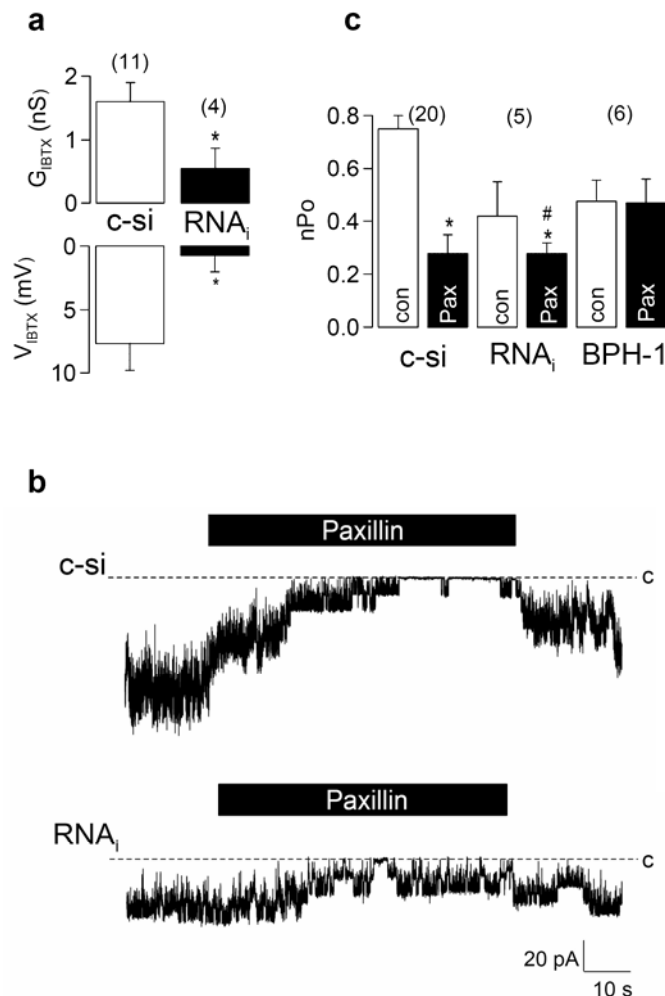


**Figure 7.** Inhibition of *KCNMA1* currents by RNAi. a) Summary of the whole cell conductances ( $G_m$ ) and membrane voltages ( $V_m$ ) of non-transfected (c-si) PC-3 cells and PC-3 cells which have been transfected with anti *KCNMA1*-RNAi.  $G_{IBTX}$  =  $G_m$  under inhibition with IBTX,  $V_{IBTX}$  =  $V_m$  under inhibition with IBTX ( $P < 0.001$  and  $P < 0.0007$ , respectively). b) Multiple BK channels in inside out membrane patches at 0 mV clamp voltage. ---c indicates current level when all channels are closed. BK channels are much more abundant in non-transfected (c-si) when compared with RNAi-transfected PC-3 cells. The BK channel inhibitor paxillin had a more pronounced effect in non-transfected (c-si) cells. c) Product of open probability and number of channels ( $nPo$ ) in non-transfected (c-si) and RNAi-transfected PC-3 cells as well as BPH-1 cells. The  $P_o$  was significantly reduced by paxillin (Pax) in non-transfected (c-si) PC-3 cells and in PC-3 cells treated by RNAi ( $P < 0.001$  and  $P < 0.02$ , respectively). The effect of paxillin was significantly greater in non-transfected PC-3 cells (c-si) than in RNAi-transfected PC-3 cells (#;  $P < 0.03$ ). \*Significance (paired t-test); (n)= number of experiments. Con= untreated controls.

The oncogenic role of *KCNMA1* found in this study is in line with the previously reported growth inhibition of human astrocytoma by IBTX (Basrai et al., 2002, Weaver et al., 2004). Interestingly, the intermediate conductance  $K^+$  channel (IK) rather than *KCNMA1* has been proposed to be important for PC-3 and LNCaP cells by Parihar et al. (Parihar et al., 2003). Parihar et al. performed the efflux experiments under non-proliferative conditions, that is, in Ringer solution rather than in growth medium. In Ringer solution, however, the cells were hyperpolarized and

thus BK channels and other voltage-gated K<sup>+</sup> channels show little activity (O'Grady and Lee, 2005, Pardo, 2004). The present data suggest that analysis of ion channels relevant to proliferation should be conducted under proliferative conditions, that is, in the presence of serum-containing culture media. Serum and glucocorticoid-inducible kinase, phospho-inositide-3 kinase and the mitogen-activated protein kinase pathway are activated by serum and have been shown to stimulate BK channels (Henke et al., 2004, O'Malley and Harvey, 2004).

The role of estrogens in prostate cancer is controversial and is also challenged by the present results. Despite the traditional use of estrogens for the treatment of prostate cancer, it is now known that estrogens can also induce neoplastic transformation in the prostate (Ho, 2004). In addition, 17 $\beta$ -estradiol directly activates BK channels by binding to the  $\beta$ 1-regulatory subunit, as shown in vascular smooth muscle cells (Valverde et al., 1999a). The present data provide evidence that 17 $\beta$ -estradiol stimulates growth of prostate cells through activation of BK channels. This growth stimulation by 17 $\beta$ -estradiol was pronounced in BPH-1 and LNCaP, but was absent in PC-3 cells. Missing activation of BK and lack of stimulation of cell proliferation by 17 $\beta$ -estradiol in PC-3 cells suggests that BK channels operate at maximal activity in these cells owing to overexpression driven by amplification. Interestingly, it has recently been shown that a proliferative effect of 17 $\beta$ -estradiol in the breast cancer cell line MCF-7 is also mediated by BK channels independently of estrogen receptor (Coiret et al., 2005). PC-3 and BPH-1 are known to express estrogen receptor alpha and beta, whereas LNCaP only expresses the estrogen receptor beta (Lau et al., 2000). Thus, 17 $\beta$ -estradiol might stimulate growth of BPH-1 and LNCaP by binding to the estrogen receptors. Alternatively, one could hypothesize that the growth effect of 17 $\beta$ -estradiol in LNCaP is due to altered ligand binding of the mutated androgen receptor (Veldscholte et al., 1992). However, the prevention of the growth stimulation of estradiol by IBTX suggests that the BK channel activity plays a central role in this growth stimulation. This is also in accordance with the previously shown direct activation of BK channels by 17 $\beta$ -estradiol (Kuruma and Hartzell, 2000, Valverde et al., 1999a). Taken together, activation of BK channel might be a major target of 17 $\beta$ -estradiol in prostate cancer in the absence of *KCNMA1* amplification and overexpression. However, it is likely that BK channels are modulated by a complex network of different molecules and molecular pathways (O'Malley and Harvey, 2004, Olsen et al., 2005).

There is increasing evidence that gene amplification leads to growth advantage of tumor cells, as a set of multiple genes rather than a single gene is overexpressed (Kauraniemi et al., 2001, Reiter et al., 2000). Along this line the urokinase-type plasminogen activator gene (uPA; syn.

*PLAU*) has previously been suggested as amplification target at 10q22 in human prostate cancer (Helenius et al., 2001, Helenius et al., 2006). As expected, *PLAU* amplification preferentially occurred in advanced prostate cancer at a similar prevalence as amplification of *KCNMA1* in our study. Prosaposin (PSAP) at 10q22, which has growth- and invasion-promoting activities, is another gene that has recently been found to be amplified in PC-3 and a few prostate cancer xenografts and lymph node metastases by single nucleotide polymorphism array and quantitative real-time PCR analysis (Koochekpour et al., 2005). Notably, *PLAU* stimulates  $\text{Ca}^{2+}$ -activated  $\text{K}^{+}$  channels in the human promyelocytic cell line U937 (Christow et al., 1999), suggesting synergistic effects of co-amplification of *KCNMA1* and *PLAU*. This challenges new promising studies on the interaction between *KCNMA1* and other genes within the amplified chromosomal region at 10q22.

In summary, the data presented in this study unmask *KCNMA1* as an amplified target gene at 10q22 that confers growth advantage to prostate cancer cells. Thus, BK channel may be a suitable pharmacological target in patients with late-stage prostate cancer that show amplification and overexpression of *KCNMA1*.





## CHAPTER 3

### Voltage-gated K<sup>+</sup> channels support proliferation of colonic carcinoma cells

#### ABSTRACT

Plasma membrane potassium (K<sup>+</sup>) channels are required for cell proliferation. Evidence is growing that K<sup>+</sup> channels play a central role in the development and growth of human cancer. Here we examine the contribution and the mechanism by which K<sup>+</sup> channels control proliferation of T<sub>84</sub> human colonic carcinoma cells. Numerous K<sup>+</sup> channels are expressed in T<sub>84</sub> cells, but only voltage-gated K<sup>+</sup> (K<sub>v</sub>) channels influenced proliferation. A number K<sub>v</sub> channel inhibitors reduced DNA synthesis and cell number, without exerting apoptotic or toxic effects. Expression of several K<sub>v</sub> channels such as Eag-1, K<sub>v</sub>3.4 and K<sub>v</sub>1.5 was detected in patch clamp experiments and in fluorescence based assays, using a voltage sensitive dye. The contribution of Eag-1 channels to proliferation was confirmed by siRNA, which abolished Eag-1 activity and inhibited cell growth. Inhibition of K<sub>v</sub> channels did not interfere with the ability of T<sub>84</sub> cells to regulate their cell volume, but restricted intracellular pH regulation. In addition, inhibitors of K<sub>v</sub> channels as well as siRNA for Eag-1 attenuated intracellular Ca<sup>2+</sup> signaling. The data suggest that K<sub>v</sub> channels control proliferation of colonic cancer cells by affecting intracellular pH and Ca<sup>2+</sup> signaling.

**Key words:** Eag, voltage-gated K<sup>+</sup> channels, colonic carcinoma cells, T<sub>84</sub>, proliferation, growth, Ussing chamber, patch clamp

## INTRODUCTION

Apart from their specific epithelial transport function, membrane ion channels are essential for maintaining cellular homeostasis and signaling. Thus they contribute to the control of essential parameters such as cell volume, intracellular pH and intracellular Ca<sup>2+</sup> concentration. K<sup>+</sup> selective ion channels form the largest ion channel protein family, which may be subdivided into voltage-gated, Ca<sup>2+</sup>-dependent, 2-pore domain, and inward rectifier K<sup>+</sup> channels. It has recently been suggested that in addition to the physiological parameters controlled by K<sup>+</sup> channels, they also affect mitotic cell cycling, proliferation and development of cancer. A role of K<sup>+</sup> channels for proliferation and tumor cell growth has been demonstrated for a number of carcinoma, like those of prostate, colon, lung, breast and others (Wang, 2004). K<sup>+</sup> channels of different subfamilies have been correlated with tumor proliferation, including Ca<sup>2+</sup>-activated K<sup>+</sup> channels, Shaker-type voltage-gated K<sup>+</sup> channels, the *ether à go-go* (Eag-1) family of voltage-gated K<sup>+</sup> channels and the 2P-domain K<sup>+</sup> channels (O'Grady and Lee, 2005, Pardo, 2004, Wang, 2004, Wonderlin and Strobl, 1996). It is not known currently, why different types of K<sup>+</sup> channels induce proliferation in the different cancer models. Most of the previous studies describe expression of a particular type of K<sup>+</sup> channel in a cancer cell line and correlate expression and functional activity of the channel with proliferation. However, mammalian cells always express a whole array of various types of K<sup>+</sup> channels, and it is not clear to what degree these individual K<sup>+</sup> channels contribute to proliferation, or if there is a specific association between particular K<sup>+</sup> channel subtypes and proliferation. Moreover the mechanisms by which these K<sup>+</sup> channels facilitate cell proliferation remain obscure.

Colonic carcinomas belong to the most frequent cancers in human. A previous study found a correlation between the activity of voltage-gated K<sup>+</sup> channels and proliferation and metastasis of a colonic cancer cell line and native colonic cancers, respectively (Abdul and Hoosein, 2002b, Lastraioli et al., 2004). Interestingly Ca<sup>2+</sup> influx into colonic cancer cells was affected by voltage-gated K<sup>+</sup> channels in one study (Abdul and Hoosein, 2002b). Identification of K<sup>+</sup> channels which are relevant for the growth of colonic carcinomas may provide novel therapeutic targets (Conti, 2004, Schonherr, 2005). Moreover, K<sup>+</sup> channels abnormally expressed in colonic cancer cells, could be potentially useful as markers for malign transformation. In the present study, we therefore screened T<sub>84</sub> colonic carcinoma cells for expression of a broad spectrum of K<sup>+</sup> channels. We then tried to identify the K<sup>+</sup> channels that have an impact on proliferation of these cells. Using a variety of K<sup>+</sup> channel blockers and siRNA, we found that voltage-gated K<sup>+</sup> channels take part in controlling cell proliferation, while other K<sup>+</sup> channel subtypes do not. A

further aim of this study was to uncover how these channels affect proliferation. The data suggest that voltage-gated K<sup>+</sup> channels control basic cellular properties like intracellular Ca<sup>2+</sup>, elicited by agonist stimulation of the cells, and regulation of the intracellular pH. Both effects are likely to be due to the hyperpolarizing effect of K<sub>v</sub> channels on the membrane voltage.

## MATERIAL AND METHODS

### *Cell culture and proliferation studies*

Human colorectal carcinoma epithelial T<sub>84</sub> cells (American Type Culture Collection, Rockville, MD, USA), were grown in DMEM/Ham's F-12 medium (1:1), supplemented with 10% fetal bovine serum (FBS), 2 mM glutamine, 100 U/ml penicillin and 100 µg/ml streptomycin (Pen/Strep) (GIBCO, Germany) in a 5% CO<sub>2</sub> atmosphere at 37°C. Cells were seeded on bovine plasma fibronectin (Invitrogen, Germany) and bovine dermal collagen (Cellon, Luxembourg) coated plastic dishes or glass cover slips. For proliferation assays, T<sub>84</sub> cells were plated at a density of 2000 cells / 0.35 cm<sup>2</sup> on coated 96 well plates (Sarstedt, Nürnberg, Germany). After 2 days, cells were incubated with inhibitors of potassium channels dissolved in serum reduced Opti-MEM 1 medium (GIBCO, Germany). After additional 2 days, cell proliferation was assessed by 5-bromo-2'-deoxyuridine (BrdU) incorporation and cell counting. BrdU incorporation was determined using an immunoassay cell proliferation ELISA kit (Roche, Germany), according to the manufacturer's protocol. For cell counting, cells were fixed with 3.7% formaldehyde and 0.5% Triton X-100 in ringer solution (mmol/l: NaCl 145; KH<sub>2</sub>PO<sub>4</sub> 0,4; K<sub>2</sub>HPO<sub>4</sub> 1,6; Glucose 5; MgCl<sub>2</sub> 1; Ca<sup>2+</sup>-Gluconate 1,3, pH 7.4) for 30 minutes and stained with Mayers Hemalaun (Merck, Darmstadt, Germany). Digital images were obtained and nuclei were counted using imaging software. Toxicity of the blockers was assessed by counting non-stained dead cells in the supernatants (Trypan Blue). Each experiment was performed in triplicate.

### *Expression of potassium channels in T<sub>84</sub> cells and real time PCR analysis*

Total RNA was isolated from T<sub>84</sub> cells using NucleoSpin RNA II columns (Macherey-Nagel, Germany). Total RNA (1 µg) was reverse transcribed for 1 h at 37°C using random primer and RT (M-MLV Reverse Transcriptase, Promega, Germany). RT-PCR was used to detect expression of the mRNAs for potassium channels. The oligonucleotide primers were designed for the mRNA of each gene product as follow

<i>name</i>	<i>gene</i>	<i>accession number</i>	<i>sense and antisense primer</i>	<i>size of PCR product (bp)</i>
K <sub>v</sub> 1.3	KCNA3	NM_002232	5'-GCCATCCTCTACTACTATCAG-3' 5'-CCACATGTCGATCAGGTTC-3'	532

<i>name</i>	<i>gene</i>	<i>accession number</i>	<i>sense and antisense primer</i>	<i>size of PCR product (bp)</i>
K <sub>v</sub> 1.5	<i>KCNA5</i>	NM_002234	5'- CTACTTCGACCCCCTGAG -3' 5'- GCTCGAAGGTGAACCAGATG -3'	555
K <sub>v</sub> LQT	<i>KCNQ1</i>	NM_000218	5'- CCACGGGGACTCTCTTCTG -3' 5'- GGCACCTTGTCCCCATAG -3'	504
K <sub>v</sub> 3.3 / K <sub>v</sub> 3.4	<i>KCNC3 / KCNC4</i>	NM_004977	5'- GACGTGCTGGGCTTCCTG -3' 5'- GCTTC TGCTTGGCCATGG -3'	442
K <sub>v</sub> 4.1	<i>KCND1</i>	NM_004979	5'- GGAAGAATACGCTGGACCG -3' 5'- GCGGCATGGGATGGTCTC -3'	472
K <sub>v</sub> 5.1	<i>KCNF1</i>	NM_002236	5'- GAGTCGTCGTGCCCCGGC -3' 5'- GTCTCTGGATGGCTCTGCTC -3'	530
K <sub>v</sub> 9.3	<i>KCNS3</i>	NM_002252	5'- GTGCAGCCTGATCTTCCTC -3' 5'- GTGTCAAACCTCTCCAGCTC -3'	540
Eag-1	<i>KCNH1</i>	NM_002238	5'- GCATGAACTACCTGAAGACG -3' 5'- CTTCTCAATGTCTG TGGATGG -3'	488
Erg-1	<i>KCNH2</i>	NM_000238	5'- CAATGCCAACGAGGAGGTG -3' 5'- GGAGAGACGTTGCCGAAG -3'	468
Elk-1	<i>KCNH8</i>	NM_144633	5'- GCCCGAACTGAAGTCATGC -3' 5'- CAAAATAAGCCAGTCCCAGC -3'	522
K <sub>ir</sub> 6.1	<i>KCNJ8</i>	NM_004982	5'- GTTTGGAGTCCACTGTGTGTG -3' 5'- CAGAATAACTATGACCTCCAAG -3'	548
TWIK1	<i>KCNK1</i>	NM_002245	5'- GCTTCGGCTTCCTGGTGC -3' 5'- GACAAACCCAAGGAGCACG -3'	505
TASK2	<i>KCNK5</i>	NM_009740	5'- GGCCATCACAGGGAACCAG -3' 5'- GCCAGGCC AGCCCCAAG -3'	496
TWIK2	<i>KCNK6</i>	NM_004823	5'- GATCTTTGCCACCTCGAG -3' 5'- GATGCTGGGAAACAAAGGAG -3'	520
BK channel α-subunit	<i>KCNMA1</i>	NM_002247	5'- GTGGATGAAAAGAGGAGGC -3' 5'- CAAATGGATGAACCCGGCTG -3'	528
BK channel β <sub>3</sub> -subunit	<i>KCNMB3</i>	NM_014407	5'- CGACCTGCACTGCCATCC -3' 5'- GGGCACC ACCTAGCAGAG -3'	398
BK channel β <sub>4</sub> -subunit	<i>KCNMB4</i>	NM_014505	5'- CCAGG TCTACGTGAACAAC -3' 5'- CTGTTGCCACTGAGGGATG -3'	520
SK4	<i>KCNN4</i>	NM_002250	5'- GATTTAGGGGCGCCGCTGAC -3' 5'- CTTGCCCCACATGGTGCCC -3'	520

The PCR reactions were performed at 94°C for 2 min, 35 cycles at 94°C for 30 sec, annealing temperature 60°C for 30 sec and 72°C for 1 min. PCR products were visualized by loading on agarose gels and were verified by sequencing.

Real-time PCR was performed in a Light Cycler (Roche, Germany), using the Quanti Tect SYBR Green PCR Kit (Quiagen, Germany). Each reaction contained 2 µl Master Mix (including Taq polymerase, DNTPs, SYBR Green buffer), 1 pM of each primer (Eag-1: 5'- GGAGTTCCA GACGGTGCAC -3', 5'- CCTCATCATCTTGGATCACC -3', 116 bp; β-actin, ACTB, NM 001101: 5'- CAACGGCTCCGGCATGTG -3', 5'- CTTGCTCTGGGCCTCGTC -3', 151 bp), 2.5 mM MgCl<sub>2</sub> and 2 µl cDNA. After 10 minutes at 94°C for activation of Taq polymerase, cDNA was amplified by 15 s at 94°C, 10 s at 60°C, and 20 s at 72°C, for 50 cycles. The amplification was

followed by a melting curve analysis to control of the PCR products. As negative controls, water instead of cDNA was run with every PCR experiment. To verify accuracy of the amplification, PCR products were further analyzed on ethidium bromide stained 2% agarose gels. Analysis of the data was performed using Light Cycler software 3.5.3. Standard curves for Eag-1 channel mRNA and  $\beta$ -actin mRNA were produced by using cDNA of 16HBE cells at different dilutions. The ratio of the amount of Eag-1 to  $\beta$ -actin mRNA was calculated for each sample.

#### *Downregulation of Eag-1 expression by small interfering RNA*

Duplexes of 21-nucleotide siRNA with 3'-overhanging TT were designed according to Ahn *et al* 2003 (Ahn *et al.*, 2003) and synthesized by IBA (Göttingen, Germany). The sense strand of the siRNA used to silence the Eag-1 gene was 5'-GACACGAUUGAAAAAGUGCTT-3', corresponding to positions 268-286 of the Eag-1 mRNA, relative to the start codon. The sense strand of the siRNA used to silence the potassium channel SK4 gene was 5'-GCGCUUGCUGGAGCAGGAGTT-3', corresponding to positions 48-66 of the SK4 mRNA relative to the start codon. A control siRNA oligonucleotide, Lmo2, designed to silence the LIM domain only 2 T-cell oncogenes (*Mus musculus*), has no target gene in T<sub>84</sub> cells and was used as a negative control for transfection. It had the sequence 5'-GCCAUCGACCAGUACUGGCTT-3' (positions 133-151 relative to the start codon) of the Lmo2 gene. Transfection of T<sub>84</sub> cells was carried out in Opti-MEM 1, one day after seeding using Oligofectamine (Invitrogen, Karlsruhe, Germany). After a 48 h rest, T<sub>84</sub> cells were used for proliferation assays, patch clamp, real time PCR and western blot.

#### *Detection of Eag-1 protein by Western blot*

Lysates of T<sub>84</sub> cells were resolved by 7% SDS-PAGE, transferred to Hybond-P (Amersham Biosciences, Germany) and incubated with mouse anti-K<sub>v</sub>10.1 (Eag-1) antibodies (alomone labs, Jerusalem, Israel). Proteins were visualized using a goat anti-mouse IgG conjugated to horseradish peroxidase (Acris Antibodies, Germany) and ECL Advance Detection Kit (Amersham Biosciences, Germany).

#### *Measurement of the intracellular Ca<sup>2+</sup> concentration, pH, cell volume and membrane potential*

T<sub>84</sub> cells were loaded with 2  $\mu$ M Fura-2 AM (Molecular Probes, USA) in Opti-MEM 1 medium with 2.5 mM probenecid (Sigma, Germany) for 1 h at room temperature. For fluorescence measurements of the intracellular Ca<sup>2+</sup> concentration [Ca<sup>2+</sup>]<sub>i</sub>, cells were perfused with ringer solution containing 2.5 mM probenecide (Sigma, Deisenhofen, Germany) at 37°C. Fluorescence was measured continuously using an inverted microscope IMT-2 (Olympus, Nürnberg, Germany) and a high speed polychromator system (VisiChrome, Visitron Systems, Germany).

Fura-2 was excited at 340/380 nm and emission were recorded between 470 and 550 nm using a CCD camera (CoolSnap HQ, Visitron Systems, Puchheim, Germany).  $[Ca^{2+}]_i$  was calculated from the ratio of 340/380 nm fluorescence values (after subtraction of background fluorescence). The formula used for calculation of  $[Ca^{2+}]_i$  was  $[Ca^{2+}]_i = K_d \times (R - R_{min}) / (R_{max} - R) \times (S_{f2}/S_{b2})$  where  $R$  is the observed fluorescence ratio. The values  $R_{max}$ ,  $R_{min}$  (maximum and minimum ratios) and the constant  $S_{f2}/S_{b2}$  (fluorescence of free and  $Ca^{2+}$ -bound fura-2 at 380 nm) were calculated using 2  $\mu$ mol/l ionomycin (free acid, Calbiochem, Merck Biosciences, Bad Soden, Germany), 5  $\mu$ mol/l nigericin (Sigma, Germany), 10  $\mu$ mol/l monensin (Sigma, Deisenhofen, Germany) and 5 mmol/l EGTA to equilibrate intracellular and extracellular  $Ca^{2+}$  in intact fura-2-loaded cells. The dissociation constant for the fura-2- $Ca^{2+}$  complex was taken as 224 nmol/l.

For assessment of intracellular pH, cells were incubated in standard bath solution (mM: 145 NaCl, 0.4  $KH_2PO_4$ , 1.6  $K_2HPO_4$ , 5 glucose, 1  $MgCl_2$ , 1.3 Ca-gluconate, pH 7.4) containing 8  $\mu$ M BCECF-AM and 0.05 % Pluronic for 30 - 60 min at room temperature (RT). For cell volume measurements  $T_{84}$  cells were loaded with 2.5  $\mu$ M calcein-AM and 0.025 % Pluronic in standard bath solution for 30 - 60 min at RT. Excitation wavelengths of 488/440 and 500 nm were used for BCECF and calcein loaded cells, respectively. Emission wavelengths were > 520 nm for BCECF fluorescence and 520-550 nm for calcein fluorescence. We screened for the effect of  $K^+$  channel blockers on the membrane voltage, using the voltage sensitive dye FMP (Baxter et al., 2002). Cells were incubated with FMP (FLIPR Membrane Potential Assay Kit, Molecular Devices, Ismaning, Germany) in ringer solution at room temperature. FLIPR was excited with 485 nm and emission was detected between 515 and 560 nm. All experiments were controlled and analyzed using the software package Meta-Fluor (Universal imaging, USA). All optical filters and dichroic mirrors were from AHF (Tübingen, Germany).

#### *Patch clamp*

Cell culture dishes were mounted on the stage of an inverted microscope (IM35, Zeiss) and kept at 37 °C. The bath was perfused continuously with Ringer solution at about 10 ml/min. Patch-clamp experiments were performed in the fast whole-cell configuration. Patch pipettes had an input resistance of 2-4 M $\Omega$ , when filled with a solution containing (mM) KCl 30, K-gluconate 95,  $NaH_2PO_4$  1.2,  $Na_2HPO_4$  4.8, EGTA 1, Ca-gluconate 0.758,  $MgCl_2$  1.034, D-glucose 5, ATP 3. pH was adjusted to 7.2, the  $Ca^{2+}$  activity was 0.1  $\mu$ M. The access resistance was measured continuously during the recordings and was 8.3-14.2 M $\Omega$ . Currents (voltage clamp) and voltages (current clamp) were recorded using a patch-clamp amplifier (EPC 7, List Medical Electronics, Germany), the LH1600 interface and PULSE (HEKA, Germany) and Chart (AD-Instruments,

Germany) software. In regular intervals, membrane voltages ( $V_c$ ) were clamped in steps of 10 mV from -50 to +50 mV relative to resting potentials. The membrane conductance  $G_m$  was calculated from the measured current ( $I$ ) and  $V_c$  values, according to Ohm's law.

#### *Materials and statistical analysis*

All compounds used were of highest available grade of purity. 4-AP, TPeA, astemizole, calciseptine, EIPA, carbachol, quinidine, and terfenadine were all from Sigma (Deisenhofen, Germany). BDS-I, charybdotoxin, and iberiotoxin were from Alamone labs (Jerusalem, Israel). Clotrimazole was from Calbiochem (Merck Biosciences, Bad Soden, Germany). Scyllatoxin was from Latoxan (Valence, France). TRAM-34 was a generous gift by Dr. H. Wulff (Department of Medical Pharmacology and Toxicology, University of California Davis, San Francisco, USA). 293B, AVE0118 and AVE1231 were gifts from Aventis Pharma (Frankfurt, Germany). All other chemicals were obtained from Merck (Darmstadt, Germany). The acetomethyl ester (2',7')-bis(carboxyethyl)-5(6)-carboxyfluorescein (BCECF-AM), calcein (calcein-AM), Fura2-AM and Pluronic were all from Molecular Probes (U.S.A.). Student's t-test (for paired or unpaired samples as appropriate) and analysis of variance (ANOVA) was used for statistical analysis.  $P < 0.05$  was accepted as significant.

## **RESULTS**

#### *Expression of cancer related K<sup>+</sup> channels in T<sub>84</sub> colonic carcinoma cells*

We broadly screened T<sub>84</sub> cells for expression of K<sup>+</sup> channels, based on previous reports indicating a role of K<sup>+</sup> channels for proliferation of cancer cells (database SAGEmap of the Cancer Genome Anatomy Project, <http://cgap.nci.nih.gov>, (Lal et al., 1999) and recent publications. RT-PCR detected transcripts of a number of voltage-gated (K<sub>v</sub>) K<sup>+</sup> channels (Figure 1A). Moreover, the ATP sensitive K<sup>+</sup> channels K<sub>ir</sub>6.1 and the two-pore (2P)-domain K<sup>+</sup> channels TWIK1, TWIK2 and TASK2 are expressed in T<sub>84</sub> cells (Figure 1B). Although, transcripts of the  $\alpha$ -subunit of the large conductance Ca<sup>2+</sup> sensitive (BK) channel could not be detected, the two  $\beta$ -subunits  $\beta$ 3 and  $\beta$ 4 are expressed in these cells, along with intermediate conductance Ca<sup>2+</sup>-activated SK4 K<sup>+</sup> channels (Figure 1C). Taken together, several K<sup>+</sup> channels are expressed in T<sub>84</sub> colonic carcinoma cells, which may potentials support cell proliferation.

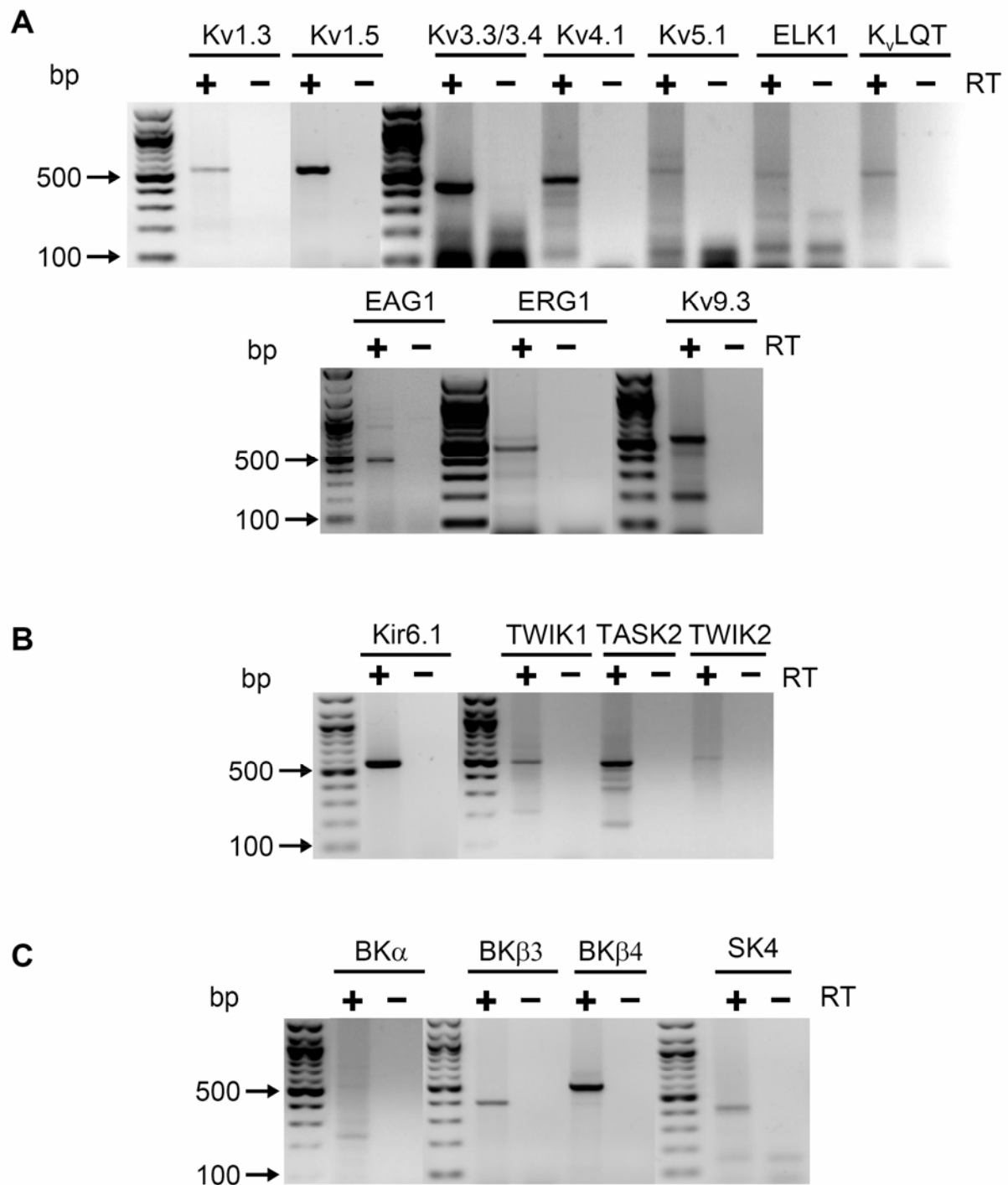


**Figure 1.** Expression of K<sup>+</sup> channels in T<sub>84</sub> cells. Expression of (A) voltage-gated (K<sub>v</sub>3.3/3.4, K<sub>v</sub>4.1, K<sub>v</sub>5.1, Elk1, K<sub>v</sub>LQT1, Eag-1, K<sub>v</sub>9.3), (B) inward rectifier (K<sub>ir</sub>6.1), two pore domain (TWIK1, TASK2, TWIK2), and (C) large (BK $\beta$ 3, BK $\beta$ 4) and small (SK4) conductance Ca<sup>2+</sup>-activated K<sup>+</sup> channels, after reverse transcription (RT).



**Table 1.** Inhibition of T<sub>84</sub> cell proliferation by K<sup>+</sup> channel blocker.

<i>Inhibitor</i>	<i>Blocked channels</i>	<i>Concentration</i>	<i>BrdU incorporation</i>	<i>cell number</i>
			(% of control)	(% of control)
293B	K <sub>v</sub> LQT	10 μM	79.0 ± 4.9 (3)*	88.0 ± 1.3 (3)*
		1 μM	79.3 ± 1.4 (3)*	90.8 ± 0.5 (3)*
		0.1 μM	80.7 ± 2.5 (3)*	97.1 ± 0.9 (3)
		0.01 μM	82.2 ± 5.1 (3)	99.7 ± 1.4 (3)
		0.001 μM	84.6 ± 5.9 (3)	99.3 ± 1.3 (3)
4-AP	K <sub>v</sub> channels	2 mM	72.2 ± 8.1 (3)*	73.8 ± 3.4 (5)*
		1 mM	84.4 ± 5.9 (4)	80.5 ± 3.5 (5)*
		0.5 mM	89.6 ± 0.2 (3)	83.2 ± 3.9 (5)*
		0.05 mM	88.1 ± 4.0 (4)	87.2 ± 3.5 (5)
		0.005 mM	92.8 ± 3.2 (5)	92.6 ± 2.1 (5)
Astemizole	Eag-1, Elk, Erg	5 μM	83.5 ± 5.1 (7)*	81.5 ± 2.1 (8)*
		0.5 μM	84.3 ± 3.0 (6)*	85.1 ± 2.7 (7)*
		0.05 μM	90.3 ± 2.8 (7)	88.5 ± 1.0 (9)*
		0.005 μM	91.3 ± 3.1 (7)	91.4 ± 1.1 (9)*
		0.5 nM	94.1 ± 3.1 (6)	96.5 ± 1.0 (8)
AVE0118	K <sub>v</sub> 1.5, 4.3, 2.1, 3.1	50 μM	67.6 ± 8.1 (5)*	60.0 ± 4.3 (5)*
		5 μM	76.1 ± 7.4 (4)	80.7 ± 2.4 (4)*
		0.5 μM	86.5 ± 4.2 (4)	82.4 ± 1.2 (5)*
		0.05 μM	89.1 ± 7.2 (4)	87.1 ± 2.3 (5)*
		0.005 μM	94.8 ± 7.3 (4)	93.4 ± 2.4 (6)
AVE1231	K <sub>v</sub> 1.5, 4.3, 2.1, 3.1	50 μM	59.7 ± 7.8 (3)*	61.6 ± 3.1 (3)*
		5 μM	89.9 ± 2.3 (4)	80.8 ± 1.6 (3)*
		0.5 μM	92.7 ± 1.0 (3)	85.2 ± 2.0 (3)*
		0.05 μM	95.0 ± 1.2 (4)	86.9 ± 0.2 (3)*
		0.005 μM	100.4 ± 0.6 (4)	95.0 ± 1.8 (3)
Charybdotoxin	BK, SK4, K <sub>v</sub> 1.3	100 nM	79.7 ± 4.5 (3)*	89.2 ± 3.1 (3)
		10 nM	87.8 ± 3.6 (3)	92.3 ± 2.3 (3)
		1 nM	89.2 ± 3.8 (3)	92.3 ± 1.7 (3)
		0.1 nM	91.5 ± 4.2 (3)	95.9 ± 1.5 (3)
		0.01 nM	91.4 ± 2.3 (3)	97.3 ± 6.1 (3)
Clotrimazole	SK4	1 μM	84.9 ± 7.7 (3)	79.1 ± 6.4 (3)
		0.1 μM	92.6 ± 6.4 (3)	80.5 ± 6.0 (3)
		0.01 μM	99.0 ± 6.9 (3)	86.0 ± 7.6 (3)
		0.001 μM	94.8 ± 10.1 (3)	88.9 ± 4.8 (3)
		10 nM	93.0 ± 4.2 (3)	76.4 ± 11.2 (3)
Iberiotoxin	BK	1 nM	93.5 ± 4.3 (4)	85.3 ± 9.8 (3)
		0.1 nM	96.0 ± 5.0 (4)	86.3 ± 9.8 (3)
		0.01 nM	94.2 ± 1.4 (4)	94.1 ± 4.8 (3)
		0.001 nM	96.7 ± 8.2 (4)	97.8 ± 4.5 (3)
		10 nM	89.8 ± 8.6 (3)	110.7 ± 13.1 (3)
Scyllatoxin	SK-family	1 nM	99.6 ± 7.7 (3)	108.8 ± 12.9 (3)
		0.1 nM	97.2 ± 5.6 (3)	103.5 ± 1.3 (3)
		0.01 nM	96.1 ± 2.6 (3)	105.8 ± 4.2 (3)
		0.001 nM	102.8 ± 4.6 (3)	117.6 ± 10.4 (3)
		100 nM	89.7 ± 3.8 (3)	94.0 ± 3.4 (3)
TRAM-34	SK4	10 nM	94.5 ± 3.0 (3)	93.2 ± 6.1 (3)
		1 nM	90.5 ± 3.1 (3)	95.8 ± 3.8 (3)
		0.1 nM	94.7 ± 1.4 (3)	93.0 ± 0.5 (3)

\* Significant difference when compared to control (ANOVA). Experiments were performed in triplicates, and numbers of different experiments are given in parentheses.

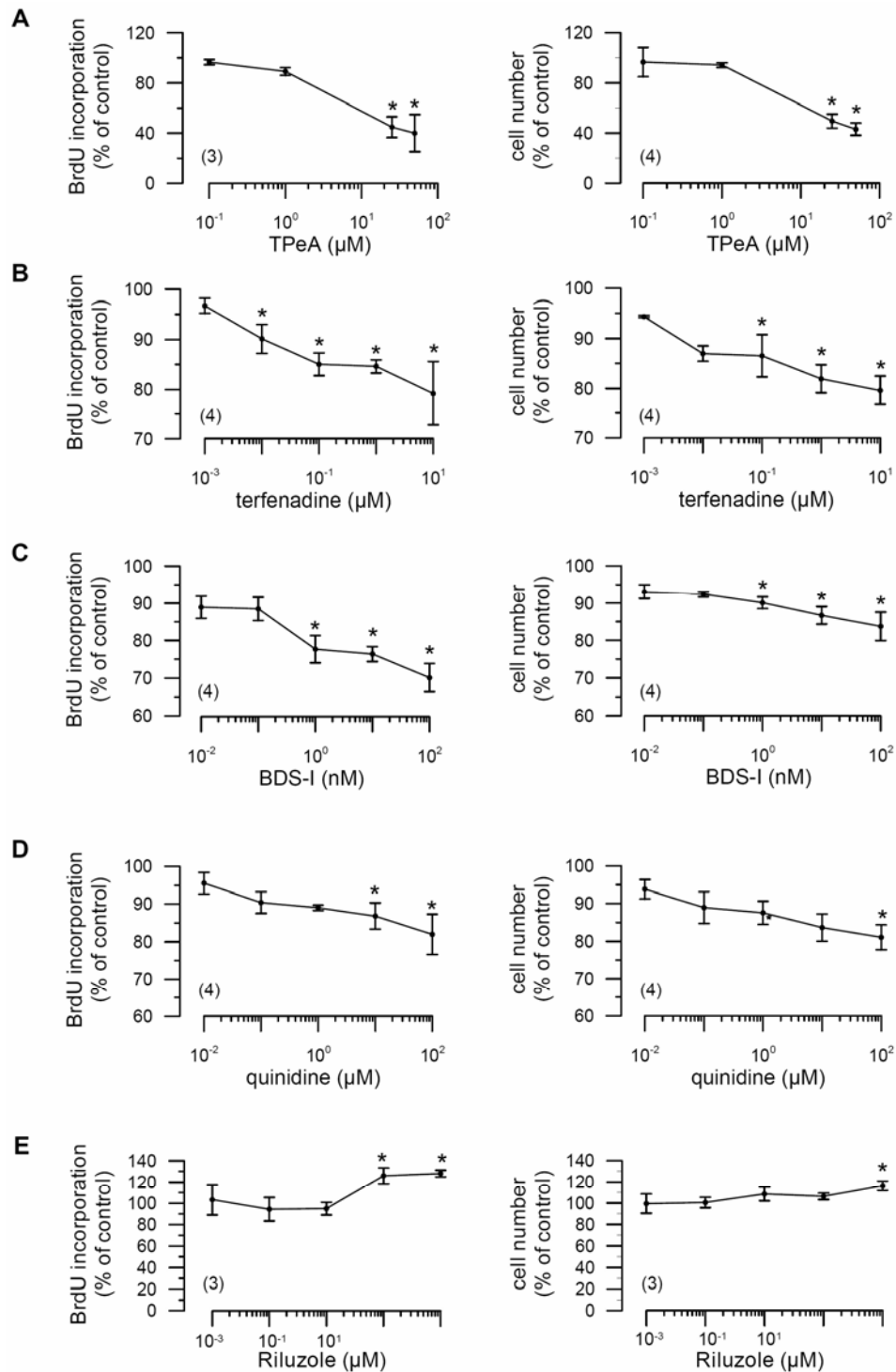


**Figure 2.** Inhibition of proliferation of T<sub>84</sub> cells by K<sub>v</sub> channel blockers. Cell proliferation of T<sub>84</sub> cells was assessed by BrdU incorporation and cell counting. The K<sup>+</sup> channel blockers TPeA (A), terfenadine (B), BDS-I (C), and quinidine (D) caused dose dependent inhibition of proliferation. E) Additional activation of SK4 channels by riluzole further enhanced proliferation. Asterisks indicate significant differences when compared to control (ANOVA). Experiments were carried out in triplicates. (number of experiments).

*Inhibition of T<sub>84</sub> cell proliferation by blockage of K<sub>v</sub> channels*

In order to identify K<sup>+</sup> channels which affect cell proliferation, we used a variety of inhibitors (Table 1, Figure 2 and 3). Cell proliferation was assessed independently, by quantifying DNA replication (BrdU incorporation) and by cell counting. Potential toxicity of the K<sup>+</sup> channel blockers was assessed by trypan blue staining. At the concentrations used in this study, the channel inhibitors caused no toxic effects on T<sub>84</sub> cells. Concentration dependent inhibition of cell proliferation was found for the non-selective K<sub>v</sub> channel blockers TPcA and Quinidine (Grace and Camm, 1998, Patel et al., 2000), for the toxin inhibitor BDS-1, which blocks K<sub>v</sub>3.4 channels (Diochot et al., 1998), and for the Eag-1 blocker terfenadine (Garcia-Ferreiro et al., 2004) (Figure 2A-D). Other K<sub>v</sub> inhibitors such as 4-AP (5  $\mu$ M - 2 mM), AVE0118 or AVE1231 (0.5 nM - 50  $\mu$ M) and the K<sub>v</sub>LQT blocker 293B (1 nM - 10 $\mu$ M) also inhibited cell proliferation, albeit at higher concentrations (Table 1). Inhibitors of Ca<sup>2+</sup>-activated K<sup>+</sup> channels, such as charybdotoxin, clotrimazole, iberiotoxin, scyllatoxin and TRAM-34 did not affect proliferation (Table 1). Thus, Ca<sup>2+</sup>-activated K<sup>+</sup> channels do not seem to support proliferation. Surprisingly, activation of SK4 channels by riluzole (Cao et al., 2002) enhanced proliferation (Figure 2E). These experiments suggest that only endogenous K<sub>v</sub> channel activity supports proliferation of T<sub>84</sub> colonic carcinoma cells, however, when up-regulated other K<sup>+</sup> channels such as intermediate conductance SK4 channels may also enhance proliferation. Endogenous K<sub>v</sub> channels not only support proliferation of T<sub>84</sub> cells, but also that of other colonic cell lines, like HT<sub>29</sub>. Proliferation of HT<sub>29</sub> cells was inhibited between 60-80% (n = 4) by 4-AP and astemizole. Moreover, K<sub>v</sub> channels have been identified recently in human and murine colonic cancers (unpublished observations).

*K<sub>v</sub> channels are active in colonic carcinoma cells*

We screened for the effects of K<sup>+</sup> channel blockers in a fluorescence based assay, using the voltage sensitive dye FMP. After loading of the cells with FMP, the K<sub>v</sub> channel blocker 4-AP (50  $\mu$ M) enhanced fluorescence intensity, due to depolarization of the membrane voltage. The effects of individual blockers were analyzed as fraction of the effect of BaCl<sub>2</sub> (5 mM), which induced maximal depolarization. The largest changes were observed for the K<sub>v</sub> channel blockers 4-AP (50  $\mu$ M), quinidine (10  $\mu$ M), terfenadine (10  $\mu$ M) and astemizole (5  $\mu$ M). This demonstrates a contribution of K<sub>v</sub> channels to the overall K<sup>+</sup> conductance in T<sub>84</sub> cells (Figure 3A, right panel). K<sup>+</sup> channel blockers were also applied in whole cell patch clamp experiments. The blockers were used at lower concentration range, in order to achieve best specificity. As shown in Figure 3B and C, K<sup>+</sup> channel blockers had small but significant effects on whole cell conductance and

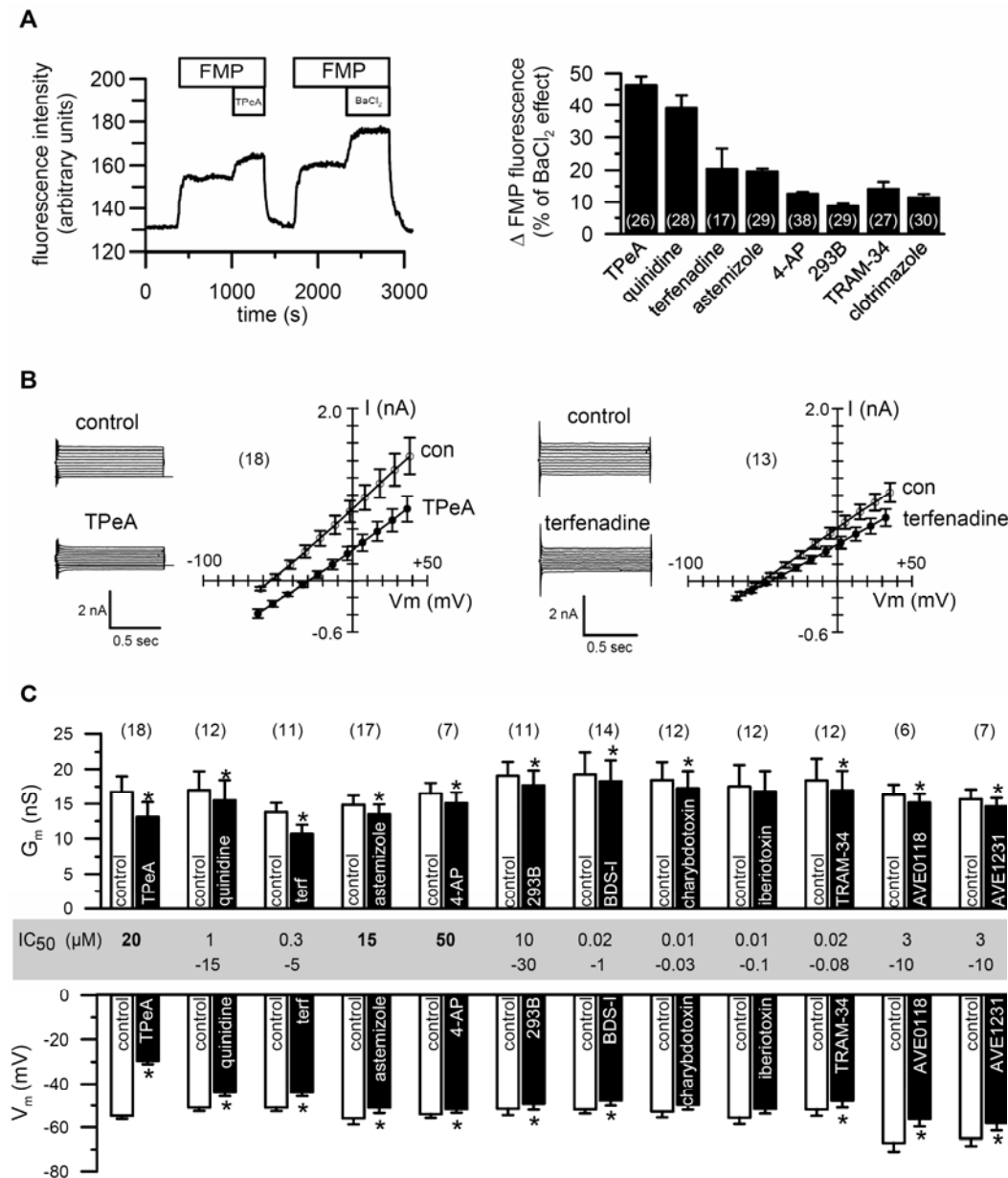


**Figure 3.** Effects of K<sub>v</sub> channel blockers on membrane voltage whole cell conductance. A) Uptake of the voltage-sensitive fluorescence dye FMP. Loading of T<sub>84</sub> cells with FMP induced fluorescence. 4-AP (50 μM) further increased fluorescence intensity due to depolarization of V<sub>m</sub>. BaCl<sub>2</sub> (5 mM) completely inhibited K<sup>+</sup> channels, thereby inducing maximal depolarization and further fluorescence increase. The right panel shows the summary of the effects of the K<sup>+</sup> channel blockers TPeA (50 μM), quinidine (10 μM), terfenadine (10 μM), astemizole (5 μM), 4-AP (50 μM), 293B (10 μM), TRAM-34 (100 nM) and clotrimazole (100 nM) on FMP fluorescence, relative to the effects of BaCl<sub>2</sub>. B) Effect of TPeA and terfenadine on whole cell currents obtained in T<sub>84</sub> cells and summary I/V curves in the absence or presence of the inhibitor. C) Summary of the effects of the K<sup>+</sup> channel blockers on whole cell conductance and membrane voltage, at concentrations as indicated above. Concentrations for the other inhibitors were: BDS-I (10 nM), charybdotoxin (100 nM), iberiotoxin (10 nM), AVE0118 (10 μM) and AVE1231 (10 μM). IC<sub>50</sub> values were determined experimentally (in bold) or were obtained from literature. Asterisks indicate significant differences when compared to control (paired Student's *t*-test). (number of experiments).

membrane voltage ( $V_m$ ). Blockers were typically applied in the presence of Ringer solution; however, similar effects were also observed when blockers were examined in the presence of culture medium (Opti-MEM 1), i.e. under proliferation assay conditions (data not shown). Taken together K<sub>v</sub> channels contribute only ~10-15% to the total membrane conductance, which is sufficient to support proliferation of T<sub>84</sub> cells. Similar has been observed in previous studies (Kunzelmann, 2005).

#### *Down-regulation of Eag-1 inhibits proliferation*

Proliferation of T<sub>84</sub> cells may be supported by a number of different K<sub>v</sub> channels. Although patch clamping and expression studies suggested a dominant role of Eag channels, we used siRNA-Eag-1 to specifically downregulate expression of Eag-1 protein. Quantitative analysis of gene expression using real-time PCR, indicated a significant loss of Eag-1 transcripts after treatment with siRNA-Eag-1 and reduced Eag-1 expression was verified by Western blotting (Figure 4A). We found that downregulation of Eag-1 expression inhibited proliferation, while mock transfection, unrelated siRNA (for Lmo2 oncogene) or siRNA inhibition of the Ca<sup>2+</sup>-activated K<sup>+</sup> channel SK4 did not reduce cell proliferation (Figure 4B). In the FMP fluorescence assay we found a reduced effect of astemizole (5  $\mu$ M) on membrane voltage, i.e. FMP uptake ( $\Delta$ FMP) (Figure 4C). Along this line suppression of astemizole sensitive Eag-1 conductance was detected in whole cell patch clamp experiments. In contrast TRAM-34 sensitive SK4 conductance was eliminated by siRNA-SK4, which had no impact on proliferation of T<sub>84</sub> cells (Figure 4D). Taken together, endogenous Eag-1 currents control proliferation of T<sub>84</sub> colonic carcinoma cells, while endogenous SK4 currents are not relevant for cell growth.

#### *K<sub>v</sub> channels control regulation of intracellular pH and Ca<sup>2+</sup> signaling, but not cell volume*

K<sub>v</sub> channels contribute to the negative membrane voltage, which may be crucial for volume and pH regulation, as well as proper Ca<sup>2+</sup> signaling particularly during cell cycling (Kahl and Means, 2003, Kunzelmann, 2005, Wakabayashi et al., 1997, Wonderlin and Strobl, 1996). We therefore asked if K<sub>v</sub> channels enhance proliferation by affecting cell volume or pH regulation, or by supporting intracellular Ca<sup>2+</sup> signaling. T<sub>84</sub> cells were swollen by removing 120 mmol/l mannitol (Hypo), or were shrunk by adding 120 mmol/l mannitol (Hyper) to an isotonic Ringer solution. Swelling and shrinkage was assessed by changes in calcein fluorescence (Figure 5A). Repetitive exposure to hypotonic bath solution produced identical changes in cell volume (n=41, data not shown). Cell swelling was not different in the presence or absence of K<sub>v</sub> channel

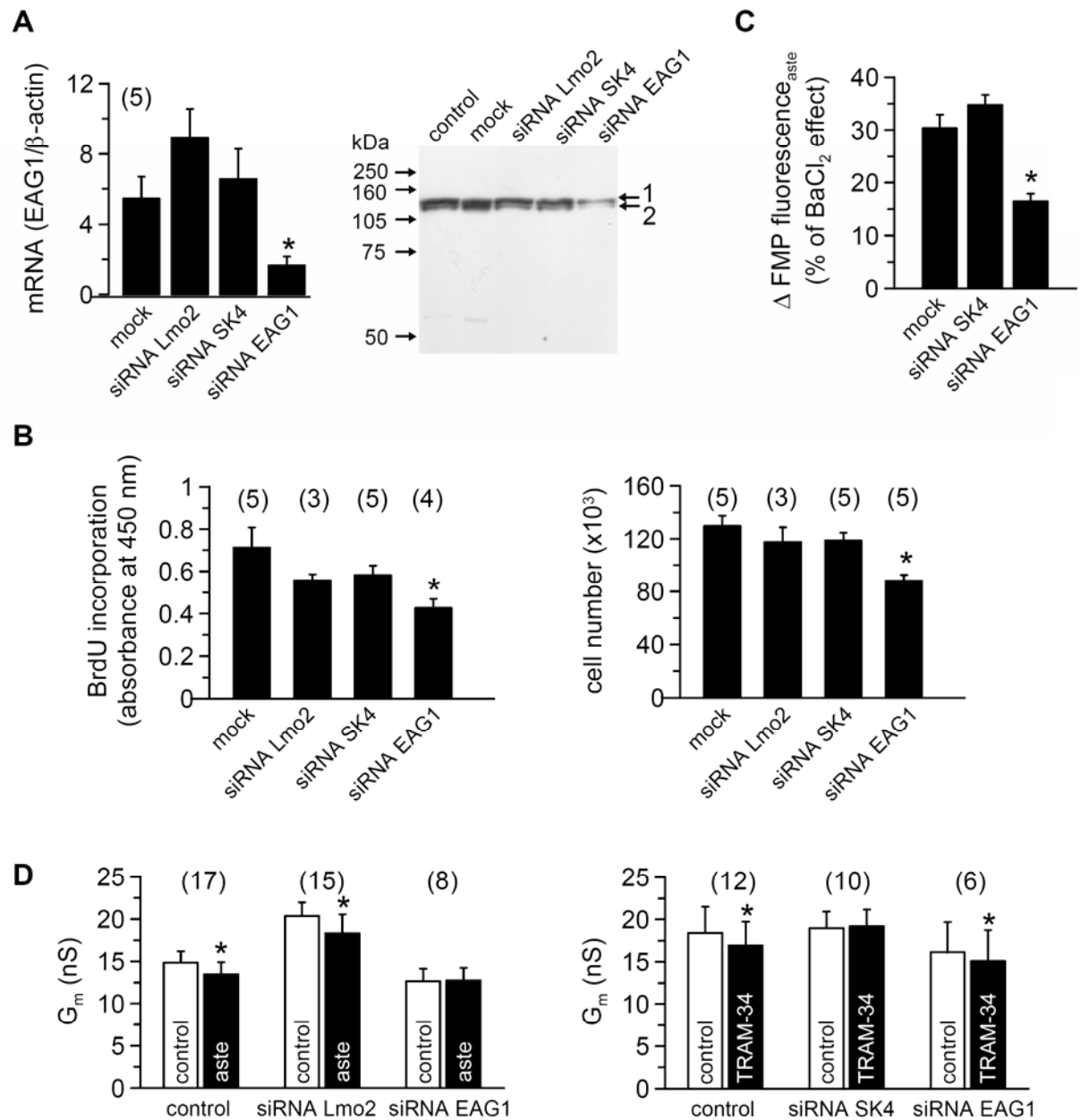


**Figure 4.** Downregulation of Eag-1 inhibits cell proliferation and astemizole sensitive currents. A) Suppression of Eag-1-mRNA and protein in T<sub>84</sub> cells by siRNA-Eag-1 but not by unrelated siRNA (Lmo2; SK4), or in mock transfected cells. B) Inhibition of cell proliferation by siRNA-Eag-1, but not by unrelated control siRNA. C) Reduced astemizole sensitive FMP fluorescence ( $\Delta$ FMP) in siRNA-Eag-1 transfected cells, but not in control cells. D). siRNA-Eag-1 abolished astemizole sensitive  $G_m$  (left panel). In contrast, siRNA-SK4 abolished TRAM-34 sensitive  $G_m$  (right panel) which, however, did not affect proliferation of T<sub>84</sub> cells (shown in B). Asterisks indicate significant difference when compared to control (ANOVA, Student's *t*-test). Proliferation assays were carried out in triplicates. (number of experiments).

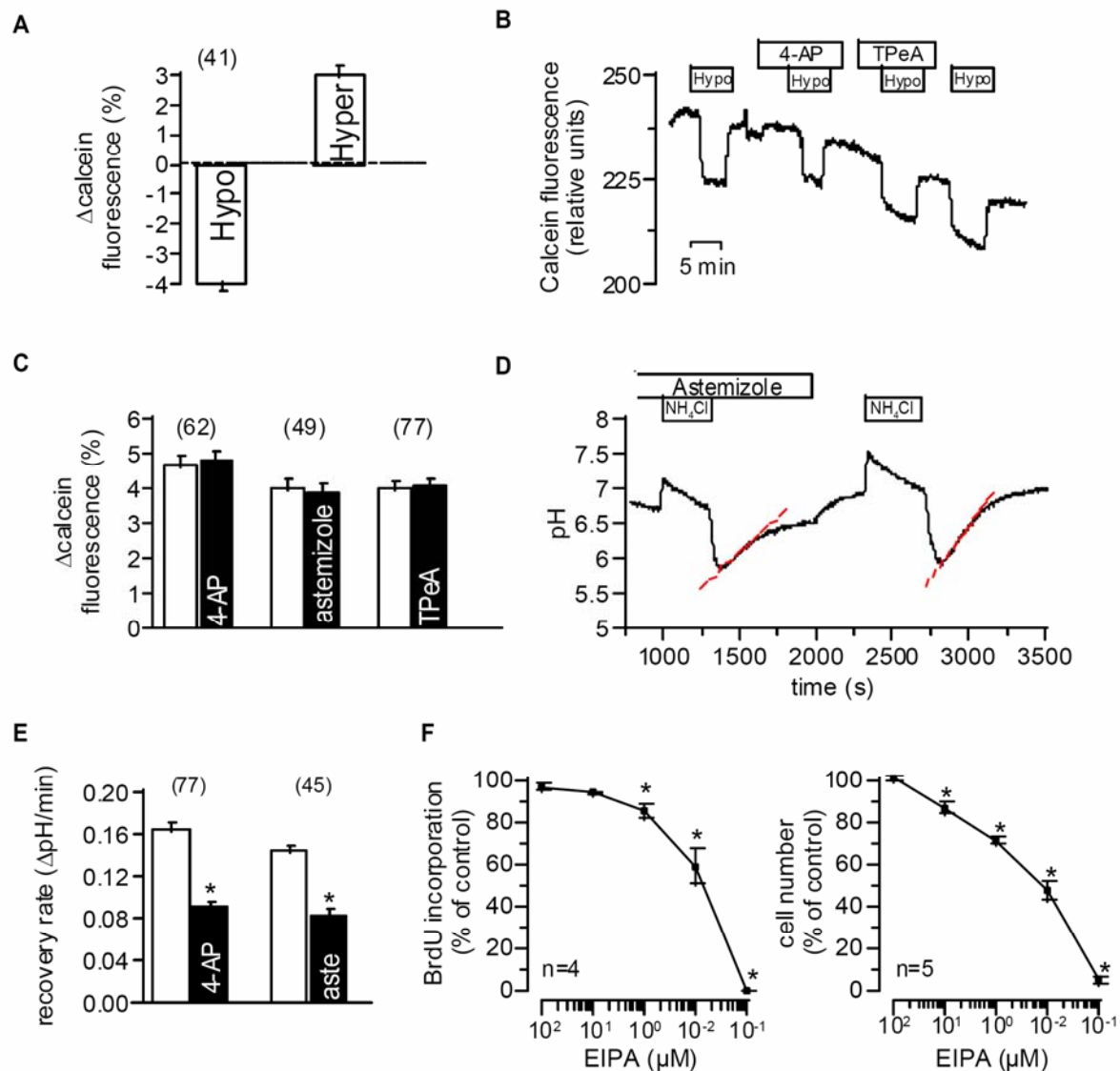


**Figure 5.** K<sub>v</sub> channels affect pH regulation but not cell swelling. A) T<sub>84</sub> cells were swollen (removal of 120 mmol/l mannitol; Hypo) or shrunken (adding 120 mmol/l mannitol; Hyper), as assessed by changes in calcein fluorescence. Repetitive exposure to hypotonic bath solution produced identical changes in cell volume (n = 41, data not shown). B) K<sub>v</sub> channel inhibitors 4-AP or TPeA did not affect cell swelling. C) Summary of the effects of 4-AP, astemizole and TPeA on cell swelling, as measured by calcein fluorescence. D) Original recording of intracellular pH and effect of astemizole on pH recovery from acid (NH<sub>4</sub>Cl) load. E) Summary of the effects of 4-AP and astemizole on pH recovery after acid load. F) Effect of the NHE1- inhibitor EIPA on cell proliferation. Asterisks indicate significant difference when compared to control (Student's *t*-test). (number of experiments).

blockers (Figure 5B, C). We further examined if pH recovery from an acid (NH<sub>4</sub>Cl; 20 mM) load and thus regulation (recovery) of intracellular pH is affected by inhibitors of K<sub>v</sub> channels. To that end cells were acid loaded using a NH<sub>4</sub>Cl pulse. The slope for initially recovery from cellular acidification was determined in the absence or presence of K<sub>v</sub> channel blockers. Repetitive

acidification under control condition showed similar recovery of the intracellular pH ( $n = 62$ , data not shown). Recordings of the intracellular pH and the summary for the recovery rates demonstrate impaired pH regulation in T<sub>84</sub> cells when exposed to the K<sub>v</sub> channel blockers 4-AP or astemizole (Figure 5 D, E). These results indicate that K<sub>v</sub> channels are important for pH regulation in colonic carcinoma cells. pH recovery is primarily due to the function of the Na<sup>+</sup>/H<sup>+</sup> exchanger NHE (Kunzelmann, 2005, Schreiber, 2005). In fact, blockage of NHE by 5-(N-Ethyl-N-Isopropyl) amiloride (EIPA) inhibited proliferation of T<sub>84</sub> cells (Figure 5F).

We further examined potential effects of K<sub>v</sub> channels on intracellular Ca<sup>2+</sup> signaling. As shown in Figure 6, baseline intracellular Ca<sup>2+</sup> in resting cells was not affected by K<sub>v</sub> channel inhibitors. We stimulated T<sub>84</sub> cells with the muscarinic secretagogue carbachol (CCH, 100  $\mu$ M). This induced a release of Ca<sup>2+</sup> from intracellular stores (transient peak response) and a subsequent influx through store operated Ca<sup>2+</sup> channels (Ca<sup>2+</sup> plateau) (original traces in Figure 6). Both Ca<sup>2+</sup> peak and plateau were significantly reduced in the presence of the non-selective K<sub>v</sub> blockers 4-AP (50  $\mu$ M) and TPcA (5  $\mu$ M) (Figure 6A). Similar effects on [Ca<sup>2+</sup>]<sub>i</sub> were observed with the Eag-1 inhibitor astemizole (0.5  $\mu$ M) and the K<sub>v</sub>3.4 blocker BDS-I (10 nM) (Figure 6). Moreover, inhibition of Eag-1 expression by siRNA also attenuated Ca<sup>2+</sup> signaling, while siRNA-suppression of SK4 had no effects on the carbachol induced Ca<sup>2+</sup> signaling (Figure 6B, C). The contribution of K<sup>+</sup> channels to Ca<sup>2+</sup> signaling was further confirmed by the nonselective K<sup>+</sup> channel inhibitor Ba<sup>2+</sup>, which also attenuated Ca<sup>2+</sup> signaling T<sub>84</sub> cells (data not shown). Taken together, K<sub>v</sub> channels affect intracellular Ca<sup>2+</sup> signaling probably by their hyperpolarizing effects which provides a driving force for Ca<sup>2+</sup> release and influx through store operated Ca<sup>2+</sup> channels (SOCs) (Fischer et al., 1996, Kazerounian et al., 2005). Although upregulation of voltage-gated Ca<sup>2+</sup> channels (VOCC) in T<sub>84</sub> cells has been reported previously (Wang et al., 2000), they are probably of limited importance for proliferation since we did observe any impact of the VOCC inhibitor calciseptine had no effect on proliferation (Figure 7A). Moreover, agonist (carbachol) induced Ca<sup>2+</sup> signaling was not affected by calciseptine in either T<sub>84</sub> or HT<sub>29</sub> cells (Figure 7B, C).

## DISCUSSION

### *K<sup>+</sup> channels and cancer*

Several types of K<sup>+</sup> channels have been detected in human cancers (Kunzelmann, 2005). Ca<sup>2+</sup>-activated K<sup>+</sup> channels were found in prostate cancer (Abdul and Hoosein, 2002a), uterine cancer (Suzuki and Takimoto, 2004b), human gliomas (Patt et al., 2004), gastric cancer (Elso et al., 2004) pituitary adenomas (Czarnecki et al., 2003) and colorectal cancer (Abdul and Hoosein,



2002a, Lastraioli et al., 2004, Yao and Kwan, 1999). In other tumors proliferation is supported by ATP sensitive K<sub>ir</sub> channels or two-pore (2P)-domain channels (Klimatcheva and Wonderlin, 1999, Mu et al., 2003b, Patel and Lazdunski, 2004). Nevertheless, in the majority of cancer

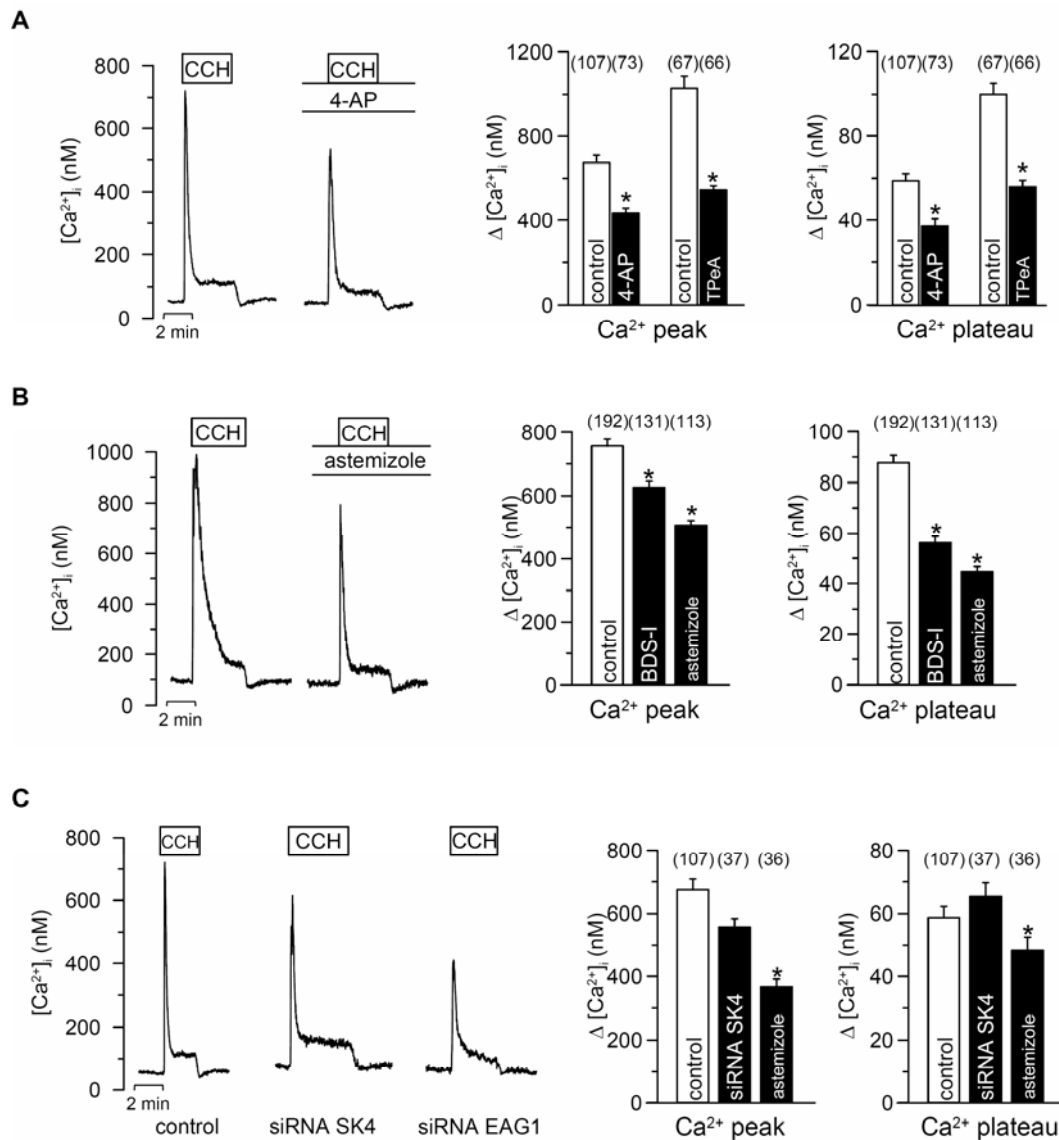


**Figure 6.** K<sub>v</sub> channels affect carbachol induced Ca<sup>2+</sup> signaling. A) Original recordings of  $[Ca^{2+}]_i$  in fura-2 loaded T<sub>84</sub> cells and effects of carbachol (CCH; 100  $\mu$ M) and 4-AP on transient (store release; peak) and persistent (influx; plateau) Ca<sup>2+</sup> increase. Right panel: Summary of the effects of 4-AP (50  $\mu$ M) and TPpA (5  $\mu$ M) on Ca<sup>2+</sup> peak and plateau. B) Original recordings of the effects of carbachol and astemizole. Right panel: Summary of the effects of BDS-I (10 nM) and astemizole (0.5  $\mu$ M) on Ca<sup>2+</sup> peak and plateau. C) Original recordings of the effects of carbachol on control cells and cells treated with siRNA-Eag-1 or siRNA-SK4. Right panel: Summary of the effects of siRNA-Eag-1 or siRNA-SK4 on Ca<sup>2+</sup> peak and plateau. Asterisks indicate significant difference when compared to control (ANOVA, Student's *t*-test). (number of experiments).

cells, K<sub>v</sub> channels were correlated to proliferation (Abdul and Hoosein, 2002b, Abdul and Hoosein, 2002c, Chang et al., 2003, Farias et al., 2004b, O'Grady and Lee, 2005, Pardo et al., 1999, Pardo, 2004). Other data from human biopsies and carcinogen treated mice suggest high levels of Eag-1 protein in colonic cancers, which is not observed in the native colon (unpublished observation). Also in the present study we found a role of K<sub>v</sub> channels for proliferation of cultured colonic carcinoma cells. Thus, the results obtained in T<sub>84</sub> cells may be representative for the changes that occur in the native colon during carcinogenesis.

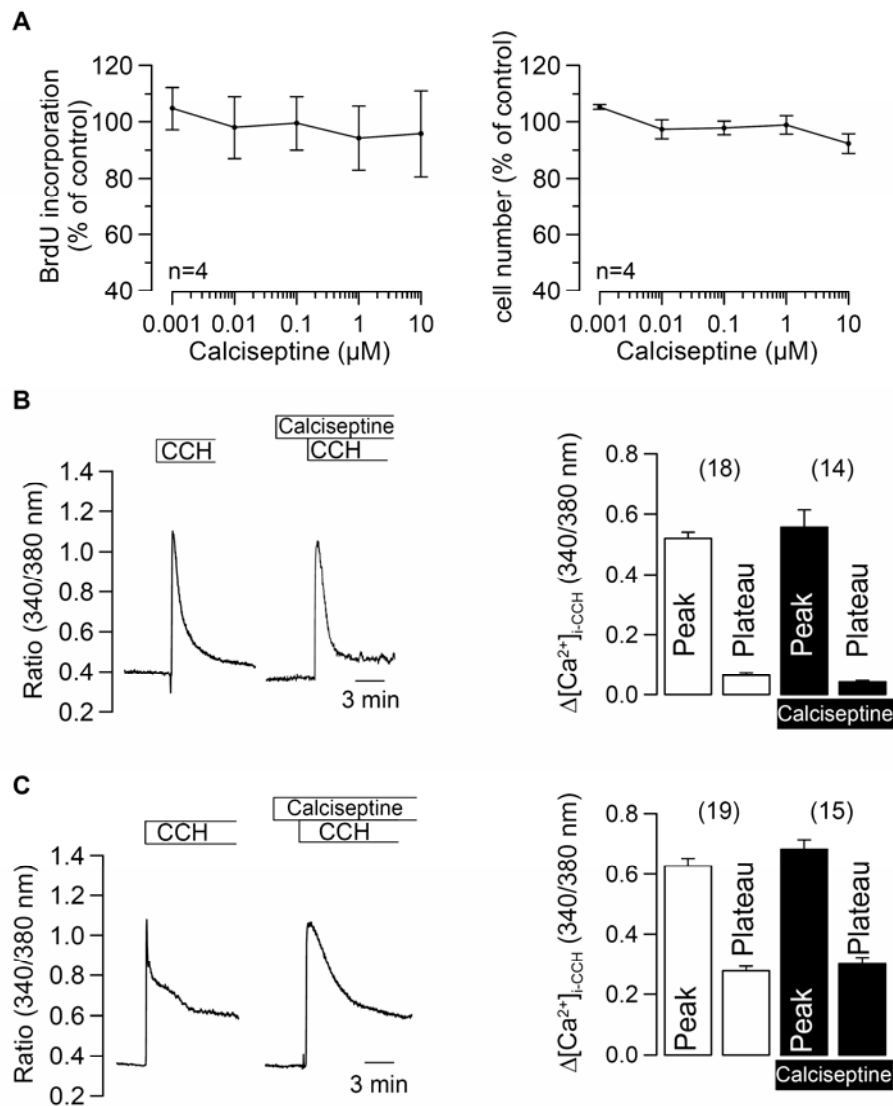


**Figure 7.** Voltage-gated Ca<sup>2+</sup> channels do not affect proliferation or Ca<sup>2+</sup> signaling in colonic cancer cells. A) Cell proliferation of T<sub>84</sub> cells was not affected by the inhibitor of L-type Ca<sup>2+</sup> channels, calciseptine. Carbachol (CCH, 100 μM) induced Ca<sup>2+</sup> increase in T<sub>84</sub> (B) or HT<sub>29</sub> (C) cells was not affected by calciseptine. (number of experiments).

*K<sub>v</sub> but not other K<sup>+</sup> channels control proliferation in T<sub>84</sub> cells*

K<sub>v</sub> channels operate at rather depolarized membrane voltages ( $V_m$ ), which are typically not found in terminally differentiated epithelial cells (O'Grady and Lee, 2005, Pardo, 2004). The depolarized  $V_m$  of carcinoma cells provides the basis for activation of K<sub>v</sub> channels (Arcangeli et al., 1995). When studied under proliferative conditions, serum containing culture medium depolarizes  $V_m$  (Peres et al., 1988). *In vivo*, cells are exposed to 20-30 g/l protein present in the interstitial fluid, which may depolarize  $V_m$  and allow for activation of K<sub>v</sub> channels in carcinoma cells *in situ* (Rutili and Arfors, 1977). Remarkably the contribution of K<sub>v</sub> channels to the overall conductance in T<sub>84</sub> cells was only 10-15%. However, this is in line with previous reports, which indicate that pro-proliferative K<sup>+</sup> currents are often of smaller amplitude, while large K<sup>+</sup> currents are detected during apoptosis (Kunzelmann, 2005, Lang et al., 2004).

Because of the limited specificity of most K<sup>+</sup> channel inhibitors (Elbashir et al., 2001), we also used siRNA to identify the K<sup>+</sup> channels in charge of cell proliferation. Only K<sub>v</sub> channels appear to affect cell proliferation, although other K<sup>+</sup> channels are expressed and functional in T<sub>84</sub> colonic carcinoma cells, such as SK4 channels. Obviously EAG-1 and other K<sub>v</sub> channels operate well in proliferating T<sub>84</sub> cells, while SK4 channels only support proliferation after additional activation by riluzole. Surprisingly, even the K<sup>+</sup> ionophore valinomycin increased proliferation of T<sub>84</sub> cells when applied at very low (100 fM) concentrations (unpublished data from the author's laboratory). We suggest that the oncogenic potential of K<sub>v</sub> channels is linked to the K<sup>+</sup> channel function. This has been demonstrated recently for TASK3 channels (Pei et al., 2003). In principle, any type of K<sup>+</sup> channel may be able to support proliferation, depending on additional cell specific properties that determine K<sup>+</sup> channel activity.

*How do K<sub>v</sub> channels control cell proliferation?*

The present study was performed to determine the mechanism by which K<sup>+</sup> channels affect cell growth. Progression through the cell cycle is dependent on K<sup>+</sup> channels and blocking of these channels causes inhibition of proliferation (Wonderlin and Strobl, 1996). This clearly suggests a cell cycle specific function of K<sup>+</sup> channels. Apart from this specific role, K<sub>v</sub> channels may also have homeostatic functions in T<sub>84</sub> cells. The present data demonstrate an impact of K<sub>v</sub> channels on intracellular Ca<sup>2+</sup> signaling and pH regulation. The importance of pH<sub>i</sub> for cell proliferation and cancer development is well established (Wakabayashi et al., 1997). pH<sub>i</sub> is varying during the cell cycle and need to be tightly controlled, probably by the Na<sup>+</sup>/H<sup>+</sup> exchanger NHE1 (Schreiber, 2005). The experiments with the NHE-blocker EIPA presented here, clearly show the importance of NHE for cell proliferation. Na<sup>+</sup>/H<sup>+</sup> exchange requires low intracellular Na<sup>+</sup> concentrations, and

V<sub>m</sub> need to stay hyperpolarized, Both is facilitated by the Na<sup>+</sup>/K<sup>+</sup>-ATPase in parallel with K<sup>+</sup> channels. K<sub>v</sub> channels may provide a K<sup>+</sup> recycling pathway and hyperpolarize the membrane voltage, and may thus contribute indirectly to pH regulation.

Equally important is the control of intracellular Ca<sup>2+</sup> in proliferating cells, especially during the mitotic cell cycle (Schreiber, 2005). We found that agonist induced Ca<sup>2+</sup> release and influx of Ca<sup>2+</sup> through SOCs, depends on the function of K<sub>v</sub> channels. Thus Ca<sup>2+</sup> dependent activation of ion currents was reduced significantly by  $3.2 \pm 0.5$  nA (100  $\mu$ M 4-AP, n=4) and  $2.8 \pm 0.4$  nA (5  $\mu$ M astemizole, n=5). It has been demonstrated by others (Fischer et al., 1996) that depolarization of the membrane voltage reduces Ca<sup>2+</sup> signaling. Since inhibitors of K<sub>v</sub> channels depolarize V<sub>m</sub>, this may explain why Ca<sup>2+</sup> signaling is affected. Furthermore, a previous study demonstrated that activation of store operated Ca<sup>2+</sup> Channels (SOCs) in T<sub>84</sub> cells induces proliferation (Kazerounian et al., 2005). Moreover, capacitative Ca<sup>2+</sup> influx through SOCs is reduced at acidic pH (Nitschke et al., 1996). Since K<sub>v</sub> channels also affect intracellular pH, this may provide an independent mechanism, by which K<sub>v</sub> channels affect intracellular Ca<sup>2+</sup> signaling. Voltage-gated Ca<sup>2+</sup> channels (VOCC) are probably not related to the effects of K<sub>v</sub> channel inhibitors, although L-type Ca<sup>2+</sup> channels are expressed in T<sub>84</sub> colonic carcinoma cells (Wang et al., 2000). This is further substantiated by the fact that the L-type Ca<sup>2+</sup> channel inhibitor calciseptine did not reduce proliferation or Ca<sup>2+</sup> signaling (Figure 7). Taken together hyperpolarization of V<sub>m</sub> by K<sub>v</sub> channels may be necessary to maintain pH regulation and Ca<sup>2+</sup> signaling, which allows progression through the G<sub>1</sub> phase of the cell cycle (Kahl and Means, 2003, Wonderlin and Strobl, 1996).

## CHAPTER 4

### Expression of voltage-gated potassium channels in human and mouse colonic carcinoma

#### ABSTRACT

**Purpose:** Voltage-gated  $K_v$  potassium channels like *ether à go-go* (Eag) channels have been recognized for their oncogenic potential in breast cancer and other malignant tumors.

**Experimental design:** We examined the molecular and functional expression of  $K_v$  channels in human colonic cancers and colon of mice treated with the chemical carcinogens dimethylhydrazine and N-methyl-N-nitrosourea. The data were compared with results from control mice and animals with chemically induced DSS colitis.

**Results:** Electrogenic salt transport by amiloride-sensitive  $Na^+$  channels and cyclic AMP-activated cystic fibrosis transmembrane conductance regulator  $Cl^-$  channels were attenuated during tumor development and colitis, while  $Ca^{2+}$ -dependent transport remained unchanged.  $K_v$  channels, in particular Eag-1 were enhanced during carcinogenesis. Multiplex reverse transcription-PCR showed increased mRNA expression for  $K_v1.3$ ,  $K_v1.5$ ,  $K_v3.1$  and members of the Eag channel family, after dimethylhydrazine and N-methyl-N-nitrosourea treatment. Eag-1 protein was detected in the malignant mouse colon and human colonic cancers. Genomic amplification of Eag-1 was found in 3.4% of all human colorectal adenocarcinoma and was an independent marker of adverse prognosis.

**Conclusions:** The study predicts an oncogenic role of  $K_v$  and Eag channels for the development of colonic cancer. These channels may represent an important target for a novel pharmacotherapy of colonic cancer.

**Key words:** DMH, MNU, DSS, voltage-gated  $K^+$  channel,  $K_v$  channel, Eag related  $K^+$  channel, colonic cancer

## INTRODUCTION

Membrane ion channels are essential for cell proliferation and have a role in the development of cancer. A substantial body of evidence exists that voltage-gated potassium ( $K_v$ ) channels have an oncogenic function (Camacho, 2006, Kunzelmann, 2005, Pardo, 2004, Pardo et al., 2005). Moreover, during carcinogenesis changes in expression or activity of ion channels may affect electrolyte transport properties in epithelia, similar to the changes observed during inflammation (Kunzelmann, 2005).  $K^+$  channels are involved in the development of cancer of prostate, colon, lung and breast (Kunzelmann, 2005, Wonderlin and Strobl, 1996).  $K^+$  channels were identified in different cancer tissues, such as  $Ca^{2+}$ -activated and voltage-gated  $K^+$  channels ( $K_v$  channel), the *ether à go-go* (Eag) family and 2P-domain  $K^+$  channels (Kunzelmann, 2005). However,  $K_v$  channels seem to play a central role in tumor cells, particularly in those of epithelial origin (Kunzelmann, 2005, Pardo, 2004, Pardo et al., 2005). Cell cycle-regulated Eag-1 channels, normally only expressed in excitable tissues and oocytes are also found in cancer cells (Camacho, 2006, Farias et al., 2004b, Pardo et al., 1999). Activation of these channels induces hyperpolarization of the plasma membrane, which may be essential for cell proliferation (Pardo, 2004). Hyperpolarization of the membrane voltage facilitates  $Ca^{2+}$  signaling, and is necessary for regulation of intracellular pH and cell volume. All of these variables ( $Ca^{2+}$ , pH, and volume) clearly affect cell proliferation (Kunzelmann, 2005, Pardo, 2004, Schreiber, 2005).

Most studies on the oncogenic role of ion channels have been done in cell lines, leaving open their relevance for tumor development *in vivo*. We therefore designed the present study to examine the role of ion channels for tumor development *in vivo* in carcinogen-treated mice. Dimethylhydrazine (DMH) and N-methyl-N-nitrosourea (MNU) were used as carcinogenic agents. DMH is organotropic for the rodent colon. It is metabolized to methylazoxymethanol and methyldiazonium and causes methylation of nucleotides (Fiala, 1977). Rectal application of MNU causes direct alkylation of DNA and also induces colonic tumors (Frei et al., 1978, Narisawa et al., 1976). During the development of colon cancer, alterations in colonic electrolyte transport have been reported in previous studies (Bleich et al., 1997, Davies et al., 1987). Electrolyte transport appears to be affected in the premalignant colon, which may contribute to the irregularities in defecation, often observed in patients with human colonic cancer. We found that electrolyte transport was affected in colitis and during carcinogenesis. However, overexpression of cell cycle regulated Eag-1  $K^+$  channels was only found in the pre-malignant mouse colon and in human colonic cancers.

## MATERIAL AND METHODS

### *Patients, tumor material for fluorescence in situ hybridization analysis, biological samples*

Three hundred eighty-six surgically resected colorectal adenocarcinomas were selected from the files of the Institutes of pathology of the University of Basel and from the Triemli Hospital, Zürich, Switzerland. Tissue microarray was constructed as previously described (Kononen et al., 1998). Specimens were kept anonymous, and experiments were conducted according to the guidelines of the ethical committee of the University of Basel. Pathologic tumor-node metastasis stage was determined according to the International Union Against Cancer. Colon biopsies were obtained from patients hospitalized at the Children's Hospital of the University of Freiburg/Germany and the department of Internal Medicine of the University of Regensburg, according to the guidelines of the local ethical committee.

### *DMH, MNU, and DSS treatment*

Animal studies were conducted according to the guidelines of the National Institute of Health guidelines for the care and use of animals in research and the German laws on protection of animals. C57BL/6NCrl mice were obtained from Charles River (Sulzfeld, Germany). DMH or control saline were dissolved in 0.9% saline and injected s.c. into the groin at a dose of 40 mg/kg once a week for 5 wks. Proximal and distal colons were removed for RNA and protein isolation, histology and functional measurements. For MNU treatment, mice were anaesthetized by i.p. injection of ketamine/xylazine (120 mg/8 mg/kg  $\times$  bodyweight). MNU (2.6 mg/0.4 ml 0.9% NaCl solution) was given intrarectally twice a week for 2 weeks and once a week for additional 4 weeks. For potential difference measurements, a catheter (PE-10 tubing) containing ringer solution was inserted 2 cm into the rectum and perfused continuously at a rate of 1 ml/h. The catheter was attached via an agar bridge to an AgCl<sup>-</sup> electrode. A s.c. needle positioned in the abdomen and connected via an agar bridge served as the reference electrode. For DSS treatment of BALB/cOlaHsd mice, 3 % DSS was added to drinking water for 7 to 10 days.

### *Histology*

Mice were sacrificed under CO<sub>2</sub> inhalation; the colon was removed and stripped mechanically from submucosal tissues. Tissues were fixed for 20 min with 4% paraformaldehyde, 0.1% glutaraldehyde, 15% picric acid in PBS (pH 7.4) followed by a 12 h incubation in 4% paraformaldehyde, 15% picric acid in PBS (pH 7.4) at 4°C. Tissues were washed in PBS and incubated in 10%, 20% and 30% sucrose solutions, dehydrated and embedded in paraffin. Paraffin-embedded tissues were cut with a rotary microtome (Leica Mikrotom RM 2165, Wetzlar, Germany). Sections were dewaxed and rehydrated and stained with hematoxylin and eosin.

Some tissues were chock frozen in iso-pentan, sectioned at 5  $\mu\text{m}$ , fixed with 4% paraformaldehyde in PBS (pH 7.4) and stained with hematoxylin.

#### *Ussing chamber experiments*

Stripped colon was put into ice cold bath solution (mM: NaCl 145,  $\text{KH}_2\text{PO}_4$  0.4,  $\text{K}_2\text{HPO}_4$  1.6, d-glucose 6,  $\text{MgCl}_2$  1, Ca-gluconate 1.3, pH 7.4) containing amiloride (20  $\mu\text{M}$ ) and indomethacin (10  $\mu\text{M}$ ). Tissues were mounted into an Ussing chamber with a circular aperture of 0.785  $\text{mm}^2$ . Luminal and basolateral sides of the epithelium were perfused continuously at a rate of 5 ml/min. Bath solutions were heated to 37°C, using a water jacket. Experiments were carried out under open-circuit conditions. Data were collected continuously using PowerLab (Spechbach, Germany). Values for transepithelial voltages ( $V_{\text{te}}$ ) were referred to the serosal side of the epithelium. Transepithelial resistance ( $R_{\text{te}}$ ) was determined by applying short (1 sec) current pulses ( $\Delta I = 0.5 \mu\text{A}$ ).  $R_{\text{te}}$  and equivalent short circuit currents ( $I_{\text{SC}}$ ) were calculated according to Ohm's law ( $R_{\text{te}} = \Delta V_{\text{te}} / \Delta I$ ,  $I_{\text{SC}} = V_{\text{te}} / R_{\text{te}}$ ).

#### *Crypt cell isolation and expression analysis of ion channels in colonic epithelial cells*

Colonic crypts were isolated from an inverted colon in  $\text{Ca}^{2+}$  free buffer solution. Total RNA was prepared from isolated crypts (NucleoSpin, Macherey-Nagel, Düren, Germany). After reverse transcription, semiquantitative multiplex reverse transcription-PCR was done. The primers as shown below were used.

Primer	Accession no.	Sense(s) and antisense(as) primer
mK <sub>v</sub> 1.3	NM_008418	5'-GTACTTTGACCCACTCCGC-3' (s) 5'-GCAAGCAAAGAACCGCACCC-3' (as)
mK <sub>v</sub> 1.5	NM_145983	5'-GCTACTTCGATCCCTTGAG-3' (s) 5'-GCTCAAAAGTGAACCAGATC-3' (as)
mK <sub>v</sub> 3.1	NM_008421	5'-CCAGACGTACCGCTCGAC-3' (s) 5'-CGAACAGCGCCCAGATGC-3' (as)
mEag-1	NM_010600	5'-GGATTCTGCAAGCTGTCTG-3' (s) 5'-GTAGAAGGTCAGGATCAAG-3' (as)
hEag-1	NM_172362, NM_002238	5'-CGCATGAACCTGAAGACG-3' (s) 5'-TCTGTGGATGGGGCGATGTTC-3' (as)
mErg-1	NM_172057	5'-CCTCGACACCATCATCCGC-3' (s) 5'-GTCCGCACAGATGATTCCC-3' (as)
mElk-1	NM_001031811	5'-GGTTTCCCCATAGTCTACTG-3' (s) 5'-CAAATGAGCCAGTCCCAGC-3' (as)
mENaC $\alpha$	NM_011324	5'-CCTTGACCTAGACCTTGACG-3' (s) 5'-CGAATTGAGGTTGATGTTGAG-3' (as)
mENaC $\beta$	NM_000336	5'-CAATAACACCAACACCCACG-3' (s) 5'-GAGAAGATGTTGGTGGCCTG-3' (as)
mENaC $\gamma$	NM_011326	5'-GCACCGACCATTAAAGGACC-3' (s) 5'-GCCTTTCCCTTCTCGTTCTC-3' (as)
mCFTR	NM_021050	5'-GAATCCCCAGCTTATCCACG-3' (s) 5'-CTTCAACCATCATCTTCCCTAG-3' (as)



PCR reactions were performed at 94°C for 2 min, 28 to 38 cycles at 94°C for 30 s, annealing temperature 56°C for 30 s, and 72°C for 1 min using GoTaq DNA Polymerase (Promega, Mannheim, Germany). Expression of mRNA of each gene product was normalized against  $\beta$ -actin expression.

#### *Detection of Eag-1 protein*

Isolated crypt cells from distal and proximal colon were lysed and total protein (50  $\mu$ g) was resolved by 7% SDS-PAGE, transferred by semi-dry blotting to Hybond-P (Amersham, Freiburg, Germany) and incubated with rabbit anti-K<sub>v</sub>10.1 (Eag-1, Alomone labs, Jerusalem, Israel) and rabbit anti-actin antibodies (Sigma, Taufkirchen, Germany). Proteins were visualized using a goat anti-rabbit IgG conjugated to horseradish peroxidase (Acris Antibodies, Hiddenhausen, Germany) and Enhanced Chemiluminescence Advance Detection kit (Amersham). Signals were detected by Fluor-S<sup>TM</sup> Multimager system (Bio-Rad Laboratories, Hercules, CA) and analyzed with Multi-Analyst software (Bio-Rad). Expression of Eag-1 protein was normalized against actin protein expression.

#### *Fluorescence in situ hybridization (FISH) analysis*

The bacterial artificial chromosome RP11-75i2, containing parts of the Eag-1 gene sequence at 1q32.2-3, was obtained from the German Resource Centre for Genome Research (Berlin, Germany). One microgram of purified plasmid DNA was labelled using a modified Bio Nick kit (Invitrogen, Carlsbad, CA). Nick translation was performed at 16°C for 90 min. The labeled FISH probe was purified by precipitation and redissolved in 50  $\mu$ l H<sub>2</sub>O. Paraffin removal (3 x 5min in Xylene followed by 2 x 2min ethanol 95% and air-drying) and enzymatic tissue pretreatment (Vysis pretreatment solution, 80°C, 15 min) of tissue sections mounted on glass slides was performed in a VP2000 Processor device (Vysis, Downers Grove, IL). A premixed hybridization cocktail containing 0.5  $\mu$ l centromere 1 probe (CEP 1 SpectrumOrange labeled; Vysis), 1.5  $\mu$ l Eag-1 probe, 1  $\mu$ l Cot DNA (Invitrogen), and 7  $\mu$ l hybridization buffer (Vysis) was added to each slide with denatured target DNA. Probes were allowed to hybridize overnight at 37°C in a humidified chamber. After washing steps, Eag-1 probe was detected using the Dig detection kit (Roche Diagnostics, Indianapolis, IN). Amplification was defined as a signal ratio of Eag-1 probe / centromere 1 of at least 2 and at least 4 gene signals.

#### *Materials and statistical analysis*

All used compounds were of highest available grade of purity. DMH, MNU, amiloride, 4-aminopyridine, astemizole, carbachol, and 3-isobutyl-1-methylxanthine (IBMX) were from Sigma-Aldrich (Taufkirchen, Germany). DSS was from ICN (Eschwege, Germany). Forskolin and 293B

were gifts from Aventis Pharma (Frankfurt, Germany). Student's t-test (for paired or unpaired samples as appropriate) and analysis of variance (ANOVA) were used for statistical analysis.  $P < 0.05$  was accepted as significant. Survival curves were plotted according to Kaplan-Meier. A log-rank test was applied to examine the relationship between alterations clinicopathological data or Esg-1 amplification status and overall survival. Patients were censored at the time of their last clinical control. Cox proportional hazard model with stepwise selection of the covariates was used to determine the parameters with greatest influence on the risk of recurrence and progression.

## RESULTS

### *Histopathology*

From week 12 on, DMH-treated animals showed a significantly reduced weight increase. MNU-treated mice also showed a reduced body weight and a growth delay compared to untreated mice. Frequently the animals developed diarrhea upon treatment with carcinogens. Six to eight weeks after DMH treatment, local mucosal infiltration of leucocytes indicated inflammatory processes in distal colon (Figure 1A and B). After 10 and 12 weeks changes of mucosal architecture such as tortuous crypts and crypt loss were observed in distal colon (Figure 1C). No obvious histological changes were found in the proximal colon. Rectal MNU application 4 times in 2 weeks induced hyperplastic crypts in distal colon, indicated by an increase of crypt heights and decreased number of goblet cells along the cryptal wall. Moreover nuclear to cytoplasmic ratio was increased (Figure 1D). Cellular redistribution and nuclear accumulation of  $\beta$ -catenin was not clearly correlated with carcinogen treatment and was therefore not used as an independent marker for carcinogenesis (data not shown). Mucosal infiltration by inflammatory cells was observed in the proximal colon. After 8 treatments (week 6), extension of the lamina submucosea and muscularis submucosea, and dysplasia of distal colonic mucosa were observed. Administration of DSS caused severe changes of the tissue architecture, ulceration, and inflammatory cell infiltration, areas of complete epithelial denudation as well as submucosal edema in distal and proximal colon. Thus, inflammation and carcinogenesis induced by chemicals is clearly demonstrated by histological changes.

### *DMH, MNU and DSS treatment inhibits $\text{Na}^+$ absorption and $\text{Cl}^-$ secretion*

In essence, electrogenic ion transport in the colon is due to  $\text{Na}^+$  absorption by amiloride sensitive  $\text{Na}^+$  channels (ENaC) and cyclic AMP- or  $\text{Ca}^{2+}$ -induced  $\text{Cl}^-$  and  $\text{K}^+$  secretion. The amount of electrogenic  $\text{Na}^+$  absorption is determined by inhibition with amiloride and calculation

of the amiloride sensitive short circuit current  $I_{SC \text{ Amil}}$  (Figure 2A). DMH treatment reduced  $I_{SC \text{ Amil}}$  in distal colon 6 and 8 weeks after the first DMH injection, which recovered at week 10 and 12 (Figure 2A and B). Similar effects on amiloride-sensitive  $\text{Na}^+$  absorption were seen in MNU-treated mice. Rectal potential difference measurements *in vivo* after 2 and 6 weeks of MNU treatment showed a reduced rectal potential different due to attenuate amiloride-sensitive transport (Figure 2C). Ussing chamber experiments and  $I_{SC}$  measurements confirmed reduced  $\text{Na}^+$  absorption in distal colon of MNU-treated mice ( $19.6 \pm 4.3 \mu\text{A}/\text{cm}^2$ ;  $n = 11$ ), when compared to control mice ( $57.8 \pm 9.6 \mu\text{A}/\text{cm}^2$ ;  $n = 13$ ) (Figure 2D). In addition, in the inflamed colon, during treatment with DSS, amiloride-sensitive rectal potential different was significantly reduced from  $-7.2 \pm 0.58 \text{ mV}$  ( $n = 7$ ) to  $-4.9 \pm 0.73 \text{ mV}$  ( $n = 10$ ).

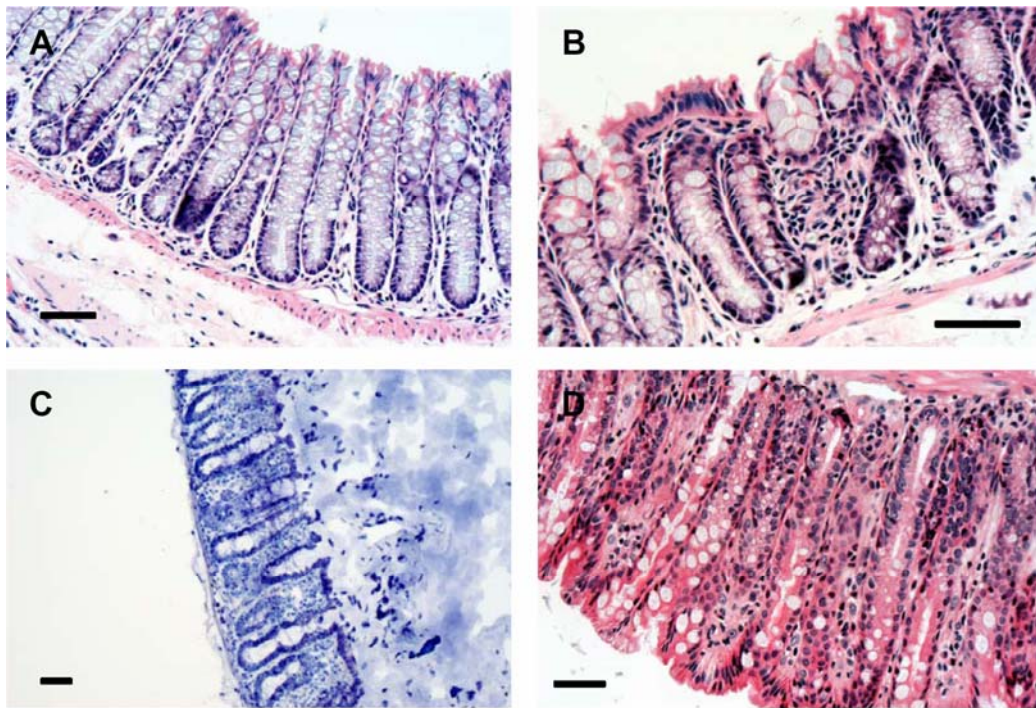


**Figure 1.** Effects of DMH, MNU, and DSS treatment on colon architecture. A) hematoxylin and eosin staining of control distal colon. B) infiltration by inflammatory cells of distal colonic mucosa after DMH treatment. C) loss of crypts in distal colonic mucosa of DMH-treated mice. D) hyperplastic crypts in distal colon after MNU treatment. Bars, 50  $\mu\text{m}$ .

Increase in intracellular cyclic AMP by IBMX (100  $\mu\text{M}$ ) and forskolin (2  $\mu\text{M}$ ) induced  $\text{Cl}^-$  secretion ( $I_{SC \text{ cAMP}}$ ) in proximal and distal colon, by activation of the cystic fibrosis transmembrane conductance regulator (CFTR). DMH caused a reduced  $I_{SC \text{ cAMP}}$  response in both proximal and

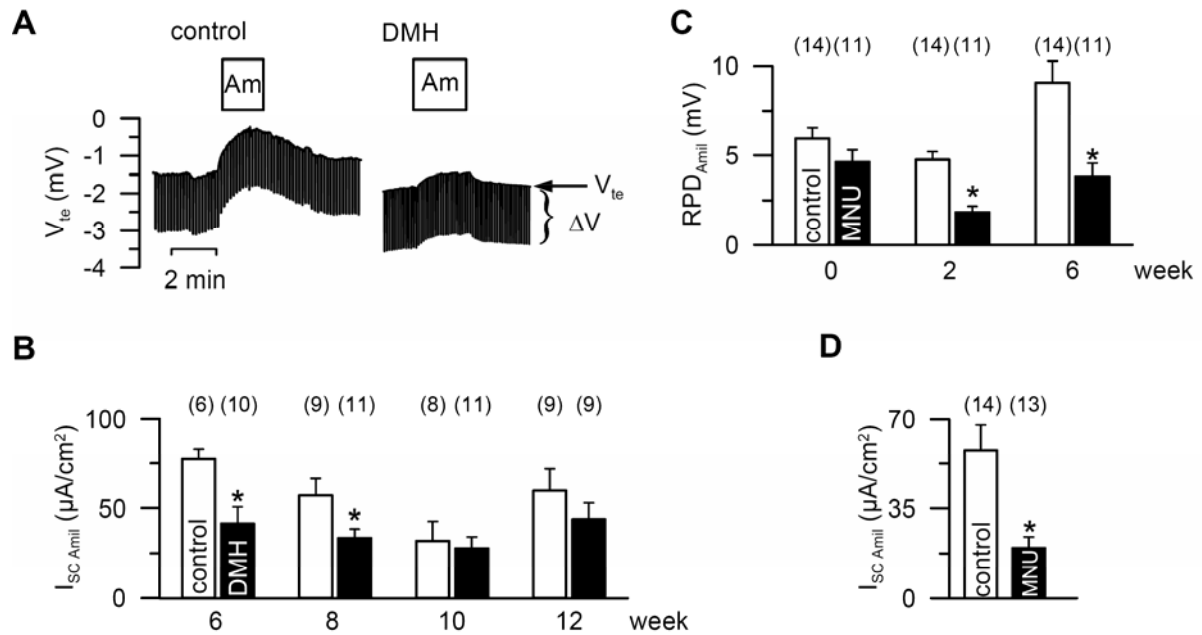


**Figure 2.** Change of amiloride-sensitive transport by carcinogens. A) Ussing chamber recordings of the transepithelial voltage. Amiloride (Am, 20  $\mu M$ ), a specific inhibitor of epithelial  $Na^+$  channels reduced  $V_{te}$  and increased  $\Delta V_{te}$  due to inhibition of  $Na^+$  absorption. The effect of amiloride on  $V_{te}$  was reduced after 6 weeks of DMH treatment. B) amiloride (20  $\mu M$ )-sensitive  $I_{SC}$  ( $I_{SC\ Aml}$ ) was reduced in Ussing chamber experiments 6 and 8 weeks after initial DMH injection. C) rectal potential difference ( $RPD_{Aml}$ ), 2 and 6 weeks after rectal application of MNU. D) Ussing chamber experiments confirmed reduced  $I_{SC\ Aml}$  in distal colon, 6 weeks after rectal application of MNU. \*, significant differences compared to control (Student's  $t$ -test). Number of mice in brackets.

distal colon at week 6 and 8. In contrast, later-stages (week 12)  $I_{SC\ cAMP}$  was significantly elevated in proximal colon (Figure 3A and B). It is well known that basolateral cAMP-dependent activation of the cotransporter NKCC1, and 293B-sensitive *KCNQ1*  $K^+$  channels ( $I_{SC\ 293B}$ ) facilitate CFTR-dependent  $Cl^-$  secretion. Accordingly DMH treatment inhibited  $I_{SC\ 293B}$  in cAMP stimulated proximal colon at week 6 and increased  $I_{SC\ 293B}$  at week 12 (Figure 3C). Similar to DMH in the early phase, MNU and DSS also reduced cAMP-dependent  $Cl^-$  secretion in rectal potential difference measurements (Figure 3D). This was further confirmed in Ussing chamber recordings. Here, cAMP-activated transport was significantly attenuated by  $62.3 \pm 5.3 \mu A/cm^2$  ( $n = 14$ ) in MNU-treated animals and by  $174.3 \pm 18.2 \mu A/cm^2$  ( $n = 7$ ) in DSS-treated mice. In contrast,  $Ca^{2+}$ -activated  $Cl^-$  secretion, stimulated by carbachol (CCH, 100  $\mu M$ ) and blockage by niflumic acid (NFA, 100  $\mu M$ ) remained unchanged (data not shown). Hence electrogenic  $Na^+$  absorption via ENaC and cAMP-dependent  $Cl^-$  secretion by CFTR are changed during inflammation and carcinogenesis, whereas  $Ca^{2+}$ -activated  $Cl^-$  secretion remains unaffected.

Because both ENaC and CFTR are the major determinants for net fluid transport in the colon, these changes are likely to affect digestive functions of the colon.

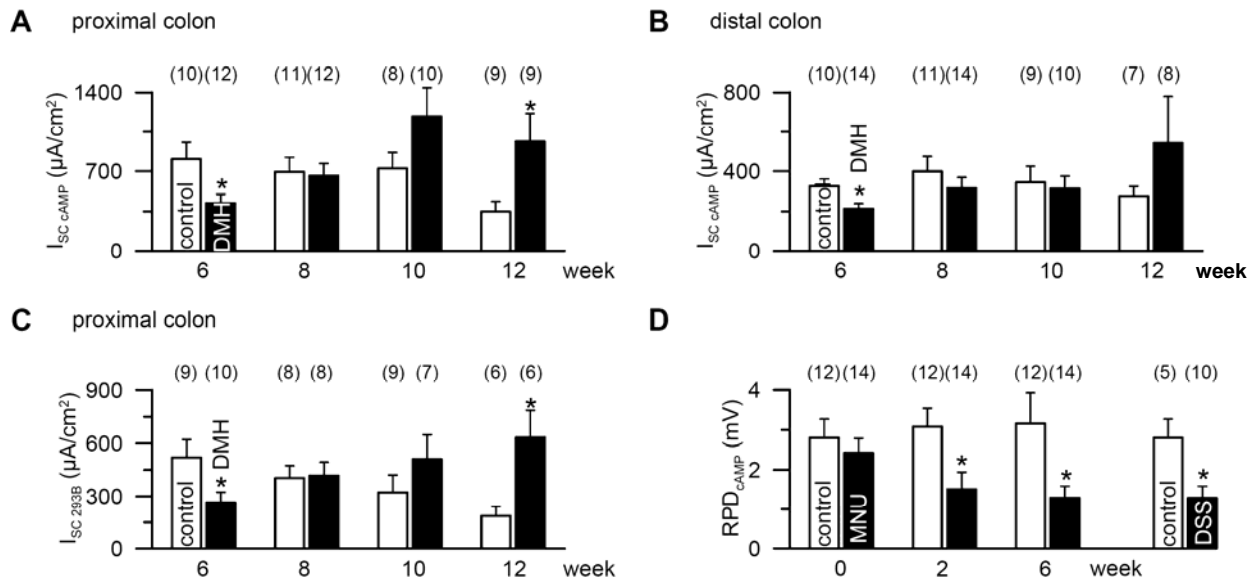


**Figure 3.** Treatment with DMH, MNU, and DSS reduced CFTR-dependent Cl<sup>-</sup> secretion. A) IBMX and forskolin increased intracellular cAMP and activated CFTR-dependent Cl<sup>-</sup> secretion. In proximal colon, cAMP-induced  $I_{SC}$  ( $I_{SC\ cAMP}$ ) was reduced 6 weeks after DMH injection, but was and elevated after 12 weeks. B) Summary of the effects of DMH on  $I_{SC\ cAMP}$  in distal colon. C) The 293B-sensitive  $I_{SC}$  ( $I_{SC\ 293B}$ ) was reduced 6 weeks after DMH injection and was elevated after 12 weeks. D) Increase in rectal potential difference by IBMX and forskolin (RPD<sub>cAMP</sub>) was reduced in MNU- and DSS-treated mice, respectively. \*, significant differences compared to control (Student's *t*-test). Number of mice in brackets.

### Carcinogens induce voltage-gated K<sup>+</sup> channels

A major goal of the present study was to identify potential oncogenic ion channels during inflammation and carcinogenesis of the colonic epithelium. It is well established that proliferation of cancer cells and metastasis require the activity of plasma membrane K<sup>+</sup> channels (Kunzelmann, 2005, Pardo, 2004). We investigated the function of K<sub>v</sub> channels in the premalignant colon using the nonselective K<sub>v</sub> channel inhibitor, 4-aminopyridine (4-AP, 100 μM) and the inhibitor of the Eag channel family, astemizole (5 μM). Application of both 4-AP and astemizole had only minor effects on  $I_{SC}$  in control animals, but inhibited  $I_{SC}$  significantly in proximal and distal colon of DMH-treated mice (Figure 4A and B). These results suggest that DMH treatment induced activation of K<sub>v</sub> and Eag-related K<sup>+</sup> channels in both distal and proximal colon. Similar results were obtained in distal colon of MNU-treated mice, where  $I_{SC\ 4AP}$  was

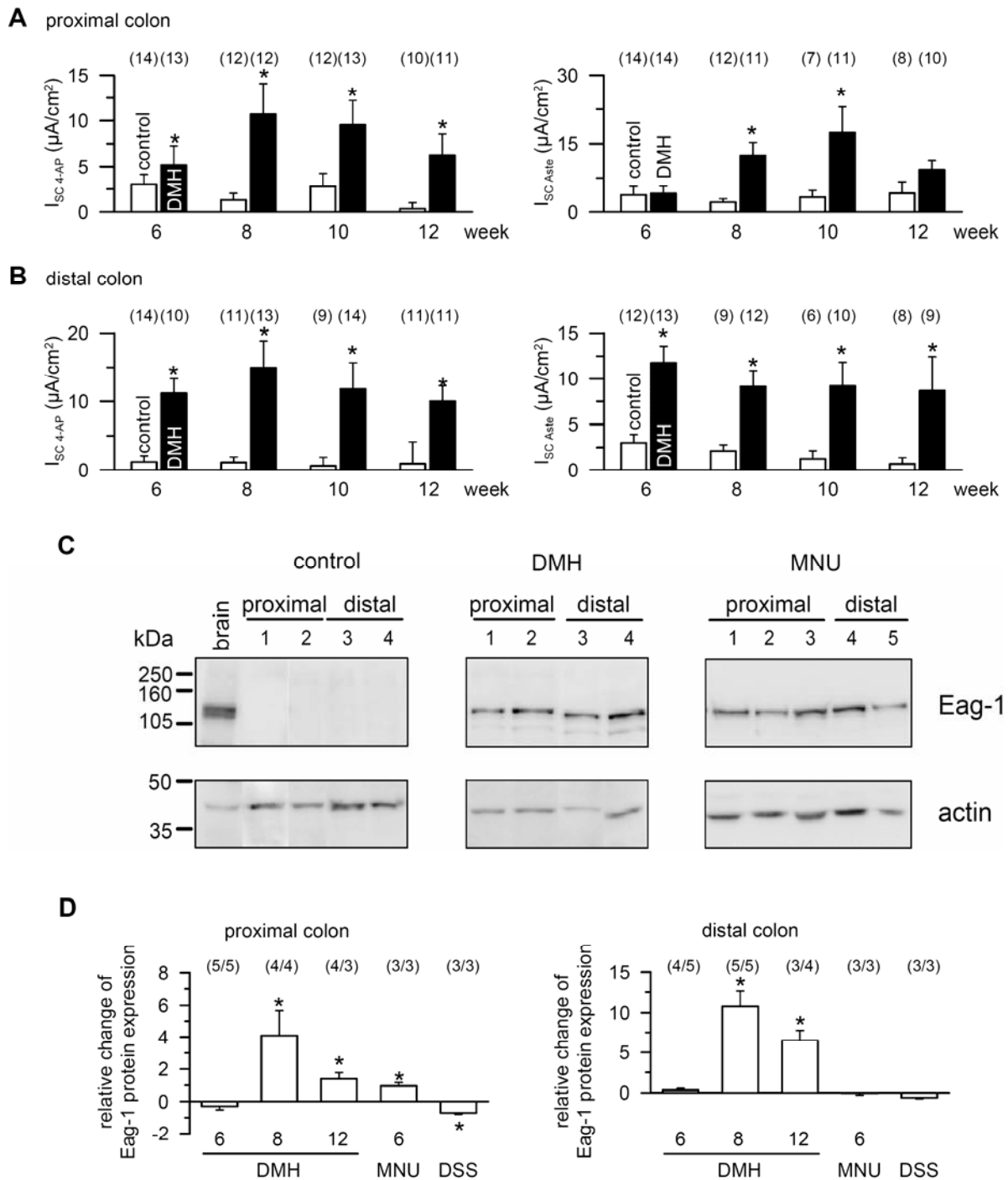


**Figure 4.** Treatment with carcinogens enhanced expression of voltage-gated  $K^+$  channels. In proximal (A) and distal (B) colon, application of 4-AP and astemizole indicated enhanced activity of voltage-gated  $K^+$  channels after treatment with carcinogens. C) Western blot analysis of Eag-1 (111 kDa) and  $\beta$ -actin (42 kDa) expression in brain (positive control) and crypt cells of proximal and distal colon of control, DMH- and MNU-treated mice. D) Summary of the changes in Eag-1 expression (normalized against  $\beta$ -actin) in crypt cells of DMH-, MNU-, and DSS-treated mice. \*, significant differences compared to control (Student's  $t$ -test). Number of mice in brackets.

**Table 1.** Changes in ion channel mRNA expression in crypt cells of proximal and distal colon of DMH-, MNU-, and DSS-treated mice

Gene	DMH wk 6	DMH wk 8	DMH wk 10	DMH wk 12	MNU wk 6	DSS
<b>Proximal colon</b>						
ENaC $\alpha$	NC (5/6)	NC (4/6)	NC (6/6)	$-0.57 \pm 0.06$ (4/5)*	NC (6/6)	NC (4/6)
ENaC $\beta$	$-0.45 \pm 0.08$ (5/5)*	NC (6/6)	NC (6/5)	$2.65 \pm 0.97$ (5/6)*	NC (5/6)	NC (4/6)
ENaC $\gamma$	NC (6/5)	NC (6/4)	NC (6/5)	$9.75 \pm 4.27$ (5/5)*	NC (6/6)	$2.21 \pm 0.62$ (4/6)*
CFTR	NC (5/6)	$-0.77 \pm 0.07$ (4/5)*	NC (6/5)	NC (6/6)	NC (6/6)	NC (4/6)
K <sub>v</sub> 1.3	NC (5/6)	$13.59 \pm 4.27$ (4/6)*	NC (6/6)	NC (5/6)	NC (6/6)	NC (4/6)
K <sub>v</sub> 1.5	NC (6/6)	NC (6/6)	NC (6/6)	NC (5/5)	$3.13 \pm 0.85$ (5/6)*	NC (4/6)
K <sub>v</sub> 3.1	NC (3/3)	$6.19 \pm 1.64$ (3/3)*	$1.36 \pm 0.43$ (6/6)*	$4.03 \pm 1.31$ (4/5)*	$1.41 \pm 0.60$ (6/6)*	NC (4/6)
Eag-1	NC (5/6)	NC (5/4)	$2.04 \pm 0.59$ (4/4)*	$8.15 \pm 2.06$ (4/5)*	NC (6/6)	NC (4/6)
Erg-1	$1.96 \pm 0.80$ (6/6)*	$6.44 \pm 2.17$ (3/3)*	$8.64 \pm 1.47$ (3/3)*	$30.38 \pm 2.81$ (3/3)*	NC (6/6)	NC (4/6)
Elk-1	NC (6/6)	$1.09 \pm 0.37$ (5/5)*	$2.83 \pm 1.42$ (5/3)*	$2.25 \pm 0.76$ (4/5)*	$-0.73 \pm 0.14$ (5/6)*	NC (3/6)
<b>Distal colon</b>						
ENaC $\alpha$	NC (6/6)	NC (5/5)	NC (6/6)	$-0.54 \pm 0.08$ (5/4)*	NC (6/6)	$-0.79 \pm 0.08$ (4/5)*
ENaC $\beta$	$-0.55 \pm 0.09$ (5/6)*	NC (5/5)	NC (6/6)	$2.54 \pm 0.56$ (5/6)*	NC (6/5)	NC (4/6)
ENaC $\gamma$	NC (6/5)	NC (5/5)	NC (6/6)	$5.60 \pm 2.22$ (5/5)*	NC (6/5)	$1.14 \pm 0.47$ (4/4)*
CFTR	NC (5/6)	$0.61 \pm 0.11$ (5/6)*	NC (6/6)	NC (6/6)	NC (6/6)	NC (4/6)
K <sub>v</sub> 1.3	NC (6/6)	NC (6/6)	NC (6/6)	NC (5/6)	$15.32 \pm 7.48$ (5/4)*	$4.13 \pm 1.57$ (4/5)*
K <sub>v</sub> 1.5	$7.52 \pm 1.86$ (6/6)*	NC (6/6)	NC (6/6)	NC (5/5)	NC (6/6)	NC (4/6)
K <sub>v</sub> 3.1	NC (3/3)	$1.80 \pm 0.65$ (3/3)*	$0.93 \pm 0.29$ (3/3)*	$1.06 \pm 0.17$ (3/3)*	NC (6/5)	NC (4/6)
Eag-1	NC (6/6)	NC (5/5)	NC (6/5)	$2.65 \pm 0.83$ (4/4)*	NC (6/6)	NC (3/6)
Erg-1	$4.44 \pm 0.37$ (3/3)*	NC (5/5)	$1.41 \pm 0.22$ (3/3)*	$2.78 \pm 2.12$ (3/2)*	$2.78 \pm 1.14$ (6/6)*	NC (4/6)
Elk-1	NC (6/6)	NC (6/6)	NC (6/6)	NC (6/6)	NC (5/5)	NC (4/6)

NOTE: Expression of mRNA was normalized against  $\beta$ -actin expression, and changes relative to the control group were calculated. Number of mice is given in parentheses.

Abbreviation: NC, no change.

\* Significant difference compared to control (Student's *t*-test).

significantly reduced by  $4.3 \pm 0.54 \mu\text{A}/\text{cm}^2$  ( $n = 14$ ). The inflamed (DSS) colon did not exhibit K<sub>v</sub> channel activity in Ussing chamber recordings and showed only small rectal potential difference changes upon application of 4-AP (data not shown). In summary, K<sub>v</sub> channels and cell cycle-regulated Eag channels were clearly detected in the premalignant colon, but were absent in the inflamed colon.

#### *Expression of ion channel mRNA in crypt cells of DMH-, MNU- and DSS-treated mice*

Because we detected changes in electrolyte transport and enhanced K<sub>v</sub> channel activity in the premalignant colon, we investigated molecular expression of the underlying ion channels. Total RNA was prepared from freshly isolated crypt cells of proximal and distal colon of DMH-, MNU- and DSS-treated (each  $n=6$ ) animals and control mice. Changes in ion channel expression relative to the control group were calculated. We found a small but significant increase in the

mRNA expression for  $\alpha$ ,  $\beta$  and  $\gamma$  subunits of ENaC in DMH-treated animals. No changes in expression of CFTR could be detected (Table 1). Thus, changes in  $\text{Na}^+$  absorption and  $\text{Cl}^-$  secretion due to the DMH treatment are not explained by changes in transcript expression of the respective ion channels but are due to other secondary changes (cf. discussion). Enhanced 4-AP-sensitive  $\text{K}^+$  currents detected in carcinogen-treated animals may also be caused by enhanced expression of  $\text{K}_v$  channels. In fact, mRNAs encoding the channels  $\text{K}_v3.1$ ,  $\text{K}_v1.3$  and  $\text{K}_v1.5$  were clearly upregulated in both distal and proximal colonic crypt cells of DMH- and MNU-treated animals. Moreover, corresponding to the enhanced astemizole-sensitive currents (Figure 4A and B), we detected enhanced mRNA expression of *ether à go-go* subtypes Eag-1, Erg-1 and Elk-1 in the premalignant proximal and distal colon of DMH- and MNU-treated mice, but not in the inflamed (DSS) colon (Table 1).

#### *DMH and MNU treatment increased expression of Eag-1 protein*

Cell cycle dependent regulation of Eag-1 is well established, thus far, expression of the channel was only found in cancer cells but not in normal epithelial tissues (Pardo et al., 1999). Because DMH treatment induced an astemizole-sensitive  $I_{\text{SC}}$  and increased Eag-1 mRNA expression in proximal and distal colon, we also examined protein expression in isolated crypt cells. In the control group, Western blot analysis showed no uniform Eag-1 expression in crypt cells (Figure 4C). In contrast, in crypt cells of DMH-treated mice, Eag-1 protein was well detected in proximal and distal colon (Figure 4C). The carcinogen MNU enhanced Eag-1 expression in the proximal colon, while no changes were observed in the inflamed colon (DSS), as indicated by densitometric analysis relative to actin staining (Figure 4D).

#### *Eag-1 protein expression in human carcinomas and diverticulitis*

Eag-1 expression was analyzed by reverse transcription-PCR in biopsies of two colorectal carcinomas and the Eag-1 transcript variants 1 and 2 were found in the centre of the carcinoma as well as in the macroscopically unaffected periphery. However, no expression of Eag-1 mRNA was found in the colon of a healthy volunteer (Figure 5A). Expression of Eag-1 protein was analyzed in isolated crypt cells from patients, diagnosed with sigma diverticulitis, ulcerative colitis, colorectal adenocarcinoma, cecum carcinoma, and colonic neoplasm (Figure 5C). Samples were also obtained from patients with unrelated diseases, such as cystic fibrosis. No expression of Eag-1 was detected in these samples. The variability of the tissue sample quality was assessed by simultaneous detection of  $\beta$ -actin expression. In summary, expression of Eag-



1 was detected in most carcinomas and in some patients diagnosed with diverticulitis, whereas the healthy colon does not seem to express cell cycle-regulated K<sup>+</sup> channels (Figure 5B).

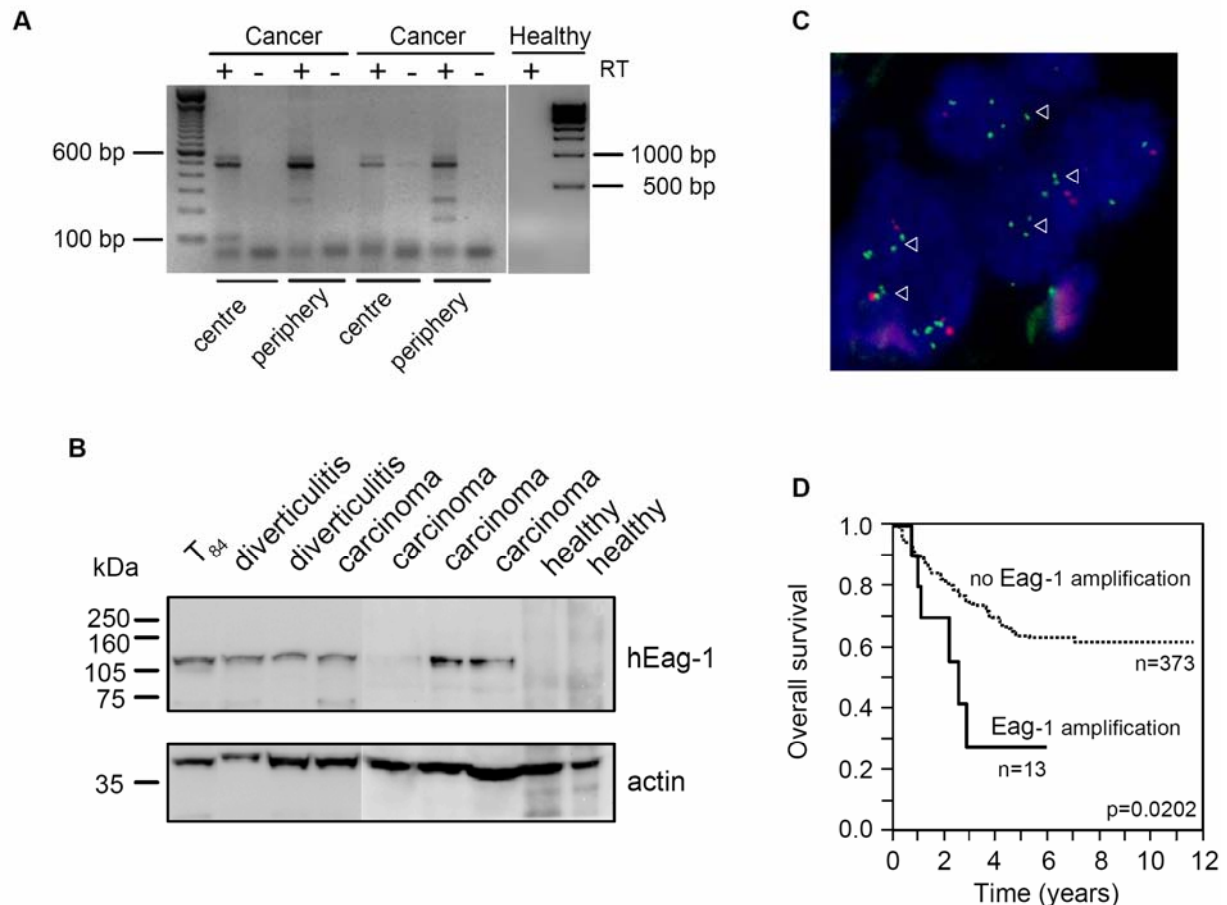


**Figure 5.** Eag-1 is expressed in colonic crypt cells of patients with cancer and diverticulitis. A) reverse transcription-PCR showed mRNA expression of the two variants of Eag-1 (variant 1, 560 bp, variant 2, 479 bp) in the center and peripheral tissue of the cancer in two patients. In a colon biopsy of a healthy volunteer, no Eag-1 transcripts were detected. B) total protein was isolated from T<sub>84</sub> colonic cancer cells and from crypt cells derived from patients with different diagnosis. Colonic biopsies of healthy patients served as controls. C) Fluorescence *in situ* hybridization of a colorectal adenocarcinoma with Eag-1 amplification. Tumor cell nuclei contain numerous Eag-1 signals (arrows), but only few reference signals in red (centromere 1;  $\times 1000$ ). Nuclei counterstained with DAPI (blue). D) Effect of Eag-1 gene amplification on overall survival in surgically resected colorectal adenocarcinoma.

*The Eag-1 gene is amplified in tumor specimens and is associated with adverse outcome*

Pathologic tumor-node-metastasis stage, histological grade, and International Union Against Cancer stage were strongly associated with overall survival ( $p < 0.0001$  each; data not shown). Fluorescence *in situ* hybridization analysis showed amplification of the Eag-1 gene in 13 (3.4%) of the 386 tumor specimens (Table 2). A representative case with Eag-1 amplification is shown

in figure 5C. Univariate survival analysis revealed that Eag-1 amplification was significantly associated with adverse outcome ( $p = 0.0202$ ; Figure 5D). If entered in a multivariate model (Cox proportional hazard), amplification of Eag-1 emerged as an independent prognostic marker ( $p = 0.0126$ , relative risk, 3.55) together with International Union Against Cancer stage ( $p < 0.0001$ , relative risk, 15.56) and histological grade ( $p = 0.0167$ , relative risk, 1.77,  $n = 386$ ). Thus expression of Eag-1 is associated with reduced overall survival in patients with colonic carcinoma.

**Table 2.** Clinicopathologic characteristics of colorectal adenocarcinomas (n=386)

Sex	
M	200 (48.1%)
F	186 (51.8%)
Age (range), year	71.6 $\pm$ 1.1 (36-96)
Localization	
Right colon	164 (43.4%)
Left colon	214 (56.6%)
pT	
pT1	7 (1.8%)
pT2	64 (16.6%)
pT3	247 (64.0%)
pT4	68 (17.6 %)
pN	
pN0	195 (50.5%)
pN1	107 (28.2%)
pN2	84 (27.7%)
pM	
pM0	309 (80.1%)
pM1	77 (19.9%)
Stage	
Stage I	53 (13.7%)
Stage II	129 (33.4%)
Stage III	127 (32.9%)
StageIV	77 (20.0%)
Grading	
G1	2 (0.5%)
G2	290 (75.1%)
G3	94 (24.4%)
Follow-up (mo)	
Mean (range)	37.7 $\pm$ 3.4 (0-140)
Median	31.0

## DISCUSSION

### *Effects of proinflammatory and carcinogenic chemicals*

For the present study, we used the mouse C57BL/6N strain, which shows a high incidence of colorectal tumors after DMH treatment (Diwan and Blackman, 1980, Greene et al., 1987).

Histological changes were identified early after DMH injection; however, definite cancers develop typically only after 24 weeks of treatment (Greene et al., 1987). Intrarectal infusion of MNU yielded a high incidence (up to 100%) of colonic cancer in previous studies with shrews (Yang et al., 1996). We detected initial inflammatory responses in both DMH- and MNU- treated animals, similar to the inflamed (DSS) colon. However, at later stages, carcinogens caused significant changes in mucosal architecture and expression of  $K_v3.1$ ,  $K_v1.3$  and  $K_v1.5$  and, particularly, Eag channels. This was not observed in the DSS model. Thus, expression of oncogenic Eag channels seems to be a consequence of the carcinogen treatment and not simply a result from inflammation. This channel was also found in human colonic cancers, but not in normal tissues. It suggests that Eag has an oncogenic potential in the colonic epithelium. Interestingly, Eag was also detected in diverticulitis, which has the potential to change into colonic cancer. We hypothesize that expression of Eag in preneoplastic tissues supports malignancy and may drive the development towards colonic cancer.

#### *Electrolyte transport changes during carcinogenesis and colitis*

Several reports show altered electrolyte transport in early stages of tumor development. Using the present models, we confirm reduction of amiloride-sensitive  $Na^+$  absorption by treatment with DMH, MNU and DSS. Inhibition of amiloride-sensitive  $Na^+$  absorption was not explained by changes in the expression profile of the three  $Na^+$  channel subunits. A likely reason for reduced  $Na^+$  absorption is an attenuation of the  $Na^+/K^+$ -ATPase in the distal colon (Davies et al., 1991). The cAMP-induced  $Cl^-$  secretion was reduced initially, but was up-regulated at later stages of DMH treatment. Stool irregularities, with changes from constipation to diarrhea, are often observed in patients with intestinal tumors or inflammatory bowel disease, and the present findings may therefore supply an explanation for these symptoms.

#### *Expression of $K_v$ channels during inflammation and carcinogenesis*

$K_v$  channels promote cell proliferation and support tumor development (Pardo, 2004, Pardo et al., 2005). In multiplex reverse transcription-PCR, we found enhanced expression of the channels  $K_v1.3$ ,  $K_v1.5$  and  $K_v3.1$  (Table 1).  $K_v1.3$  (gene locus *KCNA3*) is essential for lymphocyte proliferation and supports development of cancer in prostate, colon and breast.  $K_v1.5$  (gene locus *KCNA5*) supports proliferation of gastric cancer (Abdul and Hoosein, 2002b, Kunzelmann, 2005). Moreover, expression of  $K_v1.5$  correlates with the grade of malignancy of gliomas (Preussat et al., 2003). The apparent dissociation constants ( $K_d$ ) of 4-AP for  $K_v1.3$ ,  $K_v1.5$  and  $K_v3.1$  channels are 195  $\mu$ M, 270  $\mu$ M, and 29  $\mu$ M, respectively, which are in the range of the

4-AP concentration (100  $\mu$ M) used in the present study (Grissmer et al., 1994). We suggest that  $K_v3.1$  (gene locus *KCNC1*) is mainly responsible for the 4-AP-dependent inhibition of ion transport in the malignant colon. Thus, this is the first study which supplies evidence that  $K_v3.1$  channels are involved in development of cancer. Expression of  $K_v3.1$  is normally restricted to central nervous system and to a subpopulation of T lymphocytes (Pardo, 2004).  $K_v3.4$ , another member of this subfamily of  $K_v$  channels, controls proliferation of oral and esophageal squamous carcinoma cells (Chang et al., 2003).

#### *An oncogenic role of EAG channels in the colon*

According to previous reports, expression of Eag-1 and Erg-1 channels is strictly limited to excitable tissues. In contrast, in malign epithelial tumors, the cell cycle-controlled Eag channel determines malignancy and metastasis of breast cancer (Camacho, 2006, Pardo et al., 1999, Pardo, 2004, Stuhmer et al., 2006). Crypt cells of carcinogen-treated mice showed expression of Eag-1, Erg-1 and Elk-1 in the present study. When normalized to the actin signal, expression of Eag-1 was somewhat larger in the distal colon when compared to the proximal colon of DMH-treated animals. However, the difference was not statistically different. Moreover, expression of Eag-1 was found in human colorectal adenocarcinomas. Fluorescence *in situ* hybridization analysis showed amplification of the Eag-1 gene in 13 (3.4%) of the 386 tumor specimens. Eag-1 amplification was significantly associated with adverse outcome. The low prevalence of Eag-1 amplification does not question its importance, since mechanisms other than amplification may account for activation and over-expression in a larger fraction of tumours. For example, another potassium channel, *KCNK9* at 8q24.3, was previously found to be amplified in about 10%, but overexpressed in 44% of breast cancers (Mu et al., 2003a).

Taken together, carcinogenesis in the colon and colitis change expression of ion channels important for salt transport, which is likely to cause stool irregularities. Expression of the cell cycle-regulated  $K^+$  channel Eag-1 is closely correlated with malignancy in the human and rodent colon and Eag-1 gene amplification is associated with reduced surviving rate. These data suggested that Eag-1 expression is important for tumor development in the human colon. Because Eag-1 is already expressed at a premalignant stage, Eag-1 transcripts detected in rectal biopsies or stool samples may serve as early diagnostic and prognostic markers, as shown recently for cervical cancer (Farias et al., 2004b). The present data may also be useful in developing new therapeutic strategies for the treatment of colonic cancer.

## CHAPTER 5

### Upregulation of colonic ion channels in $APC^{Min/+}$ mice

#### ABSTRACT

**Background & Aims:** The adenomatosis polyposis coli ( $APC$ ) tumor suppressor gene is mutated in almost all human colonic cancers. Disturbances in  $Na^+$  absorption have been observed in colonic cancer and ion channels such as *ether à go-go* (Eag) or  $Ca^{2+}$ -sensitive BK channels have been recognized for their oncogenic potential.

**Methods:** The  $APC^{Min/+}$  mouse model is characterized by reduced  $APC$  expression and multiple intestinal neoplasia (Min). The activity of colonic ion channels was assessed by electrophysiological and molecular techniques.

**Results:**  $APC^{Min/+}$  mice developed polyps in proximal and distal colon and experienced a significant weight loss during an observation period of 21 weeks. Rectal potential measurements *in vivo* indicated an increase in amiloride-sensitive  $Na^+$  absorption in  $APC^{Min/+}$  mice. Quantitative Ussing chamber studies demonstrated enhanced  $Na^+$  absorption via epithelial  $Na^+$  channels (ENaC) and suggested enhanced activity of oncogenic BK and Eag-1 channels. Patch clamp experiments on mid crypt cells showed similar results for  $APC^{Min/+}$  and wt mice, suggesting that changes in channel activity take place in the surface epithelium. ENaC-mRNA and membrane protein expression was clearly enhanced in colonic surface epithelial cells.

**Conclusions:** Reduced expression of the  $APC$  gene with upregulation of the downstream proteins Akt and mTOR augments the activity of ENaC and oncogenic potassium channels. These changes reflect an imbalance due to reduced apoptosis and enhanced mitotic activity, and may have implications for the clinical outcome.

## INTRODUCTION

Membrane ion channels have been demonstrated in previous studies to control cell proliferation. Changes in ion channel expression during development of cancer have been frequently observed (for review see (Kunzelmann, 2005). Ion channel activity determines homeostatic parameters such as membrane voltage, intracellular ion concentration, and cell volume. Ion channels also control cytosolic pH and cell signaling by changes in the intracellular  $Ca^{2+}$  concentration (Kunzelmann, 2005, Schreiber, 2005, Spitzner et al., 2007). Some ion channels, like Eag-1, fulfill specific tasks during the cell cycle (Pardo et al., 1999, Pardo, 2004). Voltage-gated  $K^+$  channels are detected in breast and colonic cancer specimens and other malign tumors (Lastraioli et al., 2004, Ousingsawat et al., 2007, Pardo et al., 1999, Pardo, 2004, Spitzner et al., 2007). Large conductance  $Ca^{2+}$ -activated  $K^+$  channels are found in tumors of prostate, breast and colorectum (Bloch et al., 2007, Yao and Kwan, 1999). Previous *in vitro* studies demonstrate a contribution of  $K^+$  channels to proliferation of colonic cancer cells, and experiments performed on animal models suggest an oncogenic role of these  $K^+$  channels *in vivo* (Ousingsawat et al., 2007). To fully appreciate the changes in ion channel currents occurring during carcinogenesis in the colon, further *in vivo* studies are required, ideally on a genetically well defined mouse model (Fodde et al., 1994).

Previous studies utilized chemical tumor models in order to assess potential changes in ion conductances during carcinogenesis *in vivo*. Treatment of the animals with carcinogens like dimethylhydrazine or N-methyl-N-nitrosourea induces colonic cancer, which is paralleled by changes in ion channel expression (Fodde et al., 1994, Ousingsawat et al., 2007). While these studies supply some insight into carcinogenesis *in vivo*, the drawbacks are individual drug susceptibility and inflammation (Ousingsawat et al., 2007). Here we studied a well defined genetic mouse model that is based on a mutation in the adenomatous polyposis coli (APC) gene. Heterozygote  $APC^{Min/+}$  mice develop multiple intestinal neoplasia (Min) (Fodde et al., 1994). Mutations in the human APC gene are responsible for familial adenomatous polyposis and are found in a large majority of colorectal cancers. We found that heterozygous  $APC^{Min/+}$  animals demonstrate a change in expression of epithelial colonic  $Na^+$  channels and show an increase in BK and Eag-1 channel conductance, similar to human colonic carcinoma.

## MATERIAL AND METHODS

### *Animals*

Heterozygous  $APC^{Min/+}$  pups (Fodde et al., 1994) (Jackson laboratory, USA) were weaned at 4-5 weeks of age and genotyped by PCR. Animals were fed with complete chow with 15% corn oil (Sniff, Soest, Germany), which has an adverse effect on polyp numbers in these animals (Wasan et al., 1997).  $APC^{Min}$  were sacrificed after a weight loss of 10%. Wild-type animals of the same age served as control. Animal studies were conducted according to the guidelines of the National Institute of Health and the German laws on protection of animals.

### *Immunohistochemistry and histology*

Mice were sacrificed under CO<sub>2</sub> inhalation; Proximal and distal colon were fixed for 20 min in 0.1 M PBS with 4% paraformaldehyde. Sections were embedded in paraffin, cut in 5 µm serial sections (Leica microtome RM 2165, Wetzlar, Germany) and mounted on slides. Dehydrated sections were heat-induced for epitope retrieval for 20 min. After washing in PBS, sections were blocked and incubated in primary antibodies at 4°C overnight. Rabbit polyclonal anti- $\alpha$ , anti- $\beta$ , and anti- $\gamma$ -ENaC antibodies (BABCO, Berkely, CA, USA) and the anti-BK $\alpha$  antibody (Alamone Labs, Israel) were used in a 1:50 dilution. The polyclonal anti- $\beta$ -catenin antibody (Sigma, Taufkirchen, Germany) was used at 1:1,000 dilutions. ENaC and BK antibodies were detected using avidin-biotin complex (ABC) technique. After exposure to the primary antibody, sections were incubated in a biotinylated donkey anti-rabbit antibody diluted 1:400 (Santa Cruz Biotechnology, Heidelberg, Germany). After washes, the sections were incubated with diaminobenzidine. Tissues were counterstained with hematoxylin (Merck, Darmstadt, Germany) before mounting in Depex (SERVA Electrophoresis). Nuclei were stained with Hoe33342 (Sigma-Aldrich, Taufkirchen, Germany) and then mounted in DakoCytomation media. Endogenous peroxidase activity was blocked by incubating in 3% H<sub>2</sub>O<sub>2</sub> in PBS. Images were taken with Axiovert 200M/ApoTome (Zeiss, Munich).

### *Rectal potential different (RPD) and Ussing chamber measurement*

For RPD measurements, mice were anaesthetized by intraperitoneal injection of 20 µl (75 mg/ml) ketamine and 5 mg/ml xylazine. A catheter (polythene tube with OD 1 mm) perfused with standard ringer solution (3 ml/min) was attached to an AgCl electrode and inserted 2 cm into the rectum. A subcutaneous needle served as reference. For Ussing chamber measurement, stripped colon was put into ice cold ringer solution containing amiloride (20 µM) and indomethacin (10 µM) and tissues were measured in a perfused Ussing chamber as described previously (Ousingsawat et al., 2007).

### *Patch clamp experiments*

Crypts were isolated in  $Ca^{2+}$ -free Ringer solution. Individual crypts were held by pulled glass pipettes and whole cell patch clamp recordings were taken from mid and lower crypt cells using previously described protocols (Spitzner et al., 2007).

### *Real time PCR and Western blotting*

Expression levels for mRNAs encoding Eag-1, BK, ENaC and  $\beta$ -actin were evaluated by real time PCR using Light Cycler (Roche, Mannheim, Germany) and Quanti Tect SYBR Green PCR Kit (Qiagen, Hilden, Germany) after isolating total RNA from colonic crypt cells using standard techniques. Further details regarding primers and real time PCR are given in Supplements. Lysates of isolated proximal and distal colonic crypt cells were resolved by 7% SDS-PAGE, transferred to Hybond-P (Amersham, Freiburg, Germany) and incubated with antibodies described above. Akt antibodies were from Cell Signaling, Frankfurt, Germany). Bands were visualized with goat anti-rabbit IgG conjugated to horseradish peroxidase (Acris, Hiddenhausen, Germany) and ECL using a Fluor-STM Multimager (Bio-Rad, Hercules, USA). Expression levels were normalized to that of  $\beta$ -actin.

### *Materials and statistical analysis*

All used compounds were of highest available grade of purity. Amiloride, paxillin, 4-AP, astemizole, carbachol, forskolin, UTP, NS1619,  $\beta$ -estradiol, IBMX were all from Sigma-Aldrich (Taufkirchen, Germany). Student's t-test (for paired or unpaired samples as appropriate) and analysis of variance (ANOVA) were used for statistical analysis.  $P < 0.05$  was accepted as significant.

## **RESULTS**

### *Pathology of $APC^{Min/+}$ mice*

$APC^{Min/+}$  mice demonstrated a normal postnatal development but started to lose weight from week 12 on.  $APC^{Min/+}$  mice reached an age of  $21.21 \pm 0.81$  weeks. By then they lost more than 20% weight ( $23.22 \pm 0.8$  g;  $n = 23$ ) compared to wt animals ( $36.66 \pm 1.51$  g;  $n = 32$ ). Wt animals were sacrificed at an age of  $23.3 \pm 0.77$  weeks. Every  $APC^{Min/+}$  animal had large visible polyps in proximal ( $0.47 \pm 0.2$ ) and distal ( $2.53 \pm 1.0$ ;  $n = 14$ ) colon, but the number of polyps was much higher in small intestine and stomach ( $27.2 \pm 7$ ) (Figure 1A). Large intestinal polyps consisted of hyperplastic adenomas, which did not yet show signs of malignancy (Figure 1B). Although  $\beta$ -catenin accumulation in crypts of  $APC^{Min/+}$  animals had been described in previously (Kongkanunt et al., 1999), we found similar expression of  $\beta$ -catenin in wt and  $APC^{Min/+}$  animals



in proximal (Figure 1C) and distal (Figure 1D) colon. Confocal images of  $\beta$ -catenin staining demonstrate regular membrane staining in unaffected small (Figure 1E) and large (Figure 1F) intestinal mucosa, while the staining was more diffuse and cytosolic in the polyps (Figure 1E, F).

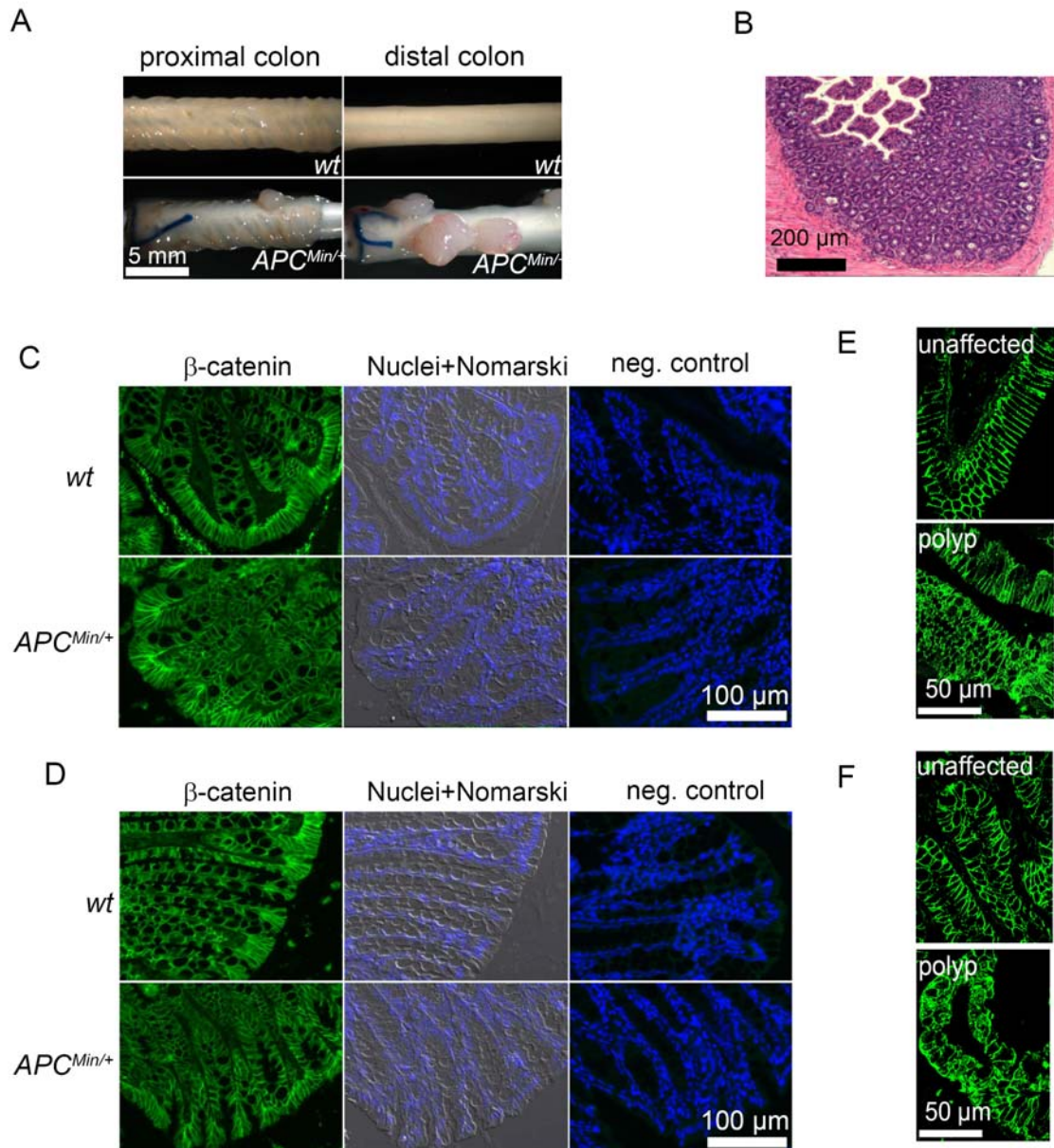


**Figure 1.** Mucosal abnormalities in  $APC^{Min/+}$  mice. A) Macroscopic aspect of inverted proximal and distal colonic mucosa of wild type (wt) and  $APC^{Min/+}$  mice. Colonic mucosa of  $APC^{Min/+}$  mice shows several large polyps. B) Hematoxylin/eosin staining of a distal colonic polyp from an  $APC^{Min/+}$  animal. C) Staining of  $\beta$ -catenin in unaffected proximal (C) and distal (D) colon of wt and  $APC^{Min/+}$  mice. Staining and confocal images of  $\beta$ -catenin in unaffected crypts and polyps from small (E) and large (F) intestine.

### Enhanced $Na^+$ absorption in $APC^{Min/+}$ mice

Rectal potentials were measured *in vivo* in anesthetized animals aged 9, 15 and 19 weeks (Table 1), using a fine polyethylene catheter (c.f. Methods). From week 15 on,  $APC^{Min/+}$  animals displayed increased lumen negative transrectal potentials (RPD), when compared to wt animals (Figure 2A, B). The RPD was mainly due to amiloride sensitive  $Na^+$  absorption ( $RPD_{am}$ ), since intrarectal application of amiloride via the catheter collapsed the lumen negative RPD. Thus, amiloride sensitive epithelial  $Na^+$  absorption is significantly enhanced in  $APC^{Min/+}$  animals (Figure 2A, C).

**Table 1.** Rectal potential difference in wt and  $APC^{Min/+}$  mice under control conditions (RPD) and changes induced by rectal perfusion of amiloride (20  $\mu$ M), forskolin 2  $\mu$ M), ATP (100  $\mu$ M), and  $Ba^{2+}$  (5 mM). Asterisks indicate significant difference when compared to wt animals. (Number of mice).

	Rectal potential difference (mV)					
	9 weeks		15 weeks		20 weeks	
	wt (n=22-30)	$Apc^{min/+}$ (n=10-19)	wt (n=19-25)	$Apc^{min/+}$ (n=8-14)	wt (n=2-9)	$Apc^{min/+}$ (n=4-5)
RPD	-12.27 $\pm$ 0.9	-10.86 $\pm$ 0.8	-9.78 $\pm$ 0.4	<b>-13.52 <math>\pm</math> 1.7*</b>	-8.52 $\pm$ 0.2	<b>-14.11 <math>\pm</math> 2.1*</b>
$RPD_{amil}$	7.41 $\pm$ 0.9	5.65 $\pm$ 0.5	4.06 $\pm$ 0.3	<b>9.36 <math>\pm</math> 1.6*</b>	4.21 $\pm$ 0.6	<b>9.76 <math>\pm</math> 2.0*</b>
$RPD_{forsk}$	2.39 $\pm$ 0.3	2.06 $\pm$ 0.4	2.66 $\pm$ 0.4	2.16 $\pm$ 0.5	3.52 $\pm$ 0.5	3.24 $\pm$ 0.7
$RPD_{ATP}$	2.09 $\pm$ 0.2	2.04 $\pm$ 0.4	1.80 $\pm$ 0.3	1.82 $\pm$ 0.6	2.02 $\pm$ 1.4	1.31 $\pm$ 0.2
$RPD_{Ba^+}$	2.38 $\pm$ 0.2	2.58 $\pm$ 0.3	2.52 $\pm$ 0.2	<b>1.66 <math>\pm</math> 0.2*</b>	2.27 $\pm$ 0.3	2.44 $\pm$ 0.7

This was further quantified in continuous recordings of the transepithelial voltage, which is a measure for the epithelial transport. Electrogenic absorption of  $Na^+$  by ENaC is normally limited to distal colon. However, in  $APC^{Min/+}$  animals amiloride sensitive  $Na^+$  transport (short circuit current,  $I_{sc}$ ) was also detected in the proximal colon (Figure 3A, C). In distal colon of  $APC^{Min/+}$  animals,  $Na^+$  absorption was largely upregulated (Figure 3B, C). Other transport properties, like forskolin induced  $Cl^-$  secretion by the cystic fibrosis transmembrane conductance regulator (CFTR)  $Cl^-$  channel, and  $Ca^{2+}$  activated electrolyte transport in the distal colon were similar in  $APC^{Min/+}$  and normal animals (data not shown).

### Expression of oncogenic $K^+$ currents in $APC^{Min/+}$ mice

Expression of cell cycle regulated Eag-1 and  $Ca^{2+}$ -dependent BK channels has been reported for colonic cancer and other malignant tumors (Bloch et al., 2007, Ousingsawat et al., 2007, Yao and Kwan, 1999). Basolateral application of the Eag-1 inhibitor astemizole (5  $\mu$ M) inhibited  $I_{sc}$  in

proximal and distal colon of both  $APC^{Min/+}$  and normal mice, however, astemizole sensitive transport ( $I_{sc\ aste}$ ) was augmented in proximal colon of  $APC^{Min/+}$  mice (Figure 3D, E). 4-aminopyridine (0.1 and 2 mM), which inhibits other types of voltage-gated  $K^+$  channels, had no effect on ion transport (data not shown). Luminal paxillin (5  $\mu$ M) inhibited  $K^+$  secretion via BK channels to the same degree in wt ( $32.8 \pm 12 \mu A/cm^2$ ;  $n = 13$ ) and  $APC^{Min/+}$  ( $31.9 \pm 19 \mu A/cm^2$ ;  $n = 6$ ) mice, suggesting similar baseline activity for BK channels. However, the activator of BK channels NS1619 (10  $\mu$ M) stimulated more  $K^+$  secretion in the distal colon of  $APC^{Min/+}$ , when compared to wt animals (Figure 3F). Moreover, after activation of  $K^+$  secretion by carbachol (100  $\mu$ M), the BK channel inhibitor paxillin showed a stronger effect in  $APC^{Min/+}$  mice ( $19.5 \pm 9.7 \mu A/cm^2$ ;  $n = 3$ ), compared to wt ( $7.2 \pm 3.4 \mu A/cm^2$ ).

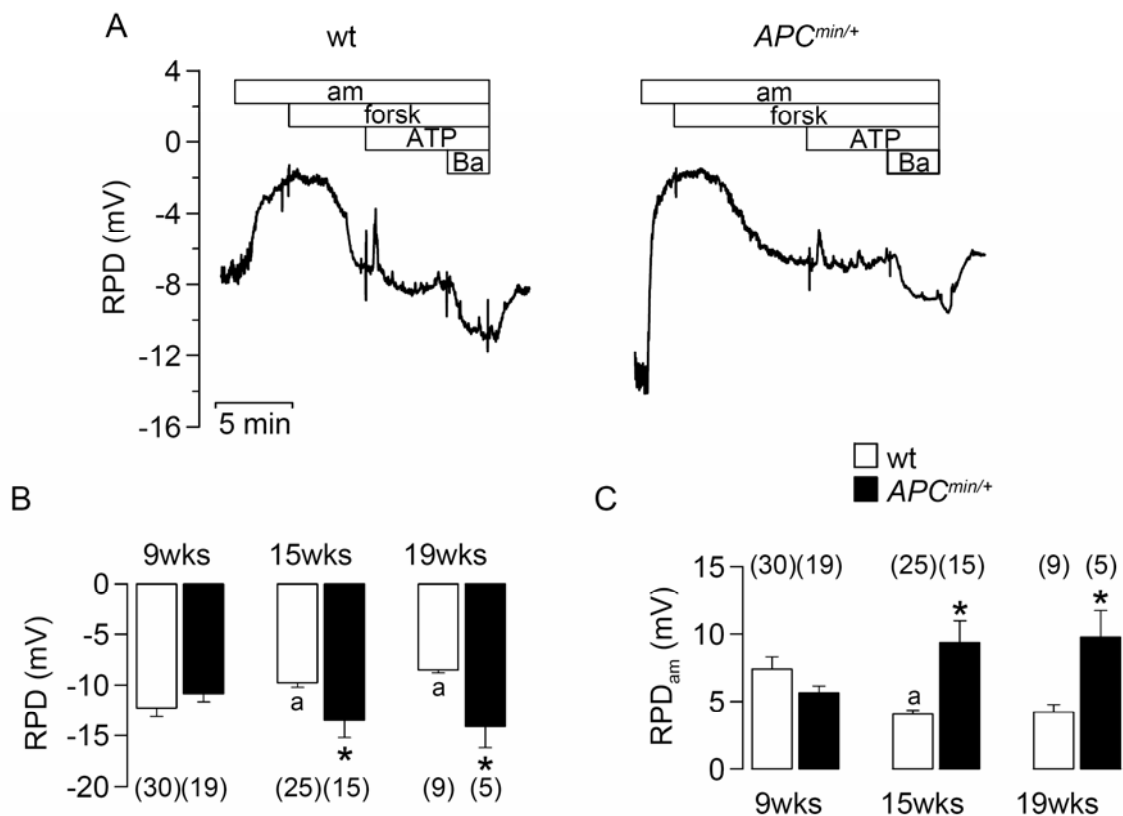


**Figure 2.** Enhanced  $Na^+$  absorption  $APC^{Min/+}$  mice. A) Original recordings of the rectal potential difference (RPD) measured in wt and  $APC^{Min/+}$  mice. Inhibition of ENaC by luminal application of amiloride (am, 20  $\mu$ M) via the catheter reduced RPD, while forskolin (forsk, 2  $\mu$ M) and barium (Ba, 5 mM) increase the rectal potential difference. ATP (100  $\mu$ M) induced a brief and transient decrease in RPD due to activation of BK  $K^+$  channels. B) Summary of RPD measured in wild type (wt) and  $APC^{Min/+}$  mice at 9, 15 and 19 weeks of age. C) Summary of the amount of RPD inhibited by amiloride in wild type (wt) and  $APC^{Min/+}$  mice at 9, 15 and 19 weeks of age. Asterisks indicate significant differences compared to control (Student's  $t$ -test). (Number of mice).

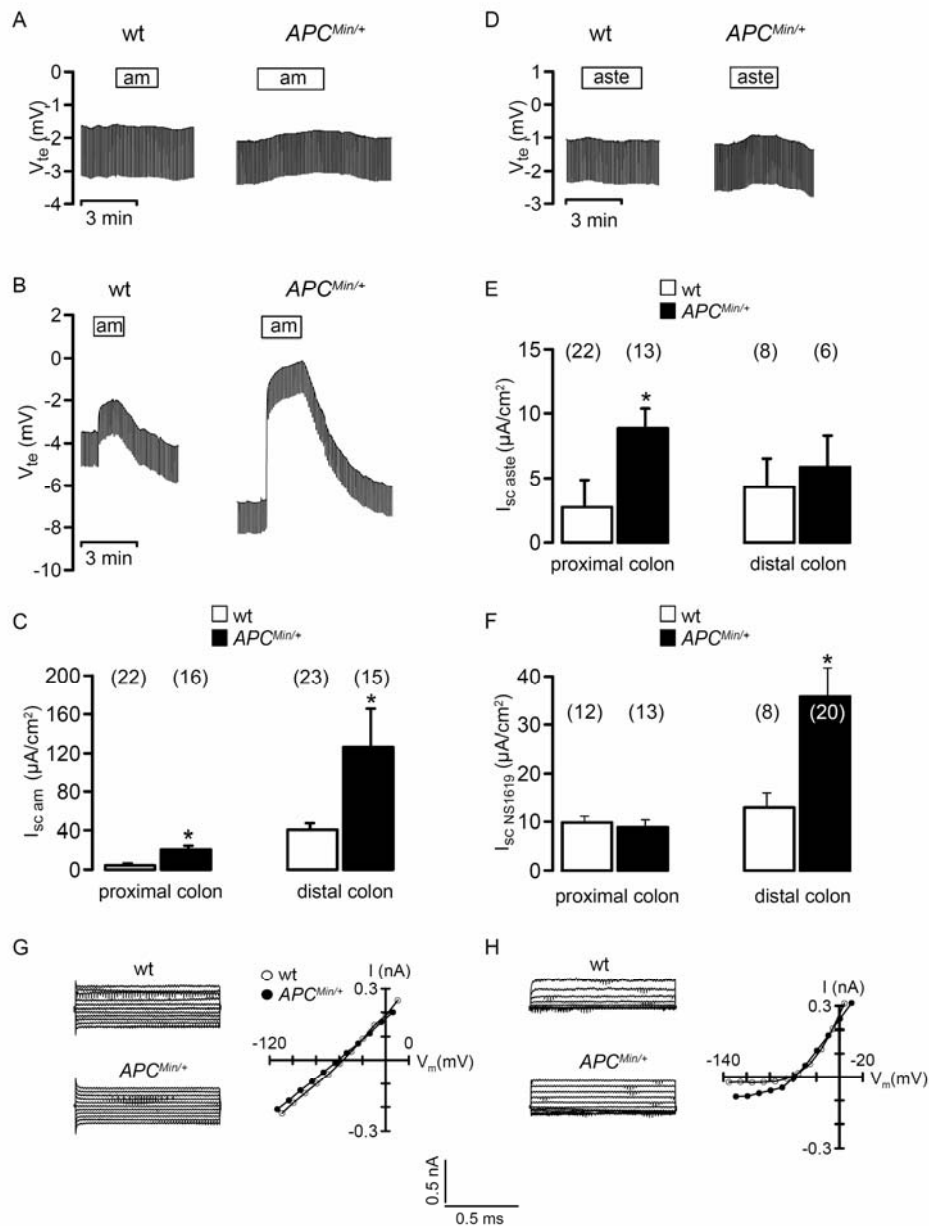


**Figure 3.** Ion channels in the colon of  $APC^{Min/+}$  mice. A), B) Original recordings of the transepithelial voltage ( $V_{te}$ ) measured in a perfused Ussing chamber. In  $APC^{Min/+}$  mice amiloride (am, 20  $\mu M$ ) slightly reduced  $V_{te}$  in the proximal colon (A) but had a large effect on  $V_{te}$  in distal colonic mucosa (B). C) Summary of the amiloride sensitive transport ( $I_{sc\ am}$ ) in proximal and distal colonic mucosa of wt and  $APC^{Min/+}$  mice. D) Original recordings of  $V_{te}$  and effects of the Eag-1-blocker astemizole (aste, 5  $\mu M$ ) in proximal colon. E) Summary of the astemizole sensitive transport ( $I_{sc\ aste}$ ) in proximal and distal colonic mucosa of wt and  $APC^{Min/+}$  mice. F) Summary of the K<sup>+</sup> secretion activated by the BK channel activator NS1619 (10  $\mu M$ ) in proximal and distal colonic mucosa of wt and  $APC^{Min/+}$  mice. G), H) Whole cell patch clamp experiments from colonic mid crypt and crypt base epithelial cells. Original current tracings (left panels) and current voltage relationships (right panels) suggest cells with linear (G) and outwardly rectifying (H) whole cell currents. Asterisks indicate significant differences compared to control (Student's *t*-test). (Number of mice).

Conductance properties were further examined in patch clamp experiments on mid and lower crypt cells. The baseline membrane voltage and conductance properties of epithelial cells from wt and  $APC^{Min/+}$  mice were indistinguishable (Table 2). We identified two populations of cells with either linear (Figure 3G) or outwardly rectifying (Figure 3H) whole cell currents. The frequency of both, however, was similar in  $APC^{Min/+}$  and wt mice. Moreover, cAMP- and  $Ca^{2+}$ -activated currents were similar in wt and  $APC^{Min/+}$ , and effects of paxillin, astemizole or 4-AP could not be detected (data not shown). Thus,  $Ca^{2+}$ -activated BK channels and astemizole sensitive Eag-1 channels must be expressed in the surface epithelium, which confirms previous results (Puntheeranurak et al., 2006).

<b>Table 2:</b> Whole cell conductance ( $G_m$ ) and membrane voltage ( $V_m$ ) of epithelial cells from colonic crypts of wt mice and $APC^{Min/+}$ animals. (Number of mice).				
	$G_m$ (nS)		$V_m$ (mV)	
	wt	$APC^{Min/+}$	wt	$APC^{Min/+}$
Proximal colon	$2.47 \pm 0.41$ (29)	$2.34 \pm 0.3$ (28)	$-65.64 \pm 2.74$ (29)	$-66.7 \pm 3.26$ (28)
Distal colon	$2.38 \pm 0.24$ (27)	$3.01 \pm 0.35$ (37)	$-68.71 \pm 2.76$ (27)	$-62.87 \pm 3.01$ (37)

#### *Enhanced expression of ENaC in $APC^{Min/+}$*

The large increase in  $Na^+$  absorption in the  $APC^{Min/+}$  colon may be due to an increase in ENaC-activity or enhanced expression of the three  $\alpha$ -,  $\beta$ -,  $\gamma$ -ENaC subunits. Immunostaining of all three ENaC-subunits was performed in proximal and distal colon (Figure 4). In contrast to wt animals,  $\alpha$ -,  $\beta$ -,  $\gamma$ -ENaC were clearly detectable in proximal colon of  $APC^{Min/+}$  mice (Figure 4A), and in the distal colon of  $APC^{Min/+}$  mice expression of  $\alpha$ -,  $\beta$ -,  $\gamma$ -ENaC was enhanced when compared to wt animals (Figure 4B). Thus, enhanced  $Na^+$  transport in the colon of  $APC^{Min/+}$  mice is due to an increase in ENaC expression. Quantification of total protein prepared from isolated colonic crypts showed an increase in  $\gamma$ -ENaC protein expression in proximal and distal colon of  $APC^{Min/+}$  mice (Figure 5D, E). Quantitative real time PCR analysis indicated enhanced expression of mRNA for  $\beta$ - and  $\gamma$ -ENaC in proximal and distal colon of  $APC^{Min/+}$  mice (Figure 5A, B).

Upregulation of the protein kinase B (Akt) in tumors of  $APC^{Min/+}$  mice has been reported previously, and patients with colorectal carcinoma have elevated levels of Akt and cytoplasmic  $\beta$ -catenin (Dihlmann et al., 2005, Moran et al., 2004). Because Akt increases ENaC activity (Lee et al., 2007), ENaC could be upregulated in the colon of  $APC^{Min/+}$  mice due to an increase in phospho-Akt. Western blot analysis indicated upregulation of activated Akt-P-Thr308 (p-Akt) in



$APC^{Min/+}$  mice in tumor tissues (polyp), but not in unaffected colonic mucosa (crypt) of  $APC^{Min/+}$  and wt mice (Figure 6A), suggesting that Akt may play a minor role in activating ENaC in  $APC^{Min/+}$  mice.

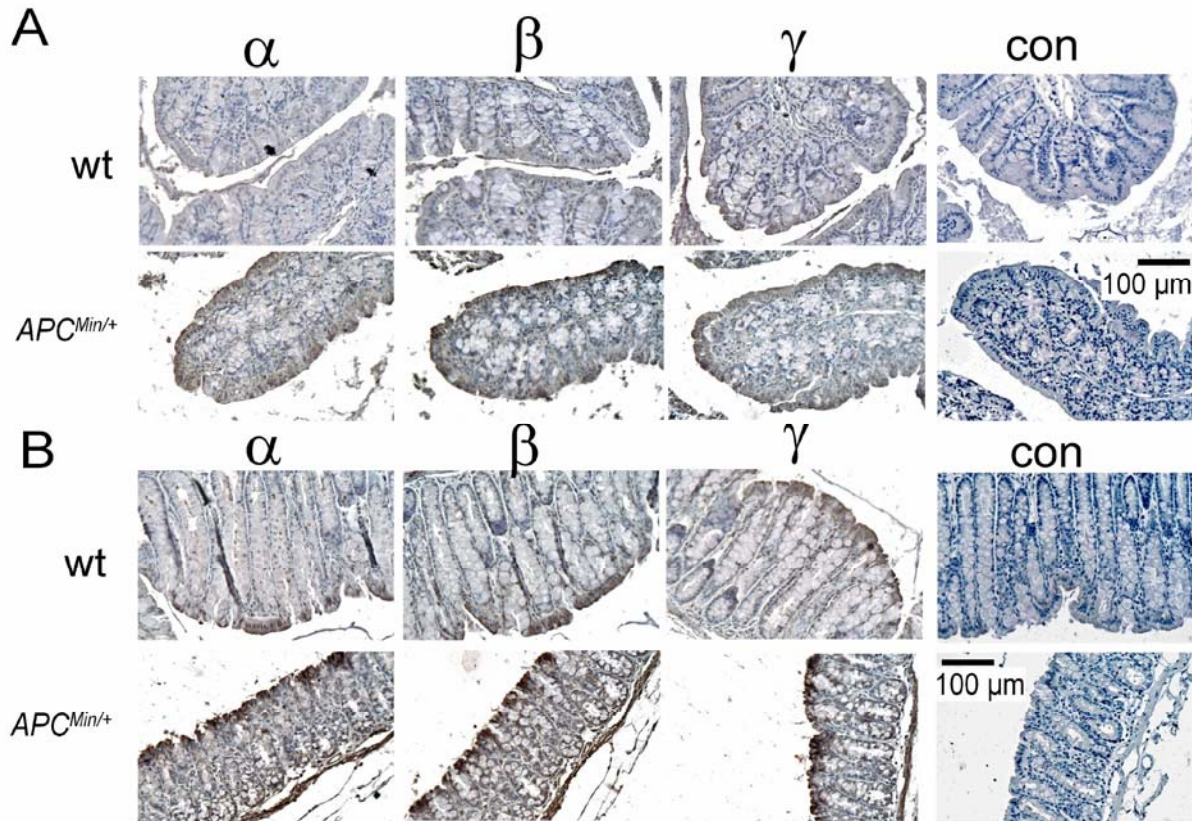


**Figure 4** Expression of ENaC in the colon of  $APC^{Min/+}$  mice. Expression of  $\alpha$ -,  $\beta$ -, and  $\gamma$ -subunits of the epithelial  $Na^+$  channel ENaC in proximal (A) and distal colon (B) of wt and  $APC^{Min/+}$  mice. No staining was obtained in the absence of primary antibodies (con).

*Enhanced  $K^+$  channel activity in  $APC^{Min/+}$  mice is not due to upregulation of  $BK\alpha$  or Eag-1*

Currents through voltage-gated Eag-1 and large conductance  $Ca^{2+}$ -activated  $BK$  channels are enhanced in the colon of  $APC^{Min/+}$  mice (Figure 3). Using real time RT-PCR, we found no increase in mRNA expression of the channel forming  $BK\alpha$  subunit or Eag-1 in  $APC^{Min/+}$  mice (Figure 6B, C). Similarly, expression of Eag-1 protein was unchanged in  $APC^{Min/+}$  animals and no obvious difference was found for  $BK\alpha$  localized in the membrane of colonic crypt cells of wt and  $APC^{Min/+}$  (Figure 6D, E). However, for  $BK$  channels the regulatory  $\beta 1$ - and  $\beta 2$ -subunits were found to be upregulated in the distal colon of  $APC^{Min/+}$  mice (Figure 6C), which probably explains the enhanced  $Ca^{2+}$  activated  $K^+$  currents in the distal colon of  $APC^{Min/+}$  mice (Figure 3F).

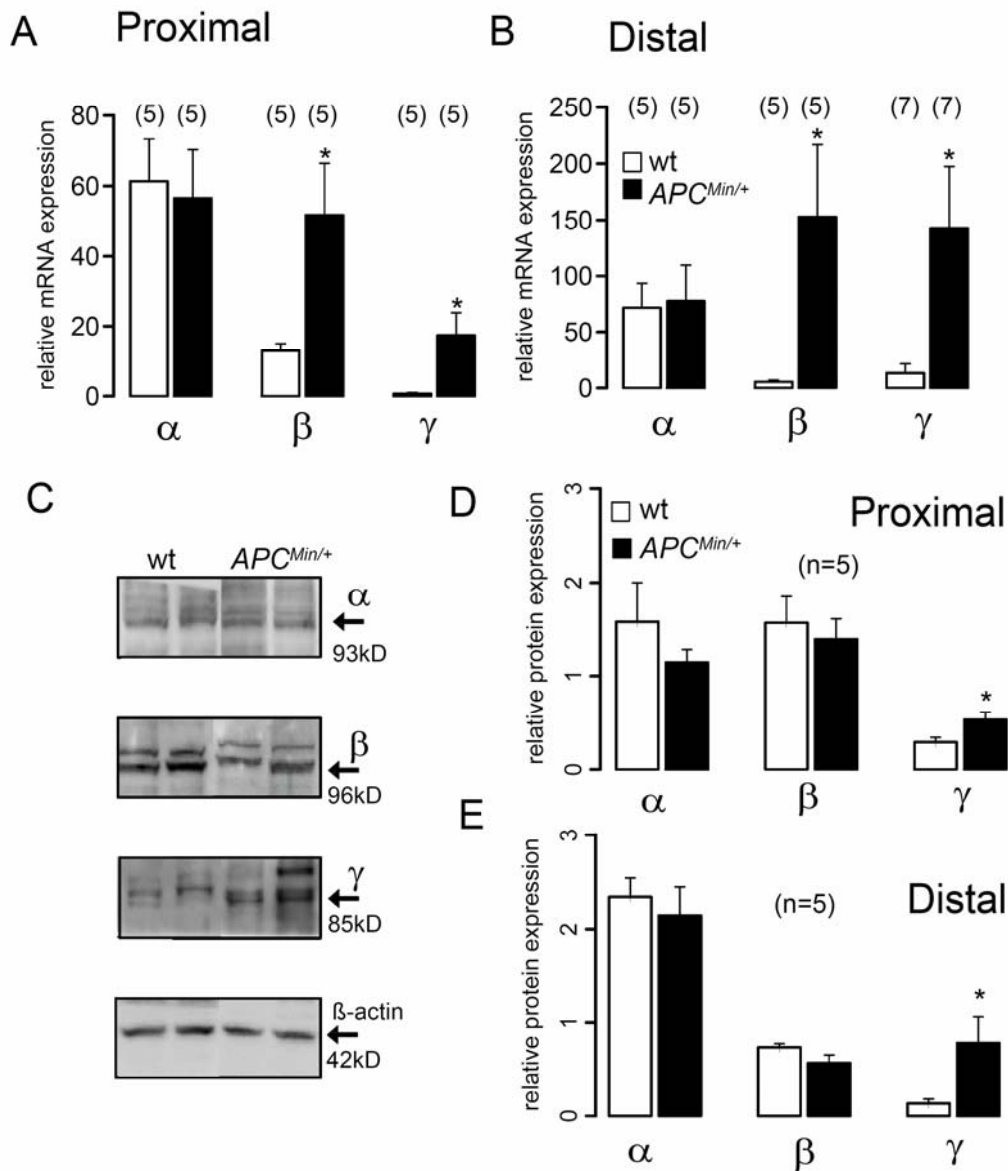


**Figure 5.** Expression of ENaC in the colon of  $APC^{Min/+}$  mice. A), B) Summary of the results from real time PCR analysis indicates upregulation of mRNA expression for  $\beta$ -ENaC and  $\gamma$ -ENaC in proximal and distal colon of  $APC^{Min/+}$  and control mice. C) Western blot analysis of the three  $\alpha$ -,  $\beta$ -, and  $\gamma$ -subunits of the epithelial  $Na^+$  channel ENaC in isolated distal colonic crypts. (D), (E) Summary of the expression of  $\alpha$ -,  $\beta$ -, and  $\gamma$ -ENaC in proximal and distal colon of wt and  $APC^{Min/+}$  mice. Asterisks indicate significant differences compared to control (Student's  $t$ -test). Number of mice = 5.

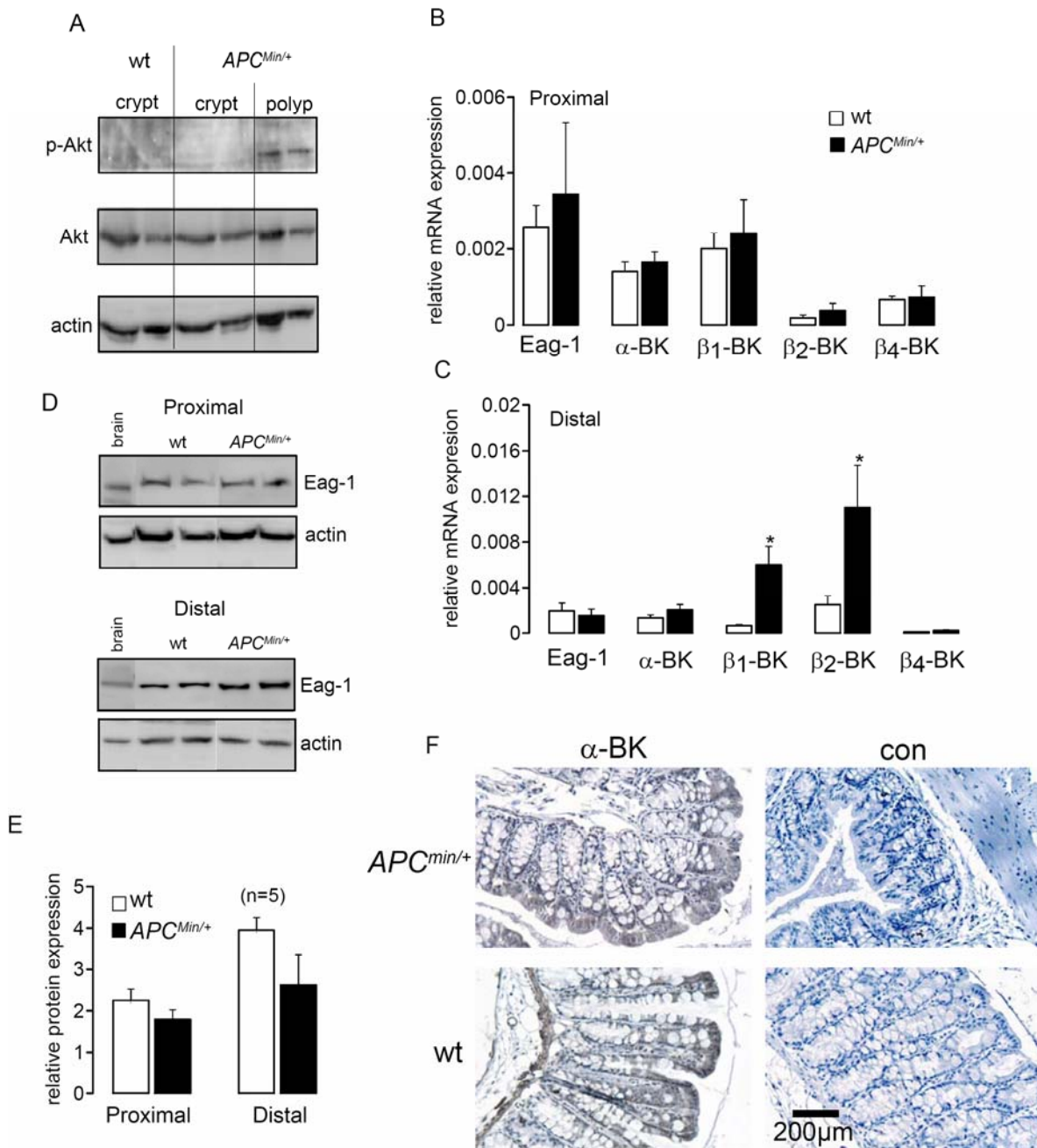


**Figure 6.** Expression of Akt, Eag-1 and BK in the colonic epithelium of  $APC^{Min/+}$  mice. A) Western blot analysis of Akt and activated phospho-Akt (Akt-P-Thr308) in unaffected mucosa and polyps. B), C) Results from quantitative analysis of mRNA expression for Eag-1 and  $\alpha/\beta$  subunits of BK channels in isolated crypts from proximal (B) and distal (C) colon. D), E) Western blot analysis of expression of Eag-1 protein in isolated crypts from proximal and distal colon (D) and quantitative comparison between wild type and  $APC^{Min/+}$  mice (E). F) Staining of  $\alpha$  subunit of BK channels in colonic epithelium of  $APC^{Min/+}$  mice and control animals. Asterisks indicate significant differences compared to control (Student's *t*-test). (Number of mice).



## DISCUSSION

### *Mutations in the APC gene reduce apoptosis and cause colonic cancer*

According to the classical Knudson' two hit model both alleles of a tumor suppressor gene need to be mutated to trigger cancer. In contrast haploinsufficiency predicts a gene dosage effect along with additional oncogenic mutations, loss of tumor suppressors or epigenetic changes that are required for tumor formation (Fodde and Smits, 2002). Heterozygous mutations in the gene encoding the adenomatosis polyposis coli (*APC*) protein are found at early stages of sporadic colorectal cancers, and are the cause for familial adenomatosis polyposis (Nathke, 2006, Su et al., 1992). *APC* has a clear role in mediating phosphorylation and degradation of  $\beta$ -catenin. Consequently loss of *APC* leads to accumulation of  $\beta$ -catenin at adherens junctions and reduced ability of epithelial cells to traverse the crypts. *APC* mutations inhibit apoptosis by allowing constitutive survivin expression. Thus the cells remain in the crypts for an extended period of time, with the potential to receive additional toxic signals (Zhang et al., 2001). Genetic instability of those crypt cells is reflected by a high anaphase bridge index with enhanced tolerance (Aoki et al., 2003, Nathke, 2006).

### *$APC^{Min/+}$ reduced apoptosis and enhanced $Na^+$ absorption*

We analyzed changes in colonic ion transport occurring in heterozygous  $APC^{Min/+}$  mice, since previous reports suggested a role of ion channels for cell proliferation and tumor formation (Kunzelmann, 2005). The remarkable upregulation of colonic  $Na^+$  absorption in  $APC^{Min/+}$  animals may be due to several reasons. i) Obviously the mammalian target of the rapamycin (mTOR) pathway is upregulated in  $APC^{Min/+}$ , which may lead to enhanced transcription of  $\alpha$ -,  $\beta$ -,  $\gamma$ -ENaC subunits (Land et al., 2007). Notably in preliminary experiments with  $APC^{Min/+}$  animals, which received the mTOR inhibitor rapamycin  $Na^+$  absorption and abnormal  $K^+$  channel expression was abolished (unpublished from the authors laboratory). ii) Although cytosolic accumulation of  $\beta$ -catenin and Akt-p-Thr308 were only observed in adenomas (Kongkanuntn et al., 1999, Moran et al., 2004), low levels of Akt-p-Thr308 in normal crypts of  $APC^{Min/+}$  mice may contribute to enhanced ENaC activity, due to a mechanism that involves phosphorylation of the ubiquitin ligase Nedd4-2 by Akt (Lee et al., 2007). iii) Expression of ENaC increases with differentiation and aging of the cells present in the surface epithelium. Reduced apoptosis in  $APC^{Min/+}$  may expand the pool of ENaC expressing epithelial cells in the surface epithelium and the upper crypt.

### *Role of $Na^+$ absorption in colonic cancer*

In the present study the animals received a chow enriched with highly saturated lipids, known to promote epithelial lesions and neoplasia (Rao et al., 2001). High fat / low fiber diet is often accompanied by constipation representing another cancer promoting factor (Sonnenberg and Muller, 1993), although the role of chronic constipation for cancer development is discussed controversially (Chan et al., 2007, Kune et al., 1988). On the other hand, colonic polyposis and colorectal cancer is often accompanied by stool irregularities and constipation (Weitz et al., 2005). The augmented  $Na^+$  absorption in  $APC^{Min/+}$  mice is likely to cause dehydration of the feces and constipation. Occasionally we observed symptoms of intestinal occlusion and rectal prolaps in  $APC^{Min/+}$  animals. Another mouse model of colonic carcinogenesis that made use of chemical carcinogens, also produced enhanced  $Na^+$  absorption (Davies et al., 1987). However reduced  $Na^+$  absorption has been found during acute application of the carcinogens, probably due to induction of an inflammation (Bleich et al., 1997, Ousingsawat et al., 2007). Colonic inflammation like in ulcerative colitis has been shown to reduce electrogenic  $Na^+$  transport and ENaC expression (Amasheh et al., 2004, Barmeyer et al., 2004).

### *Enhanced Eag-1 and $Ca^{2+}$ -activated $K^+$ currents in $APC^{Min/+}$ mice*

Apart from the change in  $Na^+$  absorption, we present evidence for upregulation of potassium currents in the colonic epithelium of  $APC^{Min/+}$  mice. These Eag-1 and BK channels were shown to support proliferation of colonic cancer cells *in vitro*, and are expressed in samples of human colorectal cancer as well as colonic epithelium of carcinogen treated mice (Kunzelmann, 2005, Lastraioli et al., 2004, Ousingsawat et al., 2007, Pardo, 2004, Spitzner et al., 2007, Yao and Kwan, 1999). The present results provide further evidence for a contribution of  $K^+$  currents to development of cancer (Kunzelmann, 2005). How are these channels activated by APC, since we did not detect a change in transcripts or total protein for Eag-1. It is likely that Eag-1 is regulated by  $\beta$ -catenin or Akt, since a close member of the same family of voltage-gated  $K^+$  channels, Erg, has been shown to be activated by Akt (Zhang et al., 2003). It is known that mutations in the APC gene alter cell cycle regulation, probably through upregulation of Erk-signaling (Dikovskaya et al., 2007). Since Eag-1 is a cell cycle regulated  $K^+$  channel, it is likely that these changes affect Eag-1 activity.

Upregulation of Akt may also increase the activity of  $Ca^{2+}$ -activated  $K^+$  channels, since membrane trafficking of BK channels was shown to be enhanced by Akt in a PI3-kinase dependent manner in neurons (Chae et al., 2005). PI3-kinase dependent regulation of BK was also found in mouse distal colon (Puntheeranurak et al., 2006). Apart from that  $\beta 1$  and  $\beta 2$

subunits of BK channels were largely increased in the distal colon of *APC<sup>Min/+</sup>* animals (Figure 5). Both channel subunits are known to increase apparent  $\text{Ca}^{2+}$  and estradiol sensitivity of BK channels (Valverde et al., 1999b). Taken together, enhanced activity of cell cycle regulated Egr-1 channels and large conductance  $\text{Ca}^{2+}$ -activated  $\text{K}^{+}$  channels are closely correlated with malignancy, and are associated with adverse outcome and reduced overall survival of patients (Ousingsawat et al., 2007). Thus the present results may provide a basis for new therapeutic strategies for the treatment of colonic cancer.



## SUMMARY

Potassium channels have been reported to control cell cycling and proliferation. Cancer cells *in vitro* and native malignant tissues show increased expression of various types of K<sup>+</sup> channels such as K<sub>v</sub>, Eag-1, Erg-1, BK and TASK-3. Here, we demonstrate a contribution of K<sup>+</sup> channels to proliferation and development of prostate and colonic cancer. Patch clamp and Ussing chamber experiments were performed in cell lines and animal tissues, and rectal potentials were measured in mice *in vivo*. With the use of K<sup>+</sup> channel activators and blockers as well as RNA interference techniques, we were able to identify functional expression of several types of K<sup>+</sup> channels. Moreover, semiquantitative RT-PCR, real time-PCR, Western blots, and immunohistochemistry were applied to quantify mRNA and expression of ion channel proteins.

### **Large conductance Ca<sup>2+</sup>-activated K<sup>+</sup> channels promote proliferation of human prostate cancer cells**

The *KCNMA1* gene encoding the  $\alpha$ -subunit of BK channels is amplified and BK channel expression was enhanced in late-stage, metastatic and hormone-refractory human prostate cancer tissues, whereas benign prostate tissues showed only a weak expression of BK channels. The role of BK channels for proliferation of late stage prostate cancer was examined in PC-3 cells, representing the hormone-insensitive prostate cancer, and was compared with hormone-sensitive prostate cancer cells (LNCaP) and the benign prostate hyperplasia cell line (BPH-1). PC-3 cells, but not LNCaP and BPH-1 cells, showed an amplification of *the KCNMA1* gene and enhanced mRNA and protein levels for BK channels. Iberitoxin, a specific BK channel blocker, inhibited whole cell currents and growth of PC-3 cells. This inhibitory effect was mimicked by downregulation of BK mRNA. BK channels were detected in excised inside/out membrane patches from PC-3 cells and were suppressed by the inhibitor paxillin and by siRNA. The BK channel activator 17 $\beta$ -estradiol did not further stimulate whole cell currents or cell proliferation in PC-3 cells, indicating maximal channel activity and hormone insensitivity of the cells. On the contrary, 17 $\beta$ -estradiol significantly enhanced both currents and proliferation in LNCaP and BPH-1 cells. These results establish a role of BK channels for proliferation of prostate cancer cells. BK channel expression in late stage prostate cancer may be used as a prognostic marker and appears as a promising target for diagnosis and therapy of prostate cancer.

### **Electrolyte transport and expression of voltage-gated K<sup>+</sup> channel are different in colonic cancer**

The role of K<sup>+</sup> channels for proliferation of colonic cancer was shown in 3 different models: i) T<sub>84</sub> human colonic carcinoma cells, ii) mouse colorectal cancer induced by chemical

carcinogens, iii) genetic mouse model of colorectal cancer ( $APC^{Min/+}$ ). Alterations in colonic electrolyte transport were found during development of colonic cancer *in vivo* and the role of  $K^+$  channels for proliferation of colonic cancer cells was assessed *in vitro*.

#### *Abnormal colonic histology in cancer mouse models*

At early stages of dimethylhydrazine (DMH) and N-methyl-N-nitrosourea (MNU) treatment, histology demonstrated inflammation of the mouse colon. At later stage of carcinogen administration, changes of mucosal architecture and dysplasia were clearly observable, indicating alterations of the colonic mucosa due to treatment by DMH or MNU. Mutations in the adenomatous polyposis coli ( $APC$ ) tumor suppressor gene are found in almost all human colonic cancers, and in familial adenomatous polyposis. Heterozygous  $APC^{Min/+}$  mice developed multiple intestinal neoplasias. Abnormal distribution of  $\beta$ -catenin and enhanced levels of phospho-Akt were detected in polyps of  $APC^{Min/+}$  mice.

#### *Changes in $Na^+$ and $Cl^-$ transport in colonic cancer mouse models.*

Initial DMH or MNU treatment decreased amiloride-sensitive epithelial  $Na^+$  absorption in the colon. The initial inflammatory response in both DMH- and MNU-treated animals was similar to that observed in the colon of dextran sulfate sodium (DSS) treated animals. A reduced  $Na^+$  absorption was also detected in the inflamed DSS-colon, indicating that ENaC activity is reduced during inflammation. Similar to ENaC, cAMP-stimulated CFTR  $Cl^-$  currents were reduced at early stage of DMH, MNU or DSS treatment. Reduced  $Na^+$  absorption and  $Cl^-$  secretion in the inflamed colon are probably a result of reduced  $Na^+/K^+$  ATPase activity. In contrast to carcinogen treated mice, amiloride-sensitive ENaC currents were significantly increased in the distal colon of  $APC^{Min/+}$  mice. Enhanced colonic  $Na^+$  absorption in  $APC^{Min/+}$  mice is due to an increase in mRNA and protein expression of ENaC, as identified by RT-PCR, immunohistochemistry, and Western blotting. Upregulation of ENaC in  $APC^{Min/+}$  mice may be due to upregulation of the mammalian target of rapamycin (mTOR) and Akt, as well as reduction of apoptosis. Taken together, inflammation reduces  $Na^+$  absorption and promotes diarrhea, which is often observed during colitis. Conversely, colonic polyposis is often accompanied by stool irregularities. The increase in colonic  $Na^+$  absorption in  $APC^{Min/+}$  mice may contribute to dehydration of the feces and constipation.

#### *Mouse models for colonic cancer show pathological expression of $K^+$ channels in the colonic epithelium*

We demonstrated a role of  $K_v$  and BK channels for development of colonic cancer both *in vitro* and *in vivo*. In T<sub>84</sub> human colonic cancer cells, we detected molecular and functional expression of voltage-gated  $K^+$  channels ( $K_v1.3$ ,  $K_v1.5$ ,  $K_v3.3/3.4$ ,  $K_vLQT$ , Eag-1, Erg-1) and  $Ca^{2+}$ -activated  $K^+$  channels (BK, SK4).  $K_v$  channel blockers inhibited cell proliferation in a concentration-dependent manner. Downregulation of Eag-1 expression by siRNA

significantly reduced proliferation, while blockers of  $\text{Ca}^{2+}$ -activated  $\text{K}^+$  channels and siRNA inhibition of SK4 did not affect proliferation of  $\text{T}_{84}$  cells. The results indicate that only  $\text{K}_v$  channels ( $\text{K}_v3.4$ ,  $\text{K}_v1.5$  and Eag-1) support proliferation of  $\text{T}_{84}$  cells. These channels assist in regulation of intracellular pH and cellular  $\text{Ca}^{2+}$  signaling, since the blockers 4-AP and astemizole reduced pH regulatory capacity and attenuated  $\text{Ca}^{2+}$  release from intracellular stores as well as  $\text{Ca}^{2+}$  influx through stored-operated  $\text{Ca}^{2+}$  channels. We also found enhanced  $\text{K}_v$  channel activity in the colon of DMH- and MNU animals. The inhibitory effects of the  $\text{K}_v$  blockers 4-AP and astemizole were significantly higher in the carcinogen treated animals. Thus,  $\text{K}_v1.3$ ,  $\text{K}_v1.5$ ,  $\text{K}_v3.1$  and members of the EAG-family are enhanced in the premalignant colon induced by chemical carcinogens. In the  $\text{APC}^{\text{Min/+}}$  model, increased astemizole-sensitive transport was observed in the proximal colon, indicating the presence of EAG family members. Apart from EAG, BK channel currents were significantly increased in the distal colon of  $\text{APC}^{\text{Min/+}}$  mice. Enhanced BK channel activity in  $\text{APC}^{\text{Min/+}}$  mice is likely due to an increase in transcription of the regulatory  $\beta 1$  and  $\beta 2$  subunits. Notably, high mRNA expression of BK channel  $\beta$ -subunits was also observed in  $\text{T}_{84}$  cells. The increase in EAG and BK channel activity was probably due to upregulation of Akt and mTOR. Akt has been shown to activate Erg, a member of the EAG family, as well as BK channels.

#### *Eag-1 and BK expression in human colorectal and prostate carcinomas*

Eag-1 protein and mRNA was also detected in colonic crypt cells from patients with colorectal carcinomas, but was not expressed in the healthy colons. The Eag-1 gene is amplified in human colonic cancers and is associated with reduced overall survival of the patients. This may serve as an early diagnostic and prognostic marker for cancer patients. Taken together, evidence is presented for a role of  $\text{K}^+$  channels during development and growth of prostate and colonic cancer. Molecular and functional expression of  $\text{K}_v$  channels, particularly Eag-1, and  $\text{Ca}^{2+}$ -activated  $\text{K}^+$  channels was detected in the different models. These channels were shown to support proliferation and are therefore likely to support progression of premalignant tissues towards cancer. Both BK and Eag-1 are markers of adverse prognosis in patients. The present data may therefore be useful in improving diagnosis, and treatment, and may have a prognostic value in patients with prostate and colonic cancer.





## REFERENCES

- Abdul, M., Hoosein, N. (2002a) Expression and activity of potassium ion channels in human prostate cancer. *Cancer Lett.* 186, 99-105
- Abdul, M., Hoosein, N. (2002b) Voltage-gated potassium ion channels in colon cancer. *Oncol.Rep* 9, 961-964
- Abdul, M., Hoosein, N. (2002c) Voltage-gated sodium ion channels in prostate cancer: expression and activity. *Anticancer Res* 22, 1727-1730
- Abdul, M., Santo, A., Hoosein, N. (2003) Activity of potassium channel-blockers in breast cancer. *Anticancer Res.* 23, 3347-3351
- Ahn, S., Nelson, C. D., Garrison, T. R., Miller, W. E., Lefkowitz, R. J. (2003) Desensitization, internalization, and signaling functions of beta-arrestins demonstrated by RNA interference. *Proc.Natl.Acad.Sci.U.S.A* 100, 1740-1744
- Amasheh, S., Barmeyer, C., Koch, C. S., Tavalali, S., Mankertz, J., Eppele, H. J., Gehring, M. M., Florian, P., Kroesen, A. J., Zeitz, M., Fromm, M., Schulzke, J. D. (2004) Cytokine-dependent transcriptional down-regulation of epithelial sodium channel in ulcerative colitis. *Gastroenterology* 126, 1711-1720
- Amberg, G. C., Bonev, A. D., Rossow, C. F., Nelson, M. T., Santana, L. F. (2003) Modulation of the molecular composition of large conductance,  $\text{Ca}^{2+}$  activated  $\text{K}^{+}$  channels in vascular smooth muscle during hypertension. *J.Clin.Invest.* 112, 717-724
- Amberg, G. C., Santana, L. F. (2003) Downregulation of the BK channel beta1 subunit in genetic hypertension. *Circ.Res.* 93, 965-971
- Amigorena, S., Choquet, D., Teillaud, J. L., Korn, H., Fridman, W. H. (1990) Ion channel blockers inhibit B cell activation at a precise stage of the G1 phase of the cell cycle. Possible involvement of  $\text{K}^{+}$  channels. *J Immunol.* 144, 2038-2045
- Aoki, K., Tamai, Y., Horiike, S., Oshima, M., Taketo, M. M. (2003) Colonic polyposis caused by mTOR-mediated chromosomal instability in  $\text{Apc}^{+/Delta716} \text{Cdx2}^{+/-}$  compound mutant mice. *Nat.Genet.* 35, 323-330
- Arcangeli, A., Bianchi, L., Becchetti, A., Faravelli, L., Coronello, M., Mini, E., Olivotto, M., Wanke, E. (1995) A novel inward-rectifying  $\text{K}^{+}$  current with a cell-cycle dependence governs the resting potential of mammalian neuroblastoma cells. *J Physiol* 489, 455-471
- Barmeyer, C., Harren, M., Schmitz, H., Heinzl-Pleines, U., Mankertz, J., Seidler, U., Horak, I., Wiedenmann, B., Fromm, M., Schulzke, J. D. (2004) Mechanisms of diarrhea in the interleukin-2-deficient mouse model of colonic inflammation. *Am.J Physiol Gastrointest.Liver Physiol* 286, G244-G252
- Barriere, H., Poujeol, C., Tauc, M., Blasi, J. M., Counillon, L., Poujeol, P. (2001) CFTR modulates programmed cell death by decreasing intracellular pH in Chinese hamster lung fibroblasts. *Am J Physiol* 281, C810-C824

- Basrai, D., Kraft, R., Bollensdorff, C., Liebmann, L., Benndorf, K., Patt, S. (2002) BK channel blockers inhibit potassium-induced proliferation of human astrocytoma cells. *Neuroreport* 13, 403-407
- Baxter, D. F., Kirk, M., Garcia, A. F., Raimondi, A., Holmqvist, M. H., Flint, K. K., Bojanic, D., Distefano, P. S., Curtis, R., Xie, Y. (2002) A novel membrane potential-sensitive fluorescent dye improves cell-based assays for ion channels. *J Biomol.Screen.* 7, 79-85
- Bernardino, J., Bourgeois, C. A., Muleris, M., Dutrillaux, A. M., Malfoy, B., Dutrillaux, B. (1997) Characterization of chromosome changes in two human prostatic carcinoma cell lines (PC-3 and DU145) using chromosome painting and comparative genomic hybridization. *Cancer Genet.Cytogenet.* 96, 123-128
- Berridge, M. J. (1995) Calcium signalling and cell proliferation. *Bioessays.* 17, 491-500
- Berridge, M. J., Bootman, M. D., Lipp, P. (1998) Calcium--a life and death signal. *Nature* 395, 645-648
- Bianchi, L., Wible, B., Arcangeli, A., Taglialatela, M., Morra, F., Castaldo, P., Crociani, O., Rosati, B., Faravelli, L., Olivotto, M., Wanke, E. (1998) herg encodes a K<sup>+</sup> current highly conserved in tumors of different histogenesis: a selective advantage for cancer cells? *Cancer Res.* 58, 815-822
- Bleich, M., Ecke, D., Schwartz, B., Fraser, G., Greger, R. (1997) Effects of the carcinogen dimethylhydrazine (DMH) on the function of rat colonic crypts. *Pflügers Arch* 433, 254-259
- Bleich, M., Riedemann, N., Warth, R., Kerstan, D., Leipziger, J., Hor, M., Driessche, W. V., Greger, R. (1996) Ca<sup>2+</sup> regulated K<sup>+</sup> and non-selective cation channels in the basolateral membrane of rat colonic crypt base cells. *Pflügers Arch* 432, 1011-1022
- Bleich, M., Warth, R. (2000) The very small-conductance K<sup>+</sup> channel K<sub>v</sub>LQT1 and epithelial function. *Pflügers Arch* 440, 202-206
- Bloch, M., Ousingsawat, J., Simon, R., Schraml, P., Gasser, T. C., Mihatsch, M. J., Kunzelmann, K., Bubendorf, L. (2007) *KCNMA1* gene amplification promotes tumor cell proliferation in human prostate cancer. *Oncogene.* 26, 2525-2534
- Bortner, C. D., Hughes, F. M. Jr., Cidlowski, J. A. (1997) A primary role for K<sup>+</sup> and Na<sup>+</sup> efflux in the activation of apoptosis. *J Biol Chem* 272, 32436-32442
- Bregestovski, P., Medina, I., Goyda, E. (1992) Regulation of potassium conductance in the cellular membrane at early embryogenesis. *J.Physiol Paris.* 86, 109-115
- Burckhardt, B. C., Gögelein, H. (1992) Small and maxi K<sup>+</sup> channels in the basolateral membrane of isolated crypts from rat distal colon: single-channel and slow whole-cell recordings. *Pflügers Arch* 420, 54-60
- Burg, E. D., Remillard, C. V., Yuan, J. X. (2006) K<sup>+</sup> channels in apoptosis. *J.Membr.Biol.* 209, 3-20

- Calderone, V. (2002) Large-conductance,  $\text{Ca}^{2+}$ -activated  $\text{K}^+$  channels: function, pharmacology and drugs. *Curr.Med.Chem.* 9, 1385-1395
- Camacho, J. (2006) *Ether à go-go* potassium channels and cancer. *Cancer Lett.* 233, 1-9
- Cao, Y. J., Dreixler, J. C., Couey, J. J., Houamed, K. M. (2002) Modulation of recombinant and native neuronal SK channels by the neuroprotective drug riluzole. *Eur.J Pharmacol.* 449, 47-54
- Chae, K. S., Martin-Caraballo, M., Anderson, M., Dryer, S. E. (2005) Akt activation is necessary for growth factor-induced trafficking of functional  $\text{K}_{\text{Ca}}$  channels in developing parasympathetic neurons. *J.Neurophysiol.* 93, 1174-1182
- Chan, A. O., Hui, W. M., Leung, G., Tong, T., Hung, I. F., Chan, P., Hsu, A., But, D., Wong, B. C., Lam, S. K., Lam, K. F. (2007) Patients with functional constipation do not have increased prevalence of colorectal cancer precursors. *Gut.* 56, 451-452
- Chang, K. W., Yuan, T. C., Fang, K. P., Yang, F. S., Liu, C. J., Chang, C. S., Lin, S. C. (2003) The increase of voltage-gated potassium channel  $\text{K}_v3.4$  mRNA expression in oral squamous cell carcinoma. *J Oral Pathol.Med* 32, 606-611
- Cherubini, A., Taddei, G. L., Crociani, O., Paglierani, M., Buccoliero, A. M., Fontana, L., Noci, I., Borri, P., Borrani, E., Giachi, M., Becchetti, A., Rosati, B., Wanke, E., Olivotto, M., Arcangeli, A. (2000) HERG potassium channels are more frequently expressed in human endometrial cancer as compared to non-cancerous endometrium. *Br.J.Cancer.* 83, 1722-1729
- Christow, S. P., Bychkov, R., Schroeder, C., Dietz, R., Haller, H., Dumler, I., Gulba, D. C. (1999) Urokinase activates calcium-dependent potassium channels in U937 cells via calcium release from intracellular stores. *Eur.J.Biochem.* 265, 264-272
- Coiret, G., Borowiec, A. S., Mariot, P., Ouadid-Ahidouch, H., Matifat, F. (2007) The antiestrogen tamoxifen activates BK channels and stimulates proliferation of MCF-7 breast cancer cells. *Mol.Pharmacol.* 71, 843-851
- Coiret, G., Matifat, F., Hague, F., Ouadid-Ahidouch, H. (2005) 17-beta-Estradiol activates maxi-K channels through a non-genomic pathway in human breast cancer cells. *FEBS Lett.* 579, 2995-3000
- Conti, M. (2004) Targeting  $\text{K}^+$  channels for cancer therapy. *J Exp Ther.Oncol.* 4, 161-166
- Crociani, O., Guasti, L., Balzi, M., Becchetti, A., Wanke, E., Olivotto, M., Wymore, R. S., Arcangeli, A. (2003) Cell cycle-dependent expression of HERG1 and HERG1B isoforms in tumor cells. *J Biol Chem* 2003.Jan.31.;278.(5.):2947.-55. 278, 2947-2955
- Cruse, G., Duffy, S. M., Brightling, C. E., Bradding, P. (2006) Functional  $\text{K}_{\text{Ca}}3.1$   $\text{K}^+$  channels are required for human lung mast cell migration. *Thorax.* 61, 880-885
- Czarnecki, A., Dufy-Barbe, L., Huet, S., Odessa, M. F., Bresson-Bepoldin, L. (2003) Potassium channel expression level is dependent on the proliferation state in the GH3 pituitary cell line. *Am.J Physiol Cell Physiol* 284, C1054-C1064

- Davies, A. G., Pierce-Shimomura, J. T., Kim, H., VanHoven, M. K., Thiele, T. R., Bonci, A., Bargmann, C. I., McIntire, S. L. (2003) A central role of the BK potassium channel in behavioral responses to ethanol in *C. elegans*. *Cell*. 115, 655-666
- Davies, R. J., Sandle, G. I., Thompson, S. M. (1991) Inhibition of the Na<sup>+</sup>, K<sup>+</sup>-ATPase pump during induction of experimental colon cancer. *Cancer Biochem.Biophys*. 12, 81-94
- Davies, R. J., Weidema, W. F., Sandle, G. I., Palmer, L., Deschner, E. E., DeCosse, J. J. (1987) Sodium transport in a mouse model of colonic carcinogenesis. *Cancer Res*. 47, 4646-4650
- Day, M. L., Johnson, M. H., Cook, D. I. (1998) Cell cycle regulation of a T-type calcium current in early mouse embryos. *Pflugers Arch* 436, 834-842
- Day, M. L., Pickering, S. J., Johnson, M. H., Cook, D. I. (1993) Cell-cycle control of a large-conductance K<sup>+</sup> channel in mouse early embryos. *Nature* 365, 560-562
- Devor, D. C., Singh, A. K., Gerlach, A. C., Frizzell, R. A., Bridges, R. J. (1997) Inhibition of intestinal Cl<sup>-</sup> secretion by clotrimazole: direct effect on basolateral membrane K<sup>+</sup> channels. *Am J Physiol*. 273, C531-C540
- Dihlmann, S., Kloor, M., Fallsehr, C., von Knebel, D. M. (2005) Regulation of Akt1 expression by beta-catenin/Tcf/Lef signaling in colorectal cancer cells. *Carcinogenesis*. 26, 1503-1512
- Dikovskaya, D., Schiffmann, D., Newton, I. P., Oakley, A., Kroboth, K., Jamieson, T. J., Meniel, V., Clarke, A., Sansom, O., Nathke, I. S. (2007) Loss of APC induces polyploidy as a result of a combination of defects in mitosis and apoptosis. *J.Cell Biol*. 176, 183-195
- Diochot, S., Schweitz, H., Beress, L., Lazdunski, M. (1998) Sea anemone peptides with a specific blocking activity against the fast inactivating potassium channel K<sub>v</sub>3.4. *J Biol Chem* 273, 6744-6749
- Diwan, B. A., Blackman, K. E. (1980) Differential susceptibility of 3 sublines of C57BL/6 mice to the induction of colorectal tumors by 1,2-dimethylhydrazine. *Cancer Lett*. 9, 111-115
- Dubois, J. M., Rouzaire-Dubois, B. (2004) The influence of cell volume changes on tumour cell proliferation. *Eur.Biophys J* 33, 227-232
- El Gedaily, A., Bubendorf, L., Willi, N., Fu, W., Richter, J., Moch, H., Mihatsch, M. J., Sauter, G., Gasser, T. C. (2001) Discovery of new DNA amplification loci in prostate cancer by comparative genomic hybridization. *Prostate*. 46, 184-190
- Elbashir, S. M., Harborth, J., Lendeckel, W., Yalcin, A., Weber, K., Tuschl, T. (2001) Duplexes of 21-nucleotide RNAs mediate RNA interference in cultured mammalian cells. *Nature* 411, 494-498
- Elble, R. C., Pauli, B. U. (2001) Tumor suppression by a proapoptotic calcium-activated chloride channel in mammary epithelium. *J Biol Chem* 276, 40510-40517
- Ellis, R. J. (2001) Macromolecular crowding: obvious but underappreciated. *Trends Biochem Sci*. 26, 597-604

- Elso, C. M., Lu, X., Culiati, C. T., Rutledge, J. C., Cacheiro, N. L., Generoso, W. M., Stubbs, L. J. (2004) Heightened susceptibility to chronic gastritis, hyperplasia and metaplasia in *Kcnq1* mutant mice. *Hum.Mol.Genet.* 13, 2813-2821
- Enomoto, K., Cossu, M. F., Maeno, T., Edwards, C., Oka, T. (1986) Involvement of the  $\text{Ca}^{2+}$ -dependent  $\text{K}^+$  channel activity in the hyperpolarizing response induced by epidermal growth factor in mammary epithelial cells. *FEBS Lett.* 203, 181-184
- Farias, L. M., Ocana, D. B., Diaz, L., Larrea, F., Avila-Chavez, E., Cadena, A., Hinojosa, L. M., Lara, G., Villanueva, L. A., Vargas, C., Hernandez-Gallegos, E., Camacho-Arroyo, I., Duenas-Gonzalez, A., Perez-Cardenas, E., Pardo, L. A., Morales, A., Taja-Chayeb, L., Escamilla, J., Sanchez-Pena, C., Camacho, J. (2004a) *Ether à go-go* potassium channels as human cervical cancer markers. *Cancer Res.* 64, 6996-7001
- Farias, L. M., Ocana, D. B., Diaz, L., Larrea, F., Avila-Chavez, E., Cadena, A., Hinojosa, L. M., Lara, G., Villanueva, L. A., Vargas, C., Hernandez-Gallegos, E., Camacho-Arroyo, I., Duenas-Gonzalez, A., Perez-Cardenas, E., Pardo, L. A., Morales, A., Taja-Chayeb, L., Escamilla, J., Sanchez-Pena, C., Camacho, J. (2004b) *Ether à go-go* potassium channels as human cervical cancer markers. *Cancer Res.* 64, 6996-7001
- Fiala, E. S. (1977) Investigations into the metabolism and mode of action of the colon carcinogens 1,2-dimethylhydrazine and azoxymethane. *Cancer* 40, 2436-2445
- Fieber, L. A. (2003) Voltage-Gated ion currents of schwann cells in cell culture models of human neurofibromatosis. *J.Exp.Zoolog.A Comp Exp.Biol.* 300, 76-83
- Fischer, K. G., Leipziger, J., Rubini-Illes, P., Nitschke, R., Greger, R. (1996) Attenuation of stimulated  $\text{Ca}^{2+}$  influx in colonic epithelial (HT<sub>29</sub>) cells by cAMP. *Pflugers Arch.* 432, 735-740
- Fodde, R., Edelmann, W., Yang, K., van Leeuwen, C., Carlson, C., Renault, B., Breukel, C., Alt, E., Lipkin, M., Khan, P. M. (1994) A targeted chain-termination mutation in the mouse *Apc* gene results in multiple intestinal tumors. *Proc.Natl.Acad.Sci.U.S.A* 91, 8969-8973
- Fodde, R., Smits, R. (2002) Cancer biology. A matter of dosage. *Science.* 298, 761-763
- Frei, J. V., Swenson, D. H., Warren, W., Lawley, P. D. (1978) Alkylation of deoxyribonucleic acid in vivo in various organs of C57BL mice by the carcinogens N-methyl-N-nitrosourea, N-ethyl-N-nitrosourea and ethyl methanesulphonate in relation to induction of thymic lymphoma. Some applications of high-pressure liquid chromatography. *Biochem.J.* 174, 1031-1044
- Galvez, A., Gimenez-Gallego, G., Reuben, J. P., Roy-Contancin, L., Feigenbaum, P., Kaczorowski, G. J., Garcia, M. L. (1990) Purification and characterization of a unique, potent, peptidyl probe for the high conductance calcium-activated potassium channel from venom of the scorpion *Buthus tamulus*. *J.Biol.Chem.* 265, 11083-11090
- Gamper, N., Fillon, S., Huber, S. M., Feng, Y., Kobayashi, T., Cohen, P., Lang, F. (2002) IGF-1 up-regulates  $\text{K}^+$  channels via PI3-kinase, PDK1 and SGK1. *Pflugers Arch* 443, 625-634
- Garcia-Ferreiro, R. E., Kerschensteiner, D., Major, F., Monje, F., Stühmer, W., Pardo, L. A. (2004) Mechanism of Block of hEag1  $\text{K}^+$  Channels by Imipramine and Astemizole. *J Gen Physiol* 124, 301-317

- Gessner, G., Schonherr, K., Soom, M., Hansel, A., Asim, M., Baniahmad, A., Derst, C., Hoshi, T., Heinemann, S. H. (2005) BK<sub>Ca</sub> channels activating at resting potential without calcium in LNCaP prostate cancer cells. *J Membr.Biol.* 208, 229-240
- Ghiani, C. A., Yuan, X., Eisen, A. M., Knutson, P. L., DePinho, R. A., McBain, C. J., Gallo, V. (1999) Voltage-activated K<sup>+</sup> channels and membrane depolarization regulate accumulation of the cyclin-dependent kinase inhibitors p27<sup>Kip1</sup> and p21<sup>CIP1</sup> in glial progenitor cells. *J Neurosci.* 19, 5380-5392
- Goldstein, S. A., Bayliss, D. A., Kim, D., Lesage, F., Plant, L. D., Rajan, S. (2005) International Union of Pharmacology. LV. Nomenclature and molecular relationships of two-P potassium channels. *Pharmacol.Rev.* 57, 527-540
- Gottlieb, R. A., Dosanjh, A. (1996) Mutant cystic fibrosis transmembrane conductance regulator inhibits acidification and apoptosis in C127 cells: possible relevance to cystic fibrosis. *Proc.Natl.Acad.Sci.U.S.A.* 93, 3587-3591
- Grace, A. A., Camm, A. J. (1998) Quinidine. *N.Engl.J Med* 338, 35-45
- Greene, F. L., Lamb, L. S., Barwick, M. (1987) Colorectal cancer in animal models--a review. *J Surg.Res.* 43, 476-487
- Grishin, A., Ford, H., Wang, J., Li, H., Salvador-Recatala, V., Levitan, E. S., Zaks-Makhina, E. (2005) Attenuation of apoptosis in enterocytes by blockade of potassium channels. *Am.J Physiol Gastrointest.Liver Physiol.* 289, G815-G821
- Grissmer, S., Nguyen, A. N., Aiyar, J., Hanson, D. C., Mather, R. J., Gutman, G. A., Karmilowicz, M. J., Auperin, D. D., Chandy, K. G. (1994) Pharmacological characterization of five cloned voltage-gated K<sup>+</sup> channels, types K<sub>v</sub>1.1, 1.2, 1.3, 1.5, and 3.1, stably expressed in mammalian cell lines. *Mol.Pharmacol.* 45, 1227-1234
- Guo, T. B., Lu, J., Li, T., Lu, Z., Xu, G., Xu, M., Lu, L., Dai, W. (2005) Insulin-activated, K<sup>+</sup>-channel-sensitive Akt pathway is primary mediator of ML-1 cell proliferation. *Am.J Physiol Cell Physiol* 289, C257-C263
- Gutman, G. A., Chandy, K. G., Adelman, J. P., Aiyar, J., Bayliss, D. A., Clapham, D. E., Covarriubias, M., Desir, G. V., Furuichi, K., Ganetzky, B., Garcia, M. L., Grissmer, S., Jan, L. Y., Karschin, A., Kim, D., Kuperschmidt, S., Kurachi, Y., Lazdunski, M., Lesage, F., Lester, H. A., McKinnon, D., Nichols, C. G., O'Kelly, I., Robbins, J., Robertson, G. A., Rudy, B., Sanguinetti, M., Seino, S., Stuehmer, W., Tamkun, M. M., Vandenberg, C. A., Wei, A., Wulff, H., Wymore, R. S. (2003) International Union of Pharmacology. XLI. Compendium of voltage-gated ion channels: potassium channels. *Pharmacol.Rev.* 55, 583-586
- Gutman, G. A., Chandy, K. G., Grissmer, S., Lazdunski, M., McKinnon, D., Pardo, L. A., Robertson, G. A., Rudy, B., Sanguinetti, M. C., Stuehmer, W., Wang, X. (2005) International Union of Pharmacology. LIII. Nomenclature and molecular relationships of voltage-gated potassium channels. *Pharmacol.Rev.* 57, 473-508
- Harguindeguy, S., Orive, G., Luis, P. J., Paradiso, A., Reshkin, S. J. (2005) The role of pH dynamics and the Na<sup>+</sup>/H<sup>+</sup> antiporter in the etiopathogenesis and treatment of cancer. Two faces of the same coin--one single nature. *Biochim.Biophys.Acta.* 1756, 1-24

- Hay-Schmidt, A., Grunnet, M., Abrahamse, S. L., Knaus, H. G., Klaerke, D. A. (2003) Localization of  $\text{Ca}^{2+}$ -activated big-conductance  $\text{K}^+$  channels in rabbit distal colon. *Pflugers Arch* 446, 61-68
- Hayward, S. W., Dahiya, R., Cunha, G. R., Bartek, J., Deshpande, N., Narayan, P. (1995) Establishment and characterization of an immortalized but non-transformed human prostate epithelial cell line: BPH-1. *In Vitro Cell Dev Biol Anim* 31, 14-24
- Helenius, M. A., Saramaki, O. R., Linja, M. J., Tammela, T. L., Visakorpi, T. (2001) Amplification of urokinase gene in prostate cancer. *Cancer Res.* 61, 5340-5344
- Helenius, M. A., Savinainen, K. J., Bova, G. S., Visakorpi, T. (2006) Amplification of the urokinase gene and the sensitivity of prostate cancer cells to urokinase inhibitors. *BJU.Int.* 97, 404-409
- Henke, G., Maier, G., Wallisch, S., Boehmer, C., Lang, F. (2004) Regulation of the voltage gated  $\text{K}^+$  channel  $\text{K}_v1.3$  by the ubiquitin ligase Nedd4-2 and the serum and glucocorticoid inducible kinase SGK1. *J Cell Physiol* 199, 194-199
- Ho, S. M. (2004) Estrogens and anti-estrogens: key mediators of prostate carcinogenesis and new therapeutic candidates. *J.Cell Biochem.* 91, 491-503
- Horoszewicz, J. S., Leong, S. S., Chu, T. M., Wajsman, Z. L., Friedman, M., Papsidero, L., Kim, U., Chai, L. S., Kakati, S., Arya, S. K., Sandberg, A. A. (1980) The LNCaP cell line--a new model for studies on human prostatic carcinoma. *Prog.Clin.Biol.Res.* 37, 115-132
- Hsing, A. W., Tsao, L., Devesa, S. S. (2000) International trends and patterns of prostate cancer incidence and mortality. *Int.J Cancer* 85, 60-67
- Hughes, F. M. Jr., Bortner, C. D., Purdy, G. D., Cidlowski, J. A. (1997) Intracellular  $\text{K}^+$  suppresses the activation of apoptosis in lymphocytes. *J Biol Chem* 272, 30567-30576
- Hughes, F. M. Jr., Cidlowski, J. A. (1999) Potassium is a critical regulator of apoptotic enzymes in vitro and in vivo. *Adv Enzyme Regul.* 39, 157-171
- Izumi, H., Torigoe, T., Ishiguchi, H., Uramoto, H., Yoshida, Y., Tanabe, M., Ise, T., Murakami, T., Yoshida, T., Nomoto, M., Kohno, K. (2003) Cellular pH regulators: potentially promising molecular targets for cancer chemotherapy. *Cancer Treat.Rev.* 29, 541-549
- Jager, H., Dreker, T., Buck, A., Giehl, K., Gress, T., Grissmer, S. (2004) Blockage of intermediate-conductance  $\text{Ca}^{2+}$ -activated  $\text{K}^+$  channels inhibit human pancreatic cancer cell growth in vitro. *Mol.Pharmacol.* 65, 630-638
- Kahl, C. R., Means, A. R. (2003) Regulation of cell cycle progression by calcium/calmodulin-dependent pathways. *Endocr.Rev.* 24, 719-736
- Kaighn, M. E., Narayan, K. S., Ohnuki, Y., Lechner, J. F., Jones, L. W. (1979) Establishment and characterization of a human prostatic carcinoma cell line (PC-3). *Invest Urol.* 17, 16-23

- Kauraniemi, P., Barlund, M., Monni, O., Kallioniemi, A. (2001) New amplified and highly expressed genes discovered in the ERBB2 amplicon in breast cancer by cDNA microarrays. *Cancer Res.* 61, 8235-8240
- Kazerounian, S., Pitari, G. M., Shah, F. J., Frick, G. S., Madesh, M., Ruiz-Stewart, I., Schulz, S., Hajnoczky, G., Waldman, S. A. (2005) Proliferative signaling by store-operated calcium channels opposes colon cancer cell cytostasis induced by bacterial enterotoxins. *J Pharmacol.Exp.Ther.* 314, 1013-1022
- Kim, C. J., Cho, Y. G., Jeong, S. W., Kim, Y. S., Kim, S. Y., Nam, S. W., Lee, S. H., Yoo, N. J., Lee, J. Y., Park, W. S. (2004) Altered expression of *KCNK9* in colorectal cancers. *APMIS* 112, 588-594
- Kim, J. A., Kang, Y. S., Lee, Y. S. (2003) Role of  $\text{Ca}^{2+}$ -activated  $\text{Cl}^-$  channels in the mechanism of apoptosis induced by cyclosporin A in a human hepatoma cell line. *Biochem Biophys Res.Commun.* 309, 291-297
- Klaerke, D. A., Wiener, H., Zeuthen, T., Jorgensen, P. L. (1996) Regulation of  $\text{Ca}^{2+}$ -activated  $\text{K}^+$  channel from rabbit distal colon epithelium by phosphorylation and dephosphorylation. *J Membr.Biol* 151, 11-18
- Klimatcheva, E., Wonderlin, W. F. (1999) An ATP-sensitive  $\text{K}^+$  current that regulates progression through early G1 phase of the cell cycle in MCF-7 human breast cancer cells. *J Membr.Biol* 171, 35-46
- Knuutila, S., Autio, K., Aalto, Y. (2000) Online access to CGH data of DNA sequence copy number changes. *Am.J.Pathol.* 157, 689
- Kongkanuntn, R., Bubbs, V. J., Sansom, O. J., Wyllie, A. H., Harrison, D. J., Clarke, A. R. (1999) Dysregulated expression of beta-catenin marks early neoplastic change in *Apc* mutant mice, but not all lesions arising in *Msh2* deficient mice. *Oncogene.* 18, 7219-7225
- Kononen, J., Bubendorf, L., Kallioniemi, A., Barlund, M., Schraml, P., Leighton, S., Torhorst, J., Mihatsch, M. J., Sauter, G., Kallioniemi, O. P. (1998) Tissue microarrays for high-throughput molecular profiling of tumor specimens. *Nat.Med.* 4, 844-847
- Koochekpour, S., Zhuang, Y. J., Beroukhi, R., Hsieh, C. L., Hofer, M. D., Zhau, H. E., Hiraiwa, M., Pattan, D. Y., Ware, J. L., Luftig, R. B., Sandhoff, K., Sawyers, C. L., Pienta, K. J., Rubin, M. A., Vessella, R. L., Sellers, W. R., Sartor, O. (2005) Amplification and overexpression of prosaposin in prostate cancer. *Genes Chromosomes.Cancer.* 44, 351-364
- Kubo, Y., Adelman, J. P., Clapham, D. E., Jan, L. Y., Karschin, A., Kurachi, Y., Lazdunski, M., Nichols, C. G., Seino, S., Vandenberg, C. A. (2005) International Union of Pharmacology. LIV. Nomenclature and molecular relationships of inwardly rectifying potassium channels. *Pharmacol.Rev.* 57, 509-526
- Kune, G. A., Kune, S., Field, B., Watson, L. F. (1988) The role of chronic constipation, diarrhea, and laxative use in the etiology of large-bowel cancer. Data from the Melbourne Colorectal Cancer Study. *Dis.Colon Rectum.* 31, 507-512
- Kunzelmann, K. (2005) Ion channels and cancer. *J Membr.Biol* 205, 159-173



- Kunzelmann, K., Mall, M. Electrolyte transport in the colon: Mechanisms and implications for disease. *Physiological Reviews* 82, 245-289. 2002.
- Kuruma, A., Hartzell, H. C. (2000) Bimodal control of a  $\text{Ca}^{2+}$ -activated  $\text{Cl}^-$  channel by different  $\text{Ca}^{2+}$  signals. *J.Gen.Physiol.* 115, 59-80
- Lal, A., Lash, A. E., Altschul, S. F., Velculescu, V., Zhang, L., McLendon, R. E., Marra, M. A., Prange, C., Morin, P. J., Polyak, K., Papadopoulos, N., Vogelstein, B., Kinzler, K. W., Strausberg, R. L., Riggins, G. J. (1999) A public database for gene expression in human cancers. *Cancer Res.* 59, 5403-5407
- Lan, M., Shi, Y., Han, Z., Hao, Z., Pan, Y., Liu, N., Guo, C., Hong, L., Wang, J., Qiao, T., Fan, D. (2005) Expression of delayed rectifier potassium channels and their possible roles in proliferation of human gastric cancer cells. *Cancer Biol. Ther.* 4, 1342-1347
- Land, S. C., McTavavish, N., Wilson, S. M. (2007) Modulation of dexamethazone-evoked  $\alpha$ -ENaC expression by the mammalian target of rapamycin (mTOR). *Acta Physiologica*. 189-S653:P08-L6-14,
- Lang, F., Friedrich, F., Kahn, E., Woll, E., Hammerer, M., Waldegger, S., Maly, K., Grunicke, H. (1991) Bradykinin-induced oscillations of cell membrane potential in cells expressing the Ha-ras oncogene. *J Biol Chem* 266, 4938-4942
- Lang, F., Gulbins, E., Szabo, I., Lepple-Wienhues, A., Huber, S. M., Duranton, C., Lang, K. S., Lang, P. A., Wieder, T. (2004) Cell volume and the regulation of apoptotic cell death. *J Mol.Recognit.* 17, 473-480
- Lang, F., Ritter, M., Gamper, N., Huber, S., Fillon, S., Tanneur, V., Lepple-Wienhues, A., Szabo, I., Gulbins, E. (2000) Cell volume in the regulation of cell proliferation and apoptotic cell death. *Cell Physiol Biochem* 10, 417-428
- Lastraioli, E., Guasti, L., Crociani, O., Polvani, S., Hofmann, G., Witchel, H., Bencini, L., Calistri, M., Messerini, L., Scatizzi, M., Moretti, R., Wanke, E., Olivotto, M., Mugnai, G., Arcangeli, A. (2004) herg1 gene and HERG1 protein are overexpressed in colorectal cancers and regulate cell invasion of tumor cells. *Cancer Res.* 64, 606-611
- Lastraioli, E., Taddei, A., Messerini, L., Comin, C. E., Festini, M., Giannelli, M., Tomezzoli, A., Paglierani, M., Mugnai, G., De Manzoni, G., Bechi, P., Arcangeli, A. (2006) hERG1 channels in human esophagus: evidence for their aberrant expression in the malignant progression of Barrett's esophagus. *J.Cell Physiol.* 209, 398-404
- Lau, K. M., LaSpina, M., Long, J., Ho, S. M. (2000) Expression of estrogen receptor (ER)- $\alpha$  and ER- $\beta$  in normal and malignant prostatic epithelial cells: regulation by methylation and involvement in growth regulation. *Cancer Res.* 60, 3175-3182
- Lee, I. A., Dinudom, A., Kumor, S., Cook, D. (2007) Akt mediates the effect of insulin on epithelial sodium channels by inhibiting Nedd4-2. *under revision*.
- Lepple-Wienhues, A., Berweck, S., Bohmig, M., Leo, C. P., Meyling, B., Garbe, C., Wiederholt, M. (1996)  $\text{K}^+$  channels and the intracellular calcium signal in human melanoma cell proliferation. *J Membr.Biol* 151, 149-157

- Lhuillier, L., Dryer, S. E. (2002) Developmental regulation of neuronal  $K_{Ca}$  channels by TGF $\beta$ 1: an essential role for PI3 kinase signaling and membrane insertion. *J Neurophysiol.* 88, 954-964
- Lomax, R. B., McNicholas, C. M., Lombes, M., Sandle, G. I. (1994) Aldosterone-induced apical  $Na^+$  and  $K^+$  conductances are located predominantly in surface cells in rat distal colon. *Am.J.Physiol.* 266, G71-82
- Maeno, E., Ishizaki, Y., Kanaseki, T., Hazama, A., Okada, Y. (2000) Normotonic cell shrinkage because of disordered volume regulation is an early prerequisite to apoptosis. *Proc.Natl.Acad.Sci.U.S.A.* 97, 9487-9492
- Magni, M., Meldolesi, J., Pandiella, A. (1991) Ionic events induced by epidermal growth factor. Evidence that hyperpolarization and stimulated cation influx play a role in the stimulation of cell growth. *J.Biol.Chem.* 266, 6329-6335
- Mall, M., Bleich, M., Greger, R., Schürlein, M., Kühr, J., Seydewitz, H. H., Brandis, M., Kunzelmann, K. (1998) Cholinergic ion secretion in human colon requires co-activation by cAMP. *Am J Physiol* 275, G1274-G1281
- Masi, A., Becchetti, A., Restano-Cassulini, R., Polvani, S., Hofmann, G., Buccoliero, A. M., Paglierani, M., Pollo, B., Taddei, G. L., Gallina, P., Di Lorenzo, N., Franceschetti, S., Wanke, E., Arcangeli, A. (2005) hERG1 channels are overexpressed in glioblastoma multiforme and modulate VEGF secretion in glioblastoma cell lines. *Br.J.Cancer.* 93, 781-792
- McCobb, D. P., Fowler, N. L., Featherstone, T., Lingle, C. J., Saito, M., Krause, J. E., Salkoff, L. (1995) A human calcium-activated potassium channel gene expressed in vascular smooth muscle. *Am.J.Physiol.* 269, H767-H777
- Meyer, R., Heinemann, S. H. (1998) Characterization of an eag-like potassium channel in human neuroblastoma cells. *J.Physiol.* 508, 49-56
- Meyer, R., Schonherr, R., Gavrilova-Ruch, O., Wohlrab, W., Heinemann, S. H. (1999) Identification of *ether à go-go* and calcium-activated potassium channels in human melanoma cells. *J Membr.Biol* 171, 107-115
- Moran, A. E., Hunt, D. H., Javid, S. H., Redston, M., Carothers, A. M., Bertagnolli, M. M. (2004) *Apc* deficiency is associated with increased *Egfr* activity in the intestinal enterocytes and adenomas of C57BL/6J-Min/+ mice. *J Biol Chem.* 279, 43261-43272
- Morrill, G. A., Robbins, E. (1984) Changes in intracellular cations during the cell cycle in HeLa cells. *Physiol Chem Phys.Med NMR* 16, 209-219
- Mu, D., Chen, L., Zhang, X., See, L. H., Koch, C. M., Yen, C., Tong, J. J., Spiegel, L., Nguyen, K. C., Servoss, A., Peng, Y., Pei, L., Marks, J. R., Lowe, S., Hoey, T., Jan, L. Y., McCombie, W. R., Wigler, M. H., Powers, S. (2003b) Genomic amplification and oncogenic properties of the *KCNK9* potassium channel gene. *Cancer Cell* 3, 297-302
- Mu, D., Chen, L., Zhang, X., See, L. H., Koch, C. M., Yen, C., Tong, J. J., Spiegel, L., Nguyen, K. C., Servoss, A., Peng, Y., Pei, L., Marks, J. R., Lowe, S., Hoey, T., Jan, L. Y., McCombie,

- W. R., Wigler, M. H., Powers, S. (2003a) Genomic amplification and oncogenic properties of the *KCNK9* potassium channel gene. *Cancer Cell* 3, 297-302
- Narisawa, T., Wong, C. Q., Maronpot, R. R., Weisburger, J. H. (1976) Large bowel carcinogenesis in mice and rats by several intrarectal doses of methylnitrosourea and negative effect of nitrite plus methylurea. *Cancer Res.* 36, 505-510
- Nathke, I. (2006) Cytoskeleton out of the cupboard: colon cancer and cytoskeletal changes induced by loss of *APC*. *Nat.Rev.Cancer.* 6, 967-974
- Nilius, B., Wohlrab, W. (1992) Potassium channels and regulation of proliferation of human melanoma cells. *J Physiol (Lond.)* 445, 537-548
- Nitschke, R., Riedel, A., Ricken, S., Leipziger, J., Benning, N., Fischer, K., Greger, R. (1996) The effect of intracellular pH on cytosolic  $\text{Ca}^{2+}$  in HT<sub>29</sub> cells. *Pflügers Arch* 433, 98-108
- O'Grady, S. M., Lee, S. Y. (2005) Molecular diversity and function of voltage-gated ( $\text{K}_v$ ) potassium channels in epithelial cells. *Int.J Biochem Cell Biol* 37, 1578-1594
- O'Malley, D., Harvey, J. (2004) Insulin activates native and recombinant large conductance  $\text{Ca}^{2+}$ -activated potassium channels via a mitogen-activated protein kinase-dependent process. *Mol.Pharmacol* 65, 1352-1363
- Okada, Y., Maeno, E., Shimizu, T., Dezaki, K., Wang, J., Morishima, S. (2001) Receptor-mediated control of regulatory volume decrease (RVD) and apoptotic volume decrease (AVD). *J Physiol.* 532, 3-16
- Olsen, M. L., Weaver, A. K., Ritch, P. S., Sontheimer, H. (2005) Modulation of glioma BK channels via erbB2. *J.Neurosci.Res.* 81, 179-189
- Orio, P., Rojas, P., Ferreira, G., Latorre, R. (2002) New disguises for an old channel: MaxiK channel beta-subunits. *News Physiol Sci.* 17, 156-161
- Ouadid-Ahidouch, H., Roudbaraki, M., Ahidouch, A., Delcourt, P., Prevarskaya, N. (2004a) Cell-cycle-dependent expression of the large  $\text{Ca}^{2+}$ -activated  $\text{K}^+$  channels in breast cancer cells. *Biochem Biophys.Res.Comm.* 316, 244-251
- Ouadid-Ahidouch, H., Roudbaraki, M., Delcourt, P., Ahidouch, A., Joury, N., Prevarskaya, N. (2004b) Functional and molecular identification of intermediate-conductance  $\text{Ca}^{2+}$ -activated  $\text{K}^+$  channels in breast cancer cells: association with cell cycle progression. *Am.J Physiol Cell Physiol* 287, C125-C134
- Ousingsawat, J., Spitzner, M., Puntheeranurak, S., Terracciano, L., Tornillo, L., Bubendorf, L., Kunzelmann, K., Schreiber, R. (2007) Expression of voltage-gated potassium channels in human and mouse colonic carcinoma. *Clin.Cancer Res.* 13, 824-831
- Pancrazio, J. J., Tabbara, I. A., Kim, Y. I. (1993) Voltage-activated  $\text{K}^+$  conductance and cell proliferation in small-cell lung cancer. *Anticancer Res.* 13, 1231-1234

- Pandiella, A., Magni, M., Lovisolo, D., Meldolesi, J. (1989) The effect of epidermal growth factor on membrane potential. Rapid hyperpolarization followed by persistent fluctuations. *J Biol Chem* 264, 12914-12921
- Pardo, L. A. (2004) Voltage-gated potassium channels in cell proliferation. *Physiology (Bethesda.)* 19, 285-292
- Pardo, L. A., Contreras-Jurado, C., Zientkowska, M., Alves, F., Stuhmer, W. (2005) Role of voltage-gated potassium channels in cancer. *J Membr.Biol.* 205, 115-124
- Pardo, L. A., del Camino, D., Sanchez, A., Alves, F., Brüggemann, A., Beckh, S., Stühmer, W. (1999) Oncogenic potential of EAG K<sup>+</sup> channels. *EMBO J* 18, 5540-5547
- Parihar, A. S., Coghlan, M. J., Gopalakrishnan, M., Shieh, C. C. (2003) Effects of intermediate-conductance Ca<sup>2+</sup>-activated K<sup>+</sup> channel modulators on human prostate cancer cell proliferation. *Eur.J Pharmacol.* 471, 157-164
- Patel, A. J., Lazdunski, M. (2004) The 2P-domain K<sup>+</sup> channels: role in apoptosis and tumorigenesis. *Pflugers Arch* 448, 261-273
- Patel, A. J., Maingret, F., Magnone, V., Fosset, M., Lazdunski, M., Honore, E. (2000) TWIK-2, an inactivating 2P domain K<sup>+</sup> channel. *J Biol Chem* 275, 28722-28730
- Patt, S., Preussat, K., Beetz, C., Kraft, R., Schrey, M., Kalff, R., Schonherr, K., Heinemann, S. H. (2004) Expression of *ether à go-go* potassium channels in human gliomas. *Neurosci.Lett.* 368, 249-253
- Pei, L., Wiser, O., Slavin, A., Mu, D., Powers, S., Jan, L. Y., Hoey, T. (2003) Oncogenic potential of TASK3 (*Kcnk9*) depends on K<sup>+</sup> channel function. *Proc.Natl.Acad.Sci.U.S.A* 100, 7803-7807
- Peres, A., Zippel, R., Sturani, E. (1988) Serum induces the immediate opening of Ca<sup>2+</sup>-activated channels in quiescent human fibroblasts. *FEBS Lett.* 241, 164-168
- Petrylak, D. P., Tangen, C. M., Hussain, M. H., Lara, P. N., Jr., Jones, J. A., Taplin, M. E., Burch, P. A., Berry, D., Moinpour, C., Kohli, M., Benson, M. C., Small, E. J., Raghavan, D., Crawford, E. D. (2004) Docetaxel and estramustine compared with mitoxantrone and prednisone for advanced refractory prostate cancer. *N.Engl.J.Med.* 351, 1513-1520
- Pillozzi, S., Brizzi, M. F., Balzi, M., Crociani, O., Cherubini, A., Guasti, L., Bartolozzi, B., Becchetti, A., Wanke, E., Bernabei, P. A., Olivotto, M., Pegoraro, L., Arcangeli, A. (2002) HERG potassium channels are constitutively expressed in primary human acute myeloid leukemias and regulate cell proliferation of normal and leukemic hemopoietic progenitors. *Leukemia.* 16, 1791-1798
- Plummer, H. K., III, Dhar, M. S., Cekanova, M., Schuller, H. M. (2005) Expression of G-protein inwardly rectifying potassium channels (GIRKs) in lung cancer cell lines. *BMC.Cancer.* 5, 104

- Plummer, H. K., III, Yu, Q., Cakir, Y., Schuller, H. M. (2004) Expression of inwardly rectifying potassium channels (GIRKs) and beta-adrenergic regulation of breast cancer cell lines. *BMC.Cancer.* 4, 93
- Potier, M., Joulin, V., Roger, S., Besson, P., Jourdan, M. L., Leguennec, J. Y., Bournoux, P., Vandier, C. (2006) Identification of SK3 channel as a new mediator of breast cancer cell migration. *Mol.Cancer Ther.* 5, 2946-2953
- Preussat, K., Beetz, C., Schrey, M., Kraft, R., Wolfl, S., Kalff, R., Patt, S. (2003) Expression of voltage-gated potassium channels K<sub>v</sub>1.3 and K<sub>v</sub>1.5 in human gliomas. *Neurosci.Lett.* 346, 33-36
- Puntheeranurak, S., Schreiber, R., Spitzner, M., Ousingsawat, J., Krishnamra, N., Kunzelmann, K. (2006) Control of ion transport in mouse proximal and distal colon and control by prolactin. *Cell Physiol Biochem (in press)* 19, 77-88
- Quirk, J. C., Reinhart, P. H. (2001) Identification of a novel tetramerization domain in large conductance K(ca) channels. *Neuron.* 32, 13-23
- Rao, C. V., Hirose, Y., Indranie, C., Reddy, B. S. (2001) Modulation of experimental colon tumorigenesis by types and amounts of dietary fatty acids. *Cancer Res.* 61, 1927-1933
- Rao, J. N., Platoshyn, O., Li, L., Guo, X., Golovina, V. A., Yuan, J. X., Wang, J. Y. (2002) Activation of K<sup>+</sup> channels and increased migration of differentiated intestinal epithelial cells after wounding. *Am.J Physiol Cell Physiol* 282, C885-C898
- Rebhan, M., Chalifa-Caspi, V., Prilusky, J., Lancet, D. (1997) GeneCards: integrating information about genes, proteins and diseases. *Trends Genet.* 13, 163
- Reiter, R. E., Sato, I., Thomas, G., Qian, J., Gu, Z., Watabe, T., Loda, M., Jenkins, R. B. (2000) Coamplification of prostate stem cell antigen (PSCA) and MYC in locally advanced prostate cancer. *Genes Chromosomes.Cancer.* 27, 95-103
- Renaudo, A., Watry, V., Chassot, A. A., Ponzio, G., Ehrenfeld, J., Soriani, O. (2004) Inhibition of tumor cell proliferation by sigma ligands is associated with K<sup>+</sup> Channel inhibition and p27<sup>kip1</sup> accumulation. *J.Pharmacol.Exp.Ther.* 311, 1105-1114
- Reshkin, S. J., Bellizzi, A., Caldeira, S., Albarani, V., Malanchi, I., Poignee, M., Alunni-Fabbroni, M., Casavola, V., Tommasino, M. (2000) Na<sup>+</sup>/H<sup>+</sup> exchanger-dependent intracellular alkalization is an early event in malignant transformation and plays an essential role in the development of subsequent transformation-associated phenotypes. *FASEB J* 14, 2185-2197
- Robitaille, R., Charlton, M. P. (1992) Presynaptic calcium signals and transmitter release are modulated by calcium-activated potassium channels. *J.Neurosci.* 12, 297-305
- Rouzaire-Dubois, B., Dubois, J. M. (1998) K<sup>+</sup> channel block-induced mammalian neuroblastoma cell swelling: a possible mechanism to influence proliferation. *J Physiol (Lond.)* 510, 93-102
- Rutili, G., Arfors, K. E. (1977) Protein concentration in interstitial and lymphatic fluids from the subcutaneous tissue. *Acta Physiol Scand.* 99, 1-8

- Sakai, H., Shimizu, T., Hori, K., Ikari, A., Asano, S., Takeguchi, N. (2002) Molecular and pharmacological properties of inwardly rectifying K<sup>+</sup> channels of human lung cancer cells. *Eur.J.Pharmacol.* 435, 125-133
- Sandle, G., Perry, M., Mathialahan, T., Linley, J., Robinson, P., Hunter, M., MacLennan, K. (2007) Altered cryptal expression of luminal potassium (BK) channels in ulcerative colitis. *J.Pathol.* 212, 66-73
- Sandle, G. I., Butterfield, I. (1999) Potassium secretion in rat distal colon during dietary potassium loading: role of pH regulated apical potassium channels. *Gut* 44, 40-46
- Sandle, G. I., McNicholas, C. M., Lomax, R. B. (1994) Potassium channels in colonic crypts. *Lancet.* 343, 23-25
- Sarkadi, B., Parker, J. C. (1991) Activation of ion transport pathways by changes in cell volume. *Biochim.Biophys.Acta.* 1071, 407-427
- Sausbier, M., Matos, J. E., Sausbier, U., Beranek, G., Arntz, C., Neuhuber, W., Ruth, P., Leipziger, J. (2006) Distal Colonic K<sup>+</sup> Secretion Occurs via BK Channels. *J Am.Soc.Nephrol.* 17, 1275-1282
- Schönherr, R. (2005) Clinical relevance of ion channels for diagnosis and therapy of cancer. *J Membr.Biol.* 205, 175-184
- Schreiber, R. (2005) Ca<sup>2+</sup> signaling, intracellular pH and cell volume in cell proliferation. *J Membr.Biol.* 205, 129-137
- Shao, X. D., Wu, K. C., Hao, Z. M., Hong, L., Zhang, J., Fan, D. M. (2005) The potent inhibitory effects of cisapride, a specific blocker for human *ether-à-go-go-related* gene (HERG) channel, on gastric cancer cells. *Cancer Biol.Ther.* 4, 295-301
- Smith, G. A., Tsui, H. W., Newell, E., Jiang, X., Zhu, X. P., Tsui, F. W., Schlichter, L. C. (2002) Functional up-regulation of HERG K<sup>+</sup> channels in neoplastic hematopoietic cells. *J Biol Chem* 277, 18528-18534
- Sonnenberg, A., Muller, A. D. (1993) Constipation and cathartics as risk factors of colorectal cancer: a meta-analysis. *Pharmacology.* 47 Suppl 1, 224-233
- Spitzner, M., Ousingsawat, J., Scheidt, K., Kunzelmann, K., Schreiber, R. (2007) Voltage-gated K<sup>+</sup> channels support proliferation of colonic carcinoma cells. *FASEB J* 11, 35-44
- Stringer, B. K., Cooper, A. G., Shepard, S. B. (2001) Overexpression of the G-protein inwardly rectifying potassium channel 1 (GIRK1) in primary breast carcinomas correlates with axillary lymph node metastasis. *Cancer Res.* 61, 582-588
- Stubbs, M., Veech, R. L., Griffiths, J. R. (1995) Tumor metabolism: the lessons of magnetic resonance spectroscopy. *Adv.Enzyme Regul.* 35, 101-115
- Stuhmer, W., Alves, F., Hartung, F., Zientkowska, M., Pardo, L. A. (2006) Potassium channels as tumour markers. *FEBS Lett.* 580, 2850-2852

- Su, L. K., Kinzler, K. W., Vogelstein, B., Preisinger, A. C., Moser, A. R., Luongo, C., Gould, K. A., Dove, W. F. (1992) Multiple intestinal neoplasia caused by a mutation in the murine homolog of the *APC* gene. *Science*. 256, 668-670
- Suzuki, T., Takimoto, K. (2004b) Selective expression of HERG and K<sub>v</sub>2 channels influences proliferation of uterine cancer cells. *Int.J.Oncol.* 25, 153-159
- Suzuki, T., Takimoto, K. (2004a) Selective expression of HERG and K<sub>v</sub>2 channels influences proliferation of uterine cancer cells. *Int.J.Oncol.* 25, 153-159
- Szabo, I., Lepple-Wienhues, A., Kaba, K. N., Zoratti, M., Gulbins, E., Lang, F. (1998) Tyrosine kinase-dependent activation of a chloride channel in CD95-induced apoptosis in T lymphocytes. *Proc.Natl.Acad.Sci.U.S.A* 95, 6169-6174
- Takahashi, A., Yamaguchi, H., Miyamoto, H. (1993) Change in K<sup>+</sup> current of HeLa cells with progression of the cell cycle studied by patch-clamp technique. *Am.J.Physiol.* 265, C328-C336
- Tilly, B. C., van den, B. N., Tertoolen, L. G., Edixhoven, M. J., De Jonge, H. R. (1993) Protein tyrosine phosphorylation is involved in osmoregulation of ionic conductances. *J.Biol.Chem.* 268, 19919-19922
- Umesaki, Y., Yajima, T., Yokokura, T., Mutai, M. (1979) Effect of organic acid absorption on bicarbonate transport in rat colon. *Pflügers Arch* 379, 43-47
- Valverde, M. A., Rojas, P., Amigo, J., Cosmelli, D., Orio, P., Bahamonde, M. I., Mann, G. E., Vergara, C., Latorre, R. (1999a) Acute activation of Maxi-K channels (hSlo) by estradiol binding to the beta subunit. *Science* 285, 1929-1931
- Valverde, M. A., Rojas, P., Amigo, J., Cosmelli, D., Orio, P., Bahamonde, M. I., Mann, G. E., Vergara, C., Latorre, R. (1999b) Acute activation of Maxi-K channels (hSlo) by estradiol binding to the beta subunit. *Science*. 285, 1929-1931
- Van Coppenolle, F., Skryma, R., Ouadid-Ahidouch, H., Slomianny, C., Roudbaraki, M., Delcourt, P., Dewailly, E., Humez, S., Crepin, A., Gourdou, I., Djiane, J., Bonnal, J. L., Mauroy, B., Prevarskaya, N. (2004) Prolactin stimulates cell proliferation through a long form of prolactin receptor and K<sup>+</sup> channel activation. *Biochem J* 377, 569-578
- Veldscholte, J., Berrevoets, C. A., Ris-Stalpers, C., Kuiper, G. G., Jenster, G., Trapman, J., Brinkmann, A. O., Mulder, E. (1992) The androgen receptor in LNCaP cells contains a mutation in the ligand binding domain which affects steroid binding characteristics and response to antiandrogens. *J.Steroid Biochem.Mol.Biol.* 41, 665-669
- Wakabayashi, S., Shigekawa, M., Pouyssegur, J. (1997) Molecular physiology of vertebrate Na<sup>+</sup>/H<sup>+</sup> exchangers. *Physiological Reviews* 77, 51-74
- Wang, H., Zhang, Y., Cao, L., Han, H., Wang, J., Yang, B., Nattel, S., Wang, Z. (2002) HERG K<sup>+</sup> channel, a regulator of tumor cell apoptosis and proliferation. *Cancer Res.* 62, 4843-4848

- Wang, X. T., Nagaba, Y., Cross, H. S., Wrba, F., Zhang, L., Guggino, S. E. (2000) The mRNA of L-type calcium channel elevated in colon cancer: protein distribution in normal and cancerous colon. *Am.J Pathol.* 157, 1549-1562
- Wang, Z. (2004) Roles of K<sup>+</sup> channels in regulating tumour cell proliferation and apoptosis. *Pflugers Arch* 448, 274-286
- Warth, R., Barhanin, J. (2003) Function of K<sup>+</sup> channels in the intestinal epithelium. *J Membr.Biol.* 193, 67-78
- Warth, R., Bleich, M. (2000) K<sup>+</sup> channels and colonic function. *Rev Physiol Biochem Pharmacol* 140, 1-62
- Warth, R., Hamm, K., Bleich, M., Kunzelmann, K., vonHahn, T., Schreiber, R., Ullrich, E., Mengel, M., Trautmann, N., Kindle, P., Schwab, A., Greger, R. (1999) Molecular and functional characterization of the small Ca<sup>2+</sup>-regulated K<sup>+</sup> channel (rSK4) of colonic crypts. *Pflügers Arch* 438, 437-444
- Wasan, H. S., Novelli, M., Bee, J., Bodmer, W. F. (1997) Dietary fat influences on polyp phenotype in multiple intestinal neoplasia mice. *Proc.Natl.Acad.Sci.U.S.A* 94, 3308-3313
- Weaver, A. K., Liu, X., Sontheimer, H. (2004) Role for calcium-activated potassium channels (BK) in growth control of human malignant glioma cells. *J.Neurosci.Res.* 78, 224-234
- Webb, S. D., Sherratt, J. A., Fish, R. G. (1999) Mathematical modelling of tumour acidity: regulation of intracellular pH. *J.Theor.Biol.* 196, 237-250
- Wei, A. D., Gutman, G. A., Aldrich, R., Chandy, K. G., Grissmer, S., Wulff, H. (2005) International Union of Pharmacology. LII. Nomenclature and molecular relationships of calcium-activated potassium channels. *Pharmacol.Rev.* 57, 463-472
- Wei, L., Xiao, A. Y., Jin, C., Yang, A., Lu, Z. Y., Yu, S. P. (2004) Effects of chloride and potassium channel blockers on apoptotic cell shrinkage and apoptosis in cortical neurons. *Pflugers Arch* 448, 325-334
- Weitz, J., Koch, M., Debus, J., Hohler, T., Galle, P. R., Buchler, M. W. (2005) Colorectal cancer. *Lancet.* 365, 153-165
- Winston, N. J., Johnson, M. H., McConnell, J. M., Cook, D. I., Day, M. L. (2004) Expression and role of the *ether-à-go-go-related* (MERG1A) potassium-channel protein during preimplantation mouse development. *Biol Reprod.* 70, 1070-1079
- Wonderlin, W. F., Strobl, J. S. (1996) Potassium channels, proliferation and G1 progression. *J Membr.Biol* 154, 91-107
- Woodfork, K. A., Wonderlin, W. F., Peterson, V. A., Strobl, J. S. (1995) Inhibition of ATP-sensitive potassium channels causes reversible cell-cycle arrest of human breast cancer cells in tissue culture. *J Cell Physiol* 162, 163-171
- Xu, B., Wilson, B. A., Lu, L. (1996) Induction of human myeloblastic ML-1 cell G1 arrest by suppression of K<sup>+</sup> channel activity. *Am J Physiol* 271, C2037-C2044



- Yang, J., Shikata, N., Mizuoka, H., Tsubura, A. (1996) Colon carcinogenesis in shrews by intrarectal infusion of N-methyl-N-nitrosourea. *Cancer Lett.* 110, 105-112
- Yao, X., Kwan, H. Y. (1999) Activity of voltage-gated K<sup>+</sup> channels is associated with cell proliferation and Ca<sup>2+</sup> influx in carcinoma cells of colon cancer. *Life Sci.* 65, 55-62
- Yu, S. P., Canzoniero, L. M., Choi, D. W. (2001) Ion homeostasis and apoptosis. *Curr. Opin. Cell Biol.* 13, 405-411
- Zhang, T., Otevrel, T., Gao, Z., Gao, Z., Ehrlich, S. M., Fields, J. Z., Boman, B. M. (2001) Evidence that APC regulates survivin expression: a possible mechanism contributing to the stem cell origin of colon cancer. *Cancer Res.* 61, 8664-8667
- Zhang, Y., Wang, H., Wang, J., Han, H., Nattel, S., Wang, Z. (2003) Normal function of HERG K<sup>+</sup> channels expressed in HEK293 cells requires basal protein kinase B activity. *FEBS Lett.* 534, 125-132
- Zhanping, W., Xiaoyu, P., Na, C., Shenglan, W., Bo, W. (2007) Voltage-gated K<sup>+</sup> channels are associated with cell proliferation and cell cycle of ovarian cancer cell. *Gynecol. Oncol.* 104, 455-460
- Zhou, Q., Kwan, H. Y., Chan, H. C., Jiang, J. L., Tam, S. C., Yao, X. (2003) Blockage of voltage-gated K<sup>+</sup> channels inhibits adhesion and proliferation of hepatocarcinoma cells. *Int. J. Mol. Med.* 11, 261-266
- Zhou, X. B., Wang, G. X., Ruth, P., Huneke, B., Korth, M. (2000) BK<sub>Ca</sub> channel activation by membrane-associated cGMP kinase may contribute to uterine quiescence in pregnancy. *Am. J. Physiol. Cell Physiol.* 279, C1751-C1759



### Appendix I. K<sup>+</sup> channel families.

The table shows the 4 major families of K<sup>+</sup> channels: voltage-gated K<sup>+</sup> channels (K<sub>v</sub>), Ca<sup>2+</sup>-activated K<sup>+</sup> channels (K<sub>Ca</sub>), two-pore domain K<sup>+</sup> channels (K<sub>2P</sub>), and inwardly rectifying K<sup>+</sup> channels (K<sub>ir</sub>). Classification according to the International Union of Pharmacology (IUPHAR) and the Human Gene Nomenclature Committee (HGNC). The table also shows other commonly used names along with the chromosomal localization (Goldstein et al., 2005, Gutman et al., 2003, Gutman et al., 2005, Kubo et al., 2005, Wei et al., 2005).

IUPHAR	HGNC	Gene chromo- somal localization	Other names	comments
<b>Voltage-gated potassium channel family (K<sub>v</sub>)</b>				
K <sub>v</sub> 1.1	<i>KCNA1</i>	12p13.3	HuK (I), MBK1, MK1, RCK1, RBK1, HBK1	6TM1P K <sub>v</sub> channel, <i>Shaker</i> -related family, can co-assemble with other K <sub>v</sub> 1 family members in heteromultimers
K <sub>v</sub> 1.2	<i>KCNA2</i>	1p13	HuK (IV), MK2, BK2, RCK5, RAK, BGK5, Xsha2, NGK1, HBK5	
K <sub>v</sub> 1.3	<i>KCNA3</i>	1p13.3?	MK3, MBK3, RCK3, hPCN3, HuK (III), HLK3, RGK5, K <sub>v</sub> 3, HGK5, <i>n</i> -channel	
K <sub>v</sub> 1.4	<i>KCNA4</i>	11p14.3-15.2	HuK (II), hPCN2, HK1, RCK4, RHK1, RK4, RK8, MK4	
K <sub>v</sub> 1.5	<i>KCNA5</i>	12p13.3	HpCN1, HK2, HCK1, K <sub>v</sub> 1, fHK, RK3, RMK2, HuK (II)	
K <sub>v</sub> 1.6	<i>KCNA6</i>	12p13.3	HBK2, MK1.6, RCK2, K <sub>v</sub> 2	
K <sub>v</sub> 1.7	<i>KCNA7</i>	19q13.3		
K <sub>v</sub> 1.8	<i>KCNA10</i>	1p13.1	K <sub>v</sub> 1.10, Kcn1	
K <sub>v</sub> 2.1	<i>KCNB1</i>	20q13.2	hDRK1, DRK1	6TM1P K <sub>v</sub> channel, <i>Shab</i> -related family
K <sub>v</sub> 2.2	<i>KCNB2</i>	8q13.2	CDRK	
K <sub>v</sub> 3.1	<i>KCNC1</i>	11p15	NGK2, K <sub>v</sub> 4, KShIIIB, Raw2, type I channel in T cells	6TM1P K <sub>v</sub> channel, <i>Shaw</i> -related family
K <sub>v</sub> 3.2	<i>KCNC2</i>	12q14.1	RKShIIIA, Raw1, K <sub>v</sub> 3.2a, rKv3.2β and rKv3.2c	
K <sub>v</sub> 3.3	<i>KCNC3</i>	19q13.3-4	HKv3.3, mKv3.3, RKShIIID, K <sub>v</sub> 3.3β	
K <sub>v</sub> 3.4	<i>KCNC4</i>	1p21	Raw3, HKShIIIC, mKv3.4	
K <sub>v</sub> 4.1	<i>KCND1</i>	Xp11.23	mShal	6TM1P K <sub>v</sub> channel, <i>Shal</i> -related family
K <sub>v</sub> 4.2	<i>KCND2</i>	7q31	Shal1, RK5	
K <sub>v</sub> 4.3	<i>KCND3</i>	1p13.3		
K <sub>v</sub> 5.1	<i>KCNF1</i>	2p25	KH1, IK8	no own function, modifier of the K <sub>v</sub> 2 channels

IUPHAR	HGNC	Gene chromosomal localization	Other names	comments
K <sub>v</sub> 6.1 K <sub>v</sub> 6.2 K <sub>v</sub> 6.3 K <sub>v</sub> 6.4	KCNG1 KCNG2 KCNG3 KCNG4	20q13 18q22-18q23 2p21 16q24.1	KH2, K13	no own function, modifier of the K <sub>v</sub> 2 channels
K <sub>v</sub> 7.1 K <sub>v</sub> 7.2 K <sub>v</sub> 7.3 K <sub>v</sub> 7.4 K <sub>v</sub> 7.5	KCNQ1 KCNQ2 KCNQ3 KCNQ4 KCNQ5	11p15.5 20q13.3 8q24 1p34 6q14	K <sub>v</sub> LQT, slow delayed rectifier KQT2	has associated subunits: KCNQ1/KCNE1, KCNQ1/KCNE3 has associated subunits: KCNQ2/KCNQ3, KCNQ2/KCNE2 has associated subunits: KCNQ3/KCNQ2, KCNQ3/KCNQ5 has associated subunits: KCNQ4/KCNQ3 has associated subunits: KCNQ5/KCNQ3
K <sub>v</sub> 8.1 K <sub>v</sub> 8.2	KCNV1 KCNV	8q22.3-24.1 9p24.2	K <sub>v</sub> 2.3, HNK A	no own function, modifier of the K <sub>v</sub> 2 channels
K <sub>v</sub> 9.1 K <sub>v</sub> 9.2 K <sub>v</sub> 9.3	KCNS1 KCNS2 KCNS3	20q12 8q22 2p24		no own function, modifier of the K <sub>v</sub> 2 channels
K <sub>v</sub> 10.1 K <sub>v</sub> 10.2	KCNH1 KCNH5	1q32-41 14q32.1	eag1a, eag1b, KCNH1a, KCNH1b, eag2	
K <sub>v</sub> 11.1 K <sub>v</sub> 11.2 K <sub>v</sub> 11.3	KCNH2 KCNH6 KCNH7	7q35-36 17q23.3 2q24.2	erg1, HERG, Hergb erg2 erg3	K <sub>v</sub> 11.1, K <sub>v</sub> 11.2, and K <sub>v</sub> 11.3 can form heteromultimers
K <sub>v</sub> 12.1 K <sub>v</sub> 12.2 K <sub>v</sub> 12.3	KCNH8 KCNH3 KCNH4	3q24.3 12q13 17q21.2	elk1, elk3 elk2, BEC1 elk1, BEC2	
<b>Ca<sup>2+</sup>-activated potassium channel (K<sub>Ca</sub>)</b>				
K <sub>Ca</sub> 1.1	KCNMA1	10q22.3	Slo, Slo1, BK, BK <sub>Ca</sub> , maxi K <sup>+</sup> channel, large Ca <sup>2+</sup> -activated K <sup>+</sup> channel	7TM/1P maxi-K <sub>Ca</sub> channel, has associated subunit 1- 4 (KCNMB1-KCNMB4)
K <sub>Ca</sub> 2.1 K <sub>Ca</sub> 2.2 K <sub>Ca</sub> 2.3	KCNN1 KCNN2 KCNN3	19p13.1 5q22.3 1q21.3	SK <sub>Ca</sub> 1, SK1 SK <sub>Ca</sub> 2, SK2 SK <sub>Ca</sub> 3, SK3, hK <sub>Ca</sub> 3	6TM/1P SK <sub>Ca</sub> channel

IUPHAR	HGNC	Gene chromo- somal localization	Other names	comments
K <sub>Ca</sub> 3.1	<i>KCNN4</i>	19q13.2	IK <sub>Ca</sub> 1, SK4, IK1, K <sub>Ca</sub> 4	6TM/1P IK <sub>Ca</sub> channel
K <sub>Ca</sub> 4.1 K <sub>Ca</sub> 4.2	<i>KCNT1</i> <i>KCNT2</i>	9q34.3 1q31.3	Slack, Slo2.2, KCNT1 Slick, Slo2.1, KCNT2	
K <sub>Ca</sub> 5.1	<i>KCNU1</i>	8p11.2	Slo3, KCNMC1, Kcnma3	
Two-pore potassium channels				
K <sub>2P</sub> 1.1	<i>KCNK1</i>	1q42-43	TWIK-1, <i>KCNK1</i> , hOHO	4TM/2P (TASK, TWIK, TREK)
K <sub>2P</sub> 2.1	<i>KCNK2</i>	1q41	TREK-1, <i>KCNK2</i> , TPKC1	
K <sub>2P</sub> 3.1	<i>KCNK3</i>	2p23	TASK-1, <i>KCNK3</i> ,	
K <sub>2P</sub> 4.1	<i>KCNK4</i>	11q13	TRAAK, <i>KCNK4</i>	
K <sub>2P</sub> 5.1	<i>KCNK5</i>	6p21	TASK-2, <i>KCNK5</i>	
K <sub>2P</sub> 6.1	<i>KCNK6</i>	19q13.1	TWIK-2, <i>KCNK6</i> , TOSS	
K <sub>2P</sub> 7.1	<i>KCNK7</i>	11q13	<i>KCNK7</i> , kcnk8	
K <sub>2P</sub> 9.1	<i>KCNK9</i>	8q24	TASK-3, <i>KCNK9</i>	
K <sub>2P</sub> 10.1	<i>KCNK10</i>	14q31	TREK-2, <i>KCNK10</i>	
K <sub>2P</sub> 12.1	<i>KCNK12</i>	2p22	THIK-2, <i>KCNK12</i>	
K <sub>2P</sub> 13.1	<i>KCNK13</i>	14q24	THIK-1, <i>KCNK13</i>	
K <sub>2P</sub> 15.1	<i>KCNK15</i>	20q12	TASK-5, <i>KCNK15</i> , KT3.3	
K <sub>2P</sub> 16.1	<i>KCNK16</i>	6p21	TALK-1, <i>KCNK16</i>	
K <sub>2P</sub> 17.1	<i>KCNK17</i>	6p21	TASK-4, <i>KCNK17</i> , TALK-2	
K <sub>2P</sub> 18.1	<i>KCNK18</i>	10q26.11	TRESK-1/TRESK-2, <i>KCNK18</i>	
Inwardly rectifying potassium channel				
K <sub>ir</sub> 1.1	<i>KCNJ1</i>	17q24	ROMK, ROMK1	2TM/1P K <sub>ir</sub> channel, 6 splice variants exist, denoted as K <sub>ir</sub> 1.1a - f
K <sub>ir</sub> 2.1 K <sub>ir</sub> 2.2	<i>KCNJ2</i> <i>KCNJ12</i>	17q23 17p11.1	IRK1 IRK2, RB-IRK2, MB-IRK2, hIRK	2TM/1P K <sub>ir</sub> channel
K <sub>ir</sub> 2.3	<i>KCNJ4</i>	22q13.10	IRK3, HIR, HRK1, BIRK2, BIR11, hIRK2, MB-IRK3, CCD-IRK3, mK <sub>ir</sub> 2.3	

IUPHAR	HGNC	Gene chromo- somal localization	Other names	comments
K <sub>ir</sub> 2.4	<i>KCNJ14</i>	19q13.1-13.3	IRK14	
K <sub>ir</sub> 3.1 K <sub>ir</sub> 3.2 K <sub>ir</sub> 3.3 K <sub>ir</sub> 3.4	<i>KCNJ3</i> <i>KCNJ6</i> <i>KCNJ9</i> <i>KCNJ5</i>	2q24.1 21q22 1q21-23 11q24	GIRK1, KGA GIRK2, hiGIRK2 GIRK3 GIRK4	G-protein-gated K <sub>ir</sub> channel
K <sub>ir</sub> 4.1 K <sub>ir</sub> 4.2	<i>KCNJ10</i> <i>KCNJ15</i>	1q22 21q22.2	K <sub>ir</sub> 1.2, K <sub>AB</sub> -2, BIR10, BIRK-10, BIRK-1, KCNJ13-PEN K <sub>ir</sub> 1.3, IRKK	Gilal ATP-dependent
K <sub>ir</sub> 5.1	<i>KCNJ16</i>	17q23.1	BIR 9	
K <sub>ir</sub> 6.1 K <sub>ir</sub> 6.2	<i>KCNJ8</i> <i>KCNJ11</i>	12p11.23 11p15.1	uKATP-1 BIR	ATP-sensitive K <sup>+</sup> channel
K <sub>ir</sub> 7.1	<i>KCNJ13</i>	2q37	K <sub>ir</sub> 1.4	

**Appendix II.** Modulators of K<sup>+</sup> channels.

Compounds	used concentration	Effects (IC <sub>50</sub> or EC <sub>50</sub> )
4-AP	50 µM - 2 mM	inhibits K <sub>v</sub> channels K <sub>v</sub> 1.3 (195 µM), K <sub>v</sub> 1.4 (13 µM), K <sub>v</sub> 1.5 (270 µM), K <sub>v</sub> 1.6 (1.5 mM), K <sub>v</sub> 1.7 (150 µM), K <sub>v</sub> 1.8 (1.5 mM), K <sub>v</sub> 2.2 (1.5 mM), K <sub>v</sub> 3.1 (29 µM), K <sub>v</sub> 3.3 (1.2 mM)
Astemizole	0.5 nM - 5 µM	inhibits members of the <i>ether à go-go</i> K <sub>v</sub> family (Eag, Erg, Elk)
AVE0118	0.005 - 50 µM	inhibits K <sub>v</sub> 1.3, K <sub>v</sub> 1.5 (5.6 µM), K <sub>v</sub> 2.1, K <sub>v</sub> 3.1, K <sub>v</sub> 4.3
AVE1231	0.005 - 50 µM	inhibits K <sub>v</sub> 1.5 (3.6 µM), K <sub>v</sub> 4.3/KChIP2.2b (5.9 µM) I <sub>KACH</sub> current (K <sub>ir</sub> 3.4) (8.4 µM), I <sub>Kr</sub> current (Erg-1) (30 µM) K <sub>ATP</sub> current (K <sub>ir</sub> 6.1, 6.2)
BaCl <sub>2</sub>	5 mM	non selective K <sup>+</sup> channel blocker
BDS-I	0.01 - 100 nM	inhibits K <sub>v</sub> 3.4
293B	0.001 - 10 µM	inhibits K <sub>v</sub> LQT1 (K <sub>v</sub> 7.1)
Charybdotoxin	0.01 - 100 nM	inhibits K <sub>v</sub> 1.2 (14 nM), K <sub>v</sub> 1.3 (3 nM), K <sub>v</sub> 1.8 (100 nM), BK (2.9 nM), SK4 (5nM)
Clotrimazole	10 nM - 1 µM	inhibits SK4 (70 nM)
Iberiotoxin	0.001 - 10 nM	inhibits BK (10 nM)
Paxillin	1 µM - 5 µM	inhibits BK (less than 10 nM)
Quinidine	0.01 - 100 µM	inhibits K <sub>v</sub> 1.4 (10 µM-1 mM), K <sub>v</sub> 1.5 (0.6 µM), K <sub>v</sub> 1.7 (15 µM), Eag-1 (1.4 µM)
Riluzole	1 nM - 1 mM	activate SK1 (2 µM), SK2 (2 µM), SK3 (3 µM), SK4 (1 µM) inhibits K <sub>v</sub> 1.4 (70 µM)
Scyllatoxin	0.001 - 20 nM	inhibits SK1 (325 nM), SK2 (200 pM), SK3 (1.1 nM)
TRAM-34	0.1 - 100 nM	inhibits SK4 (20 nM)
Terfenadine	0.001 - 10 µM	inhibits members of the <i>ether-à-go-go</i> K <sub>v</sub> family, inhibits Eag, Erg-1 (56 nM), Elk-2 (1.µM)
TPeA	0.1 – 100 µM	non selective K <sup>+</sup> channel blocker
NS1619	10 µM	activates BK (10-30 µM)
17β-estradiol	10 µM	activates BK

note:  
4-AP = 4-aminopyridine  
TPeA = Tetrapentylammonium chloride  
I<sub>KACH</sub> current = acetylcholine-activated K<sup>+</sup> current  
I<sub>Kr</sub> current = the fast delayed outward rectifying K<sup>+</sup> current





## ACKNOWLEDGEMENTS

I would like to express my deepest gratitude and appreciation to my advisor, Prof. Dr. Karl Kunzelmann for his encouragement, invaluable advice, supervision and patience throughout my study. He considerably contributed to the whole concept of this work. I am equally grateful to Dr. Rainer Scheiber for his constructive comments and excellent guidance.

I really appreciate Prof. Dr. Geissler, Prof. Dr. Schneuwly, Prof. Dr. Tamm, and Prof. Dr. Warth for accepting to be examining committees of this thesis.

Generous financial support for my studies and the work presented here has been provided by the Deutsche Forschungsgemeinschaft DFG SCHR 752/2-1 & SCHR 752/2-2, and Wilhelm Sander-Stiftung 2005.063.1.

I would also like to thank particularly Agnes (Agnes Paech) and Tini (Ernestine Tartler) for their excellent technical assistance. I am also thankful to my colleagues for their help, support, and friendship. Special thanks are given to Gabi for translation summary into German language and René for correcting my thesis.

I would like to acknowledge all other contributors of this work, Dr. L Bubendorf, Dr. Michel Bloch, Hedvika Novotny (Institute for Pathology, University of Basel), Dr. Marcus Mall (Kinderklinik der Universität Heidelberg), Dr. F. Obermeier, Dr. Frauke Bataille (Department of Medicine I and Pathology, University of Regensburg), Dr. H. Wulff, (Department of Medical Pharmacology and Toxicology, University of California Davis, USA), and Prof. Dr Peter Ruth (Institute of Pharmacy, University of Tübingen).

Finally, a special note of my deep thankfulness is extended to my parents, my brothers, my sisters, and my friends in Thailand for their love, warm-hearted encouragement and everlasting support. I would like to express all my love to my mother for giving my life, her endless love and true understanding.



## CURRICULUM VITAE

**Name:** Miss Jiraporn Ousingsawat  
**Address:** Lieblstrasse 8, 93059 Regensburg  
**E-mail:** jira\_ae@yahoo.com

### Personal information

Date of birth December, 27<sup>th</sup>, 1972  
Citizenship Thai

### Education:

2003 – at present Ph.D., Faculty of Natural Sciences III: Biology and Preclinical medicine,  
University of Regensburg.  
1996 - 1998 M.Sc. (Physiology), Mahidol University. Research topic: Acute effect of  
prolactin on calcium transport in the colon of rats.  
1991 – 1995 B.Sc. (Physiotherapy), Mahidol University, with second Honors.

### Professional experience:

2001 – 2003 : Lecture at the Department of Physiology, Faculty of Medical Science,  
Naresuan University, Phitsanulok, Thailand.  
2001 : Assistant Dean (Quality Assurance), Faculty of Medical Science,  
Naresuan University, Phitsanulok, Thailand.  
1999 – 2001 : Lecture at the Department of Physiology, Faculty of Medicine, Naresuan  
University  
1995 – 1996 : Physiotherapist at The Central Hospital, Bangkok, Thailand

### Publications:

1. Bloch, M., **Ousingsawat, J.**, Simon, R., Schraml, P., Gasser, T. C., Mihatsch, M. J., Kunzelmann, K., Bubendorf, L. (2007) KCNMA1 gene amplification promotes tumor cell proliferation in human prostate cancer. *Oncogene*. 26, 2525-2534
2. **Ousingsawat, J.**, Spitzner, M., Puntheeranurak, S., Terracciano, L., Tornillo, L., Bubendorf, L., Kunzelmann, K., Schreiber, R. (2007) Expression of voltage-gated potassium channels in human and mouse colonic carcinoma. *Clin.Cancer Res.* 13, 824-831
3. Sousa, M., **Ousingsawat, J.**, Seitz, R., Puntheeranurak, S., Regalado, A., Schmidt, A., Grego, T., Jansakul, C., Amaral, M. D., Schreiber, R., Kunzelmann, K. (2007) An extract

- from the medicinal plant *Phyllanthus acidus* and its isolated compounds induce airway chloride secretion: A potential treatment for cystic fibrosis. *Mol.Pharmacol.* 71, 366-376
4. Spitzner, M., **Ousingsawat, J.**, Scheidt, K., Kunzelmann, K., Schreiber, R. (2007) Voltage-gated K<sup>+</sup> channels support proliferation of colonic carcinoma cells. *FASEB J* 11, 35-44
  5. Kunzelmann, K., Spitzner, M., **Ousingsawat, J.**, Martins, J. R., Schreiber, R. (2006) Expression von Ionenkanälen beim Kolonkarzinom: Neue diagnostische und therapeutische Möglichkeiten? *Onkologie heute* 2, 18-21
  6. Kunzelmann, K., Scheidt, K., Scharf, B., **Ousingsawat, J.**, Schreiber, R., Wainwright, B. J., McMorran, B. (2006) Pseudomonas flagellin inhibits Na<sup>+</sup> transport in airway epithelia. *FASEB J* 20, 545-546
  7. Puntheeranurak, S., Schreiber, R., Spitzner, M., **Ousingsawat, J.**, Krishnamra, N., Kunzelmann, K. (2006) Control of ion transport in mouse proximal and distal colon and control by prolactin. *Cell Physiol Biochem (in press)* 19, 77-88
  8. Adam, G., **Ousingsawat, J.**, Schreiber, R., Kunzelmann, K. (2005) Increase in intracellular Cl<sup>-</sup> concentration by cAMP and Ca<sup>2+</sup> dependent stimulation of M1 collecting duct cells. *Pflügers Arch* 449, 470-478
  9. da Paula, A. C., Ramalho, A. S., Farinha, C. M., Cheung, J., Maurisse, R., Gruenert, D. C., **Ousingsawat, J.**, Kunzelmann, K., Amaral, M. D. (2005) Characterization of novel airway submucosal gland cell models for cystic fibrosis studies. *Cell Physiol Biochem.* 15, 251-262
  10. Krishnamra, N., **Ousingsawat, J.**, Limlomwongse, L. (2001) Study of acute pharmacologic effects of prolactin on calcium and water transport in the rat colon by an in vivo perfusion technique. *Can J Physiol Pharmacol.* 79, 415-421.

#### Presentation:

1. Poster presentation. Epithelial Na<sup>+</sup> channels are upregulated in the colon of *APC<sup>Min/+</sup>* mice. The 86<sup>th</sup> annual meeting of the Deutsche Physiologische Gesellschaft, 2007, Hannover.
2. Oral presentation. The carcinogen 1,2- Dimethylhydrazin activates K<sub>v</sub> and EAG potassium channels in mouse colon. The 85<sup>th</sup> annual meeting of the Deutsche Physiologische Gesellschaft, 2006, Munich.
3. Oral presentation. Large conductance Ca<sup>2+</sup>-activated K<sup>+</sup> channels promote proliferation of prostate cancer cells. The 84<sup>th</sup> annual meeting of the Deutsche Physiologische Gesellschaft, 2005, Göttingen.
4. Poster presentation. Cellular effects of a medicinal plant extract from *Phyllanthus Acidus*. The 83<sup>rd</sup> annual meeting of the Deutsche Physiologische Gesellschaft, 2003, Leipzig.